Contributions to Financial Econometrics: Asset Pricing in a DSGE Framework and Volatility Discovery in Cryptocurrency Markets

Dissertation

zur Erlangung des Doktorgrades

der Wirtschafts- und Sozialwissenschaftlichen Fakultät

der Eberhard Karls Universität Tübingen

vorgelegt von

Dalia Elshiaty

aus Kairo, Ägypten

Tübingen

2022

1. Betreuer:	Prof. Dr. Joachim Grammig
2. Betreuer:	Prof. Dr. Martin Biewen
Tag der mündlichen Prüfung:	24.04.2023
Dekan:	Prof. Dr. Ansgar Thiel
1. Gutachter:	Prof. Dr. Joachim Grammig
2. Gutachter:	Prof. Dr. Martin Biewen

Acknowledgments

This dissertation bears my name as the sole author of this work. Yet, there are many hidden players to whom I am eternally grateful, and without whom this dissertation would have never seen the light of day. I hope that with the following words, I would be able to acknowledge their efforts and give them some of the credit which I indefinitely owe.

My doctoral years have spanned the times of the Corona pandemic. This has added an unimaginable burden to an already stressful situation being experienced by my family. As a family of immigrants in Germany, the isolation that came with the lock-downs was especially draining, and as the sole-caretakers of a then three-year old child, my husband and I were stretched beyond our limits. This is to say that without the patience, support and encouragement from my husband, Dr. Muhammad Alshahed, I would have never been able to complete this work.

I owe the greatest debt to my supervisor, Prof. Dr. Joachim Grammig. Back in 2014, when I was still in Egypt, he decided that I was worthy of a chance to join the Master program in Economics and Finance. He really did set my life on a new trajectory with that decision. His support continued through out my "HiWi" position, the supervision of my Master thesis and his insistence that my, at that time, pregnancy comes first before any work, and later on through the tough balancing act between my duties as a mom and my doctoral studies. Throughout my professional

career, any accomplishments I achieve will always be indebted to him.

The quality of the work in this dissertation benefited greatly from the experiences of my co-authors Prof. Dr. Thomas Dimpfl and Dr. Julie Schnaitmann. I learned a lot from their deep insights, critical thinking as well as their perfectionism. Dr. Schnaitmann along with Dr. Jantje Sönksen have exerted great efforts in proofreading several drafts of this dissertation. I am incredibly grateful for their endless patience.

I will forever miss the family spirit that we shared in the Chair of Prof. Grammig. As a foreigner, you made me feel at home away from home. Thank you to all my former and current colleagues; Prof. Dr. Thomas Dimpfl, Dr. Jantje Sönksen, Dr. Eva-Maria Küchlin, Dr. Johannes Bleher, Constantin Hanenberg and Alex Reining. A special thank you goes to Sylvia Bürger for helping me navigate all of the required paperwork throughout the years, and for enduring my broken German. She was the one who went the extra mile towards correcting my spoken German. I owe her many proper German phrases.

Our temporary residence as a Chair at the tiny apartment in Sigwartstraße will always be cherished in my memories. The close contact with Prof. Dr. Martin Biewen's Chair, that could have resulted in conflicts, was actually a time spent with friends. For this, I thank Prof. Dr. Martin Biewen, Lea Eiting, Alexandra Klotz, Dr. Matthias Seckler, Dr. Jakob Schwerter, Marian Rümmele, Miriam Sturm and Pascal Erhardt.

I cannot end the acknowledgments without giving due credit to my parents, Prof. Dr. Ayman Elshiaty and Prof. Dr. Saly Elkholy. They have provided the role model, that I have followed my entire life. I am also grateful to my sisters, Mariam and Yara, for all the babysitting duties that were forced on them and which they were more than happy to undertake. Finally, to Nelly, my daughter, who has long known me as the busy, always working, doctoral student-mom, I am finally done.

Contents

List of Figures

List of Tables

Chapter 1

Introduction

The hallmark of financial economics is uncertainty (Campbell, Lo and MacKinlay, 1997). The representative investor faces uncertainty while deciding to optimally allocate her resources. This propagates into uncertainty in the market prices of investment assets in the economy, which is then observed in the volatility of those assets' prices. Empirical research in financial economics aims at reconciling the reality of financial markets with theoretical economic models. Yet, as uncertainty is the de facto phenomenon in this field, methodological work relies heavily on probability theory and statistical methods. This is essentially the origin story behind the emergence of the field of financial econometrics.

In this dissertation, three essays are presented each using financial econometric techniques to address the challenges posed by uncertainty. The first two essays are concerned with the challenges faced when estimating a complex dynamic stochastic general equilibrum (DSGE) asset pricing model. In these models, both households and firms make investment decisions under uncertainty that ultimately determine the pricing kernel of assets in this given economy. The third essay is concerned with the manifestation of uncertainty in the form of volatility in the market of cryptocurren-

cies. This dissertation has been under development at a time when cryptocurrencies were monopolizing the financial news with their bubble burst in 2018.[1] Naturally, the examination of their volatility dynamics is a question of interest then and now.

In 2001, Tim Bollerslev's essay in the Journal of Econometrics (Bollerslev, 2001) highlighted the future outlook of financial econometrics at that time. He advocated for research efforts focused in two main areas; the development of flexible methods in estimation procedures, and the use of long-memory properties in the modeling of the volatility of financial markets. Twenty years later, these topics are still of viable interest, and the three financial econometrics essays, presented in this dissertation, make use of remarkable developments in these two areas to tackle the financial economic challenges of the current time.

The first two essays rely on developments made by Dridi, Guay and Renault (2007) to the infamous Indirect Inference estimation method by Gourieroux, Monfort and Renault (1993). Indirect inference estimation enables the estimation of complex structural economic models with intractable likelihood functions, that otherwise cannot be estimated by standard maximum likelihood methods. The theoretical developments made by Dridi et al. (2007) enable misspecification in the underlying structural model to be taken into account during the estimation process. The technique is also flexible enough to allow for some parameters of the model to be calibrated, while the main parameters of interest are consistently estimated. The third essay, on the other hand, utilizes developments in methods that can account for the inherent long-memory property of volatility series. These are then used to conduct a careful scrutiny of the volatility dynamics in the latest FinTech innovation; cryptocurrencies.

[1] See for example `https://www.wsj.com/articles/bitcoin-falls-below-4-000-as-cryptocurrency-collapse-worsens-1543241154`

The first essay is presented in Chapter 2 and is based on the paper *Empirical Asset Pricing in a DSGE Framework: Reconciling Calibration and Econometrics using Partial Indirect Inference*. It is joint work with Prof. Dr. Joachim Grammig and Dr. Julie Schnaitmann. The second essay, titled *The Price of Misspecification in DSGE Asset Pricing Models* is presented in Chapter 3 and is entirely my own contribution to the field of asset pricing. The third essay is presented in Chapter 4 and is based on the paper *Volatility Discovery in Cryptocurrency Markets*. It is joint work with Prof. Dr. Thomas Dimpfl and has been published in *The Journal of Risk Finance* (Dimpfl and Elshiaty, 2021).

In Chapter 2, *Empirical Asset Pricing in a DSGE Framework: Reconciling Calibration and Econometrics using Partial Indirect Inference*, the main aim is to use rigorous econometric methodology to critically examine the acclaimed success of DSGE asset pricing models. In our paper, we focus on a recent variant of these models; namely the model proposed by Chen (2017). The model uses the equilibrium dynamics in the DSGE model to generate a pricing kernel that claims to resolve the well-known asset pricing puzzles in financial economics while also delivering reasonable macroeconomic dynamics. The success of these DSGE asset pricing models, including that of Chen's, is primarily based on confirmatory evidence delivered via calibration exercises. In our study, however, we examine this model under the diligent scheme of econometric analysis to determine whether it indeed resolves two of the famous asset pricing puzzles; namely, the equity premium puzzle and the risk-free rate puzzle. Our econometric approach adapts the partial indirect inference estimation technique from Dridi et al. (2007) to the problem at hand. This allows us to consistently estimate the parameters of interest in the pricing kernel, while all other nuisance parameters, that come from potentially misspecified macroeconomic dynamics, remain calibrated. We explicitly specify the assumptions under which

consistency is maintained, and develop the asymptotic distribution necessary for statistical inference to be performed. Our results suggest that the acclaimed success of DSGE models to resolve the asset pricing puzzles should be viewed with caution. Our analyses indicate that the risk-free rate puzzle still poses a considerable problem, and while the equity premium puzzle is indeed resolved, this is achieved at a relative risk aversion rate that is higher than what is conventionally accepted.

In Chapter 3, *The Price of Misspecification in DSGE Asset Pricing Models*, the main aim is to shed light on the estimation challenges posed by the potential misspecification in DSGE asset pricing models, and the disastrous ramifications that this might have on the estimation quality of the models' parameters. This problem of non-identification of the model's structural parameters might be why calibration exercises, rather than due diligence via econometric methods, have thus far been the norm in evaluating the performance of these models. Towards this end, a comparison of the results of three competing econometric strategies is performed on Chen (2017)'s model; the classical Indirect Inference (II) method developed by Gourieroux et al. (1993), and its two recent modifications proposed by Dridi et al. (2007); the full encompassing partial indirect inference (FII) method and the partial indirect inference (PII) method that was thoroughly discussed in Chapter 2. A fragility measure, known as the "dark matter" measure, recently developed by Chen, Dou and Kogan (2019), is used to challenge the underlying assumption of the previous chapter. Namely, that misspecification exists in the entirety of the macroeconomic dynamics. The findings indicate that ignoring misspecification has dire consequences on the estimation precision of the parameters of the model. However, the answer is not to simply calibrate all the macroeconomic parameters. Rather, the dark matter measure reveals that it is advantageous to add the Gross Domestic Product (GDP) moments to the original PII estimation. The new modified PII method then deliv-

ers comparably precise estimation results with slightly better implied asset pricing moments, and remarkably better business cycle dynamics.

Chapter 4, *Volatility Discovery in Cryptocurrency Markets*, focuses on using the long memory properties of the volatility time series of four famous cryptocurrencies (Bitcoin, Ethereum, Litecoin, and Ripple) that are traded on three prominent exchanges (Bitfinex, Bitstamp, and Kraken). The main aim is to discover whether a certain exchange is a volatility leader for the other two, and whether a certain cryptocurrency is the volatility driver for the other three considered cryptocurrencies. The theoretical approach is a discretized version of Dias, Scherrer and Papailias (2018). It extends the classic price discovery framework to include the long memory property that characterizes the common latent volatility process, which is assumed to govern the volatility on all exchanges. Empirically, the different volatility time series are individually modeled via a stochastic volatility scheme (Sandmann and Koopman, 1998), and altogether modeled using a fractionally cointegrated vector autoregressive (FCVAR) model (Johansen, 2008; Johansen and Nielsen, 2012). The latter model accounts for the long memory nature of the latent volatility processes. The FCVAR estimation results are then used to calculate the volatility information share of each exchange for each cryptocurrency and, in a later step, for each cryptocurrency using the leading exchange market. In a similar fashion to the price discovery methodology, the Hasbrouck (1995) information share and the modified information share of Lien and Shrestha (2009) are utilized for this purpose. Our analyses indicate that the market with the highest trading volume share is not necessarily the market where volatility discovery takes place. Yet, we interpret our findings for all cryptocurrencies other than Bitcoin with caution, as they are relatively newer. Therefore, their sampled data is not long enough to ensure the estimation precision of the FCVAR model.

Finally, Chapter 5 concludes this dissertation by summarizing the findings put forth by the three essays comprising the entire work. It can thus be thought of as a résumé of the contributions of this dissertation to the financial econometrics field.

Chapter 2

Empirical Asset Pricing in a DSGE Framework:

Reconciling Calibration and Econometrics using Partial Indirect Inference[*]

2.1 Introduction

Embedding preference-based asset pricing within a dynamic stochastic general equilibrium (DSGE) framework holds the promise to resolve the prominent puzzles of financial economics by using a pricing kernel that is consistent with macroeconomic processes. However, the apparent empirical success of such approaches is predomi-

[*]This chapter is based on Grammig, Schnaitmann and Elshiaty (2020) and is available at `https://ssrn.com/abstract=3648085`. We are grateful for the comments given by the participants at the Society for Financial Econometrics annual conference, Cambridge 2022, the European Finance Association's virtual meeting from Helsinki, Finland 2020, the Econometric Society's virtual World congress 2020 from Bocconi University, the European Economic Association's virtual meeting, 2020 and the International Conference on Computational and Financial Econometrics in 2018 at the University of Pisa for their helpful feedback. In particular, we thank Bertille Antoine, Giorgio Calzolari, Roxana Halbleib, Alastair Hall, Frank Kleibergen, Tim Landvoigt, Olivier Scaillet and Jantje Sönksen for their insightful comments and suggestions.

nantly based on calibration methods, which Hansen and Heckman (1996) have criticized for lacking the rigor of econometric analysis.

This study aims at delivering a critical assessment of the DSGE asset pricing approach, and to return the empirical analysis of these models to the econometrics fold. For that purpose, we focus on the most recent exponent proposed by Chen (2017). Applying the partial indirect inference method (PII) introduced by Dridi et al. (2007), we acknowledge that parts of the model (the production technology) are misspecified, while other parts (the pricing kernel) have the claim of capturing financial economic reality. Adapting the PII philosophy to the present problem, we use binding functions that facilitate the consistent estimation of some structural model parameters of interest, while treating others as nuisance parameters. The latter do not truly capture economic reality, but are necessary to generate model-implied data within the simulation-based estimation procedure.

The class of DSGE models considered here connects asset prices to an exogenous technology process and an endogenously generated consumption process. In this model economy, households try to smooth their consumption stream in response to technology shocks, and the fluctuations in consumption determine asset prices. Capital adjustment costs induce that the supply of new capital via household investment and consumption decisions is not perfectly flexible. Jermann (1998) pioneers this literature by considering a real business cycle (RBC) model that explains both business cycle moments and asset pricing facts. He introduces linear habit persistence, which creates volatility in the pricing kernel without the need for an unreasonably high relative risk aversion. While the model-implied time-varying risk premium resolves the equity premium puzzle, the linear habit specification also generates an implausibly high volatility of the risk-free rate. Chen (2017) accounts for this drawback by accounting for nonlinear habit preferences as in Campbell and Cochrane

(1999), and convex capital adjustment costs. The empirical validation of this most recent exponent of DSGE asset pricing models is performed by means of a calibration study. The results are interpreted such that the calibrated model resolves many empirical asset pricing puzzles.

Quite different to such a calibration study, econometric analysis challenges a model's specification, instead of seeking confirmatory evidence. The model parameters are estimated using empirical data, which entails a careful discussion of identifying restrictions. The key questions are whether these restrictions facilitate consistent parameter estimation, and how informative the available data are to accomplish that task. The analysis is deeply concerned with parameter estimation uncertainty, which translates into confidence intervals for the parameters and model-implied indicators of interest. These are all non-issues for calibration studies.

However, the econometric analysis of DSGE asset pricing models is a challenging task. Proponents of calibration may even argue that such highly stylized models are not suitable for econometric analysis in the first place. Notwithstanding, there exists a large body of literature that deals with the estimation of DSGE models (not necessarily concerned with asset pricing). Early studies rely on likelihood methods[1], although the complex model structures often render the likelihood function intractable. A more fundamental caveat concerns the notion of "true" model parameters that one seeks to estimate by maximum likelihood. Parts of a DSGE asset pricing model are openly misspecified; as put by Dridi et al. (2007), they represent a "caricature of reality". As such, it is unclear what an asymptotically efficient estimation achieves in the first place. Bayesian methods are regularly used for the estimation of DSGE models[2], but they lack the intuitive appeal of frequen-

[1]See, e.g. Altug (1989), Leeper and Sims (1994), McGrattan, Rogerson and Wright (1997) and Ireland (2004).

[2]An and Schorfheide (2007) and Fernández-Villaverde, Rubio-Ramírez and Schorfheide (2016) provide reviews of the Bayesian DSGE model estimation approach.

tist approaches, which are capable of directly linking the structural parameters to the DSGE model's equilibrium conditions, as noted by Fernández-Villaverde (2010). Moment matching strategies (generalized or simulated method of moments) are an alternative to likelihood-based methods[3], but the aforementioned caveat applies, if one doubts that data generated from the DSGE model endowed with the "true" parameters corresponds to the real world data generating process.

The present study pursues a matching approach that acknowledges that parts of the DSGE asset pricing model are evidently misspecified, while others claim to reflect economic reality. Specifically, we implement, for the first time in the context of DSGE asset pricing, the partial indirect inference philosophy proposed by Dridi et al. (2007) and focus our estimation efforts on those parameters and parts of the DSGE asset pricing model that are assumed to reflect economic reality: its asset pricing implications. We thereby build a bridge between the data generated by the DSGE asset pricing model and the data that we observe in the real world. To the best of our knowledge, this is the first study that provides a comprehensive application of partial indirect inference to econometrically analyze a DSGE asset pricing model. We make the general assumptions of Dridi et al. (2007) explicit, and derive the limiting distribution implied by the instrumental model that we employ for our study, which facilitates statistical inference about the estimated parameters. Applying the PII method to estimate the structural parameters of interest, we provide confidence

[3]Christiano and Eichenbaum (1992) and Burnside, Eichenbaum and Rebelo (1993) pioneer the literature that uses the generalized method of moments to estimate the full vector of structural parameters of DSGE models with analytically tractable unconditional moments. Regarding more complex models, for which unconditional moments cannot be provided in closed form, the literature resorts to matching the impulse response function parameters from Vector Autoregressions (VARs) generated from both simulated data and empirical data, see for example Rotemberg and Woodford (1997), Christiano, Eichenbaum and Evans (2005) and Altig, Christiano, Eichenbaum and Linde (2011). Ruge-Murcia (2007) and Ruge-Murcia (2012) match simulated moments à la Duffie and Singleton (1993) and McFadden (1989), while Ruge-Murcia (2014) uses indirect inference estimation introduced by Smith (1993) and Gourieroux et al. (1993) to match the parameters of a non-linear VAR.

intervals for these parameters as well as model-implied key economic indicators, which rely on the derived limiting distribution.

Our econometric analysis shows that the empirical performance of the model proposed by Chen (2017) is not unfavorable, but the claim that the DSGE approach can resolve the notorious asset pricing puzzles should be viewed with caution. On the upside, the model-implied equity premium and Sharpe ratio as well as the business cycle and consumption growth moments are economically plausible, also when taking estimation uncertainty into consideration. Moreover, the macroeconomic moments are largely unaffected by the choice of the preference parameters and are mainly impacted by a sensible calibration choice. However, there are two notable caveats. First, the economically plausible equity premium and Sharpe ratio are not achieved by a level of risk aversion conventionally thought to be plausible.[4] Provided that one is willing to accept a steady-state relative risk aversion coefficient of about 20, it can be claimed that the DSGE asset pricing model with nonlinear habit persistence may help to resolve the equity premium puzzle. Second, while the estimated model does not imply an excessively volatile risk-free rate, which is often encountered in production-based models (Jermann, 1998), it fails to match the empirical level of the risk-free rate. The elevated level of the model-implied risk-free rate is associated with a time preference point estimate above unity. Accordingly, the risk-free rate puzzle remains unresolved.

The remainder of the paper is organized as follows: In Section 2.2.1, we present the anatomy of the DSGE asset pricing model to be analyzed, and we highlight its key features in Section 2.2.2. Calibration results are then presented in Section 2.2.3. Section 2.3.1 outlines the econometric methodology. We use a brief exposition in the main text and explain methodological details in the appendix. We elaborate

[4]This is is a well-documented feature of partial equilibrium habit-based asset pricing models (see, e.g. Campbell and Cochrane (1999), Cochrane (2016), Cochrane (2017)).

on the specific assumptions used for our instrumental model choice in Appendix 2.A, and we derive the asymptotic distribution of the PII estimator in Appendix 2.B. Section 2.3.2 motivates the parameters' separation into structural parameters of interest and nuisance parameters. Section 2.4 presents the estimation results as well as a critical assessment of the empirical performance of the estimated model. Section 2.5 concludes.

2.2 Asset pricing in a DSGE framework

In this section, we elaborate on the DSGE asset pricing model proposed by Chen (2017). This model is built on a standard RBC model that is augmented by nonlinear habit preferences in the spirit of Campbell and Cochrane (1999) and by convex capital adjustment costs. Section 2.2.1 gives details about the model specification. We focus on the model's asset pricing features in Section 2.2.2. More specifically, we investigate the model-implied risk-free rate and Sharpe ratio. In Section 2.2.3, we present calibration results of the model similar to those in Chen (2017).

2.2.1 Anatomy of the DSGE asset pricing model

The representative household chooses consumption and hours of labor such that the following expected lifetime utility function is maximized.

$$\mathbb{E}_0 \left[\sum_{t=0}^{\infty} \beta^t \frac{(C_t - H_t)^{1-\gamma} - 1}{1-\gamma} \right], \tag{2.2.1}$$

where C_t and H_t are consumption and habit in time t, respectively, while β and γ represent the time preference and the utility curvature parameters. Chen (2017) assumes that there is no leisure, and that, in equilibrium, $N_t = 1$, i.e. the household is endowed with a single unit of labor. Following Campbell and Cochrane (1999),

surplus consumption, S_t, determines the evolution of habit, such that $S_t \equiv \frac{C_t - H_t}{C_t}$. Surplus consumption follows an autoregressive process

$$s_{t+1} = (1 - \rho_s)\bar{s} + \rho_s s_t + \lambda(\Delta c_{t+1} - \mu), \tag{2.2.2}$$

where $s_t = \ln S_t$ indicates the log of the variable, ρ_s is an autoregressive parameter, μ is the steady-state growth rate of technology and λ is a constant fixed to $\lambda = 1/\bar{S} - 1$ as in Campbell and Cochrane (1999).

The utility function in Equation (2.2.1) is a power utility augmented with non-linear external habit preferences. This specification ensures that the model has a time-varying risk premium given by $rra_t = \gamma / S_t$. Markets are complete and the stochastic discount factor (SDF) of the household is given by

$$M_{t,t+1} = \beta \left(\frac{C_{t+1}}{C_t} \frac{S_{t+1}}{S_t} \right)^{-\gamma}. \tag{2.2.3}$$

On the production side, the representative firm produces output, Y_t, according to a constant returns to scale production function $Y_t = Z_t K_t^{\alpha} (X_t N_t)^{1-\alpha}$, where Z_t, K_t and N_t refer to the level of production technology, capital and labor available at time t, respectively. X_t is the deterministic long-run growth component of productivity which evolves as $x_{t+1} = x_t + \mu$. As in a standard RBC model, the log of the production technology evolves in an autoregressive manner

$$z_{t+1} = \rho_z z_t + \sigma_z \varepsilon_{z,t+1}, \tag{2.2.4}$$

where $\varepsilon_{z,t+1} \sim \mathcal{N}(0,1)$ i.i.d. The technology shock is a homoskedastic shock, and it constitutes the only source of uncertainty in the model. Capital accumulation in this economy evolves according to

$$K_{t+1} = I_t + (1-\delta)K_t, \tag{2.2.5}$$

where I_t refers to investment at time t, and δ refers to the capital depreciation rate. Moreover, the representative firm faces convex capital adjustment costs $\Phi(I_t, K_t) = \frac{\phi}{2}\left(\frac{I_t}{K_t} - (\mathrm{e}^{\mu} - 1 + \delta)\right)^2 K_t$. These adjustment costs become zero in the steady state. The firm seeks to maximize the expected discounted value of future dividends, i.e.

$$\max_{\{I_t, K_{t+1}, N_t\}} \mathbb{E}_0\Big[\sum_{t=0}^{\infty} M_{0,t}\left\{Z_t K_t^{\alpha}(X_t N_t)^{1-\alpha} - W_t N_t - \Phi(I_t, K_t) - I_t\right\}\Big], \tag{2.2.6}$$

subject to capital accumulation in Equation (2.2.5).

In equilibrium, both the labor market and the goods market clear which gives rise to the equilibrium wage and the budget constraint, respectively

$$W_t = (1-\alpha) Z_t X_t K_t^{\alpha} (X_t N_t)^{-\alpha}, \tag{2.2.7}$$

$$C_t + I_t = Z_t K_t^{\alpha}(X_t N_t)^{1-\alpha} - \Phi(I_t, K_t), \tag{2.2.8}$$

as well as the asset pricing equation for investment return, $R^I_{t,t+1}$.

$$\mathbb{E}_t\left[M_{t,t+1} R^I_{t,t+1}\right] = 1, \tag{2.2.9}$$

with

$$R^I_{t,t+1} = \frac{\alpha \frac{Y_{t+1}}{K_{t+1}} + \left(1 + \phi\left(\frac{I_{t+1}}{K_{t+1}}\right)\right)(1-\delta) + \frac{\phi}{2}\left(\frac{I_{t+1}}{K_{t+1}}\right)^2}{1 + \phi\left(\frac{I_t}{K_t}\right)}, \tag{2.2.10}$$

where $\alpha\frac{Y_{t+1}}{K_{t+1}}$ is the marginal product of capital, $\frac{I_{t+1}}{K_{t+1}}$ is the investment rate, and ϕ is the quadratic adjustment cost parameter.

2.2.2 Features of the model

In the following, we discuss the main features of this model that resolve the asset pricing puzzles. We are primarily concerned with the risk-free rate puzzle and the equity premium puzzle.

Empirical data show that the firm or equity return volatility, $\sigma(R^I_{t,t+1})$, is 15% while the volatility of the investment return rate, $\frac{I_{t+1}}{K_{t+1}}$, is only 2% annually. Thus, the volatility of the investment return will not reconcile, see Equation (2.2.10), unless the adjustment cost parameter, ϕ, is calibrated at a very high value. In fact, Chen sets $\phi = 100$. This implies that productivity shocks are absorbed by asset prices rather than investment. This fact is also demonstrated in Jermann (1998), Kogan (2004), Jermann (2010), and Kogan and Papanikolaou (2012). Thus, high adjustment costs discourage volatile investments. Consequently, market clearing indicates that productivity shocks will alternatively lead to volatile consumption which defies consumption smoothing preferences by households as indicated in empirical data. This dilemma, in turn, is solved by incurring low elasticity of intertemporal substitution EIS $= \frac{\partial \mathbb{E}_t[\Delta c_{t+1}]}{\partial r^f_{t+1}} = \frac{\bar{s}}{\gamma} \approx 0.035$.

However, low EIS propagates the problem to a different part in the model, as it implies a more volatile risk-free rate relative to empirical data (see the caveat in Jermann, 1998), which is precisely the risk-free rate puzzle. Persistent external habit preferences in this model smooth risk-free rate volatility via a precautionary savings effects. The log-normal approximation of the risk-free rate is given by

$$r^f_{t+1} \approx -\log\beta + \frac{\gamma}{\bar{S}}\mathbb{E}_t[\Delta c_{t+1}] - \gamma(1-\rho_s)(s_t - \bar{s}) - \frac{1}{2}\frac{\gamma^2}{\bar{S}^2}\mathrm{Var}_t[\Delta c_{t+1}], \qquad (2.2.11)$$

where $\overline{rra} = \gamma/\bar{S}$ gives the steady-state relative risk aversion of the representative investor. Here, intertemporal substitution, the second to last term from the r.h.s of the above equation, implies that in bad times, investors want to borrow from the future by selling the risk-free asset which, in turn, pushes r^f_{t+1} up. On the other hand, precautionary savings, the last term on the r.h.s, work in the opposite direction as they entail that, in a volatile economy, investors are more reluctant to sell the risk-free asset. As a result, given high persistence of habit, i.e. $\rho_s = 0.98$, a relatively smooth risk-free rate can coexist together with low EIS.

In this model, consumption volatility risk is endogenously generated. As the model is driven by an homoskedastic productivity shock, the heteroskedasticity arises from the nonlinearity in the law of motions of the model. This nonlinearity leads to counter-cyclical consumption volatility, as consumption is more sensitive to shocks in bad times. The precautionary savings channel is summarized as follows: a negative shock to wealth strengthens the motive to save which leads to an increase in savings and a decrease in consumption. The opposite effect occurs for a positive wealth shock. Consequently, this uncertainty in the need for precautionary savings causes consumption volatility. Chen (2017) further shows that external habit amplifies the effect of this channel.

Consumption volatility risk in this model plays a crucial role in valuing assets as the asset pricing dynamics are derived from the time-varying risk premium which, in turn, is driven by the time-varying consumption volatility. From the model, the conditional maximum Sharpe ratio is derived via a log-normal approximation of the SDF as follows

$$\max_{\{\text{all assets}\}} \left[\frac{\mathbb{E}_t(R_{t+1} - R^f_{t+1})}{\sigma_t(R_{t+1})} \right] \approx \frac{\gamma}{\bar{S}} \sigma_t(\Delta c_{t+1}). \tag{2.2.12}$$

Equation (2.2.12) shows that the steady-state relative risk aversion, $\overline{rra}$, amplifies the effect of consumption volatility. Thus, a small increase in the latter can result in a large increase in risk premium.

2.2.3 Calibration

In this section, we replicate the results of Chen (2017). Towards this end, we calibrate the model and calculate the asset pricing implications and the business cycle moments. The moments that are targeted and their resulting parameter values are comparable to those reported in Campbell and Cochrane (1999) and Kaltenbrunner and Lochstoer (2010). The parameter values used to simulate the model are provided in Table 2.1. The technology parameters are calibrated to values common in the RBC literature: The capital share of GDP, α, is matched to the empirical target of this ratio and set to 0.35. The depreciation rate is guided by the mean investment rate and chosen to be $\delta = 0.016$. The total factor productivity (TFP) parameters are chosen as follows: long-run productivity growth $\mu = 0.0045$ is given by the mean output growth, the volatility of TFP is matched to the volatility of HP-filtered GDP, i.e. $\sigma_z = 0.012$, whereas the persistence of TFP is set to the persistence of the output-to-capital ratio, i.e. $\rho_z = 0.98$. The quadratic capital adjustment cost is chosen to be $\phi = 100$ comparable to Guvenen (2009) and Kaltenbrunner and Lochstoer (2010). This choice implies that productivity shocks are absorbed by asset prices and leads to around 0.11% mean adjustment costs in relation to output, as shown in Table 2.2.

The subjective time-preference rate of the representative agent, β, is chosen to match the mean return on the 90-day Treasury bill and is given by 0.995. Relative risk aversion is captured by the ratio of the utility curvature parameter, γ, to the surplus consumption S_t, i.e. $rra_t = \gamma/S_t$, and is time-varying. In the steady-

Table 2.1: Calibrated values

Parameter		Value	Target Moment	Data
Preferences				
β	Time Preference	0.995	90-Day T-bill Return (%)	0.17
ρ_s	Persistence of Surplus Consumption	0.980		
$\bar{S}$	Steady-State Surplus Consumption	0.070		
γ	Utility Curvature	2.00	for comparison with Campbell-Cochrane	
$\overline{rra} = \gamma/\bar{S}$	Steady-State Relative Risk Aversion	28.57		
Long-run Technology				
α	Capital Share	0.35	Mean Output/Capital	0.143
δ	Depreciation Rate	0.016	Mean Investment Rate	0.025
μ	TFP Growth	0.0045	Mean Output Growth (%)	0.48
Cyclical Technology				
σ_z	Volatility of TFP	0.012	Vol HP-filtered GDP (%)	1.72
ρ_z	Persistence of TFP	0.980	Persistence of Output/Capital	0.997
ϕ	Adjustment Cost	100.00		

Note: This table replicates Table 1 in Chen (2017). It reports the parameter values obtained from matching empirical target moments. The time series used span a period from 1948 to 2012 on quarterly frequency from US data.

state, risk aversion is given by $\overline{rra} = \gamma/\bar{S}$, and we cannot uniquely identify the two associated parameters. Here, the utility curvature parameter, γ, is set to 2 without targeting a specific moment, and the steady-state surplus consumption is chosen to be $\bar{S} = 0.07$ as in Campbell and Cochrane (1999).[5] Hence, the steady state relative risk aversion is calibrated to $\overline{rra} = 28.57$. Lastly, the persistence of surplus consumption, ρ_s, is set similar to Chen (2017) at 0.98. The value is guided by the persistence of Tobin's Q and the first autocorrelation of the price-dividend ratio which are reported in his paper.

We simulate the model 500 times over a time series length of $T = 260$, i.e., the length is equivalent to the number of quarters in our observed sample. The

[5]In Campbell and Cochrane (1999) a closed form solution for the steady-state surplus consumption exists and risk aversion is only captured in γ. Here, no closed form solution exist as the system is impacted by endogenous consumption volatility risk.

calibration results, as well as their counterparts from Chen (2017), are provided in Table 2.2. For the business cycle moments, the results implied by the simulations and the observed data, are quite similar, for both pairs of moments, with the exception of the mean output to capital ratio.[6] As for the consumption growth moments, we find that the mean and the standard deviation of log consumption growth, implied by the model, match the empirical moments well.

For the asset pricing moments, the mean quarterly Sharpe ratio of the CRSP index is given by 0.22 which is equivalent to the sample average over the ensembles. The observed quarterly equity premium is equal to 1.82%, whereas the ensemble mean is 2.46%. Furthermore, the volatility of the excess return is sensible in the simulations. We use the 90-day T-bill return as a proxy of the risk-free rate. The average quarterly risk-free rate is given by 0.17% in the data, whereas it is considerably higher in our simulations and given by 0.65%. The volatility of the model-implied risk-free rate at 0.74% is not excessively volatile and is in line with the observed counterpart at 0.90%. We can, therefore, conclude that the trade-off between the intertemporal substitution and the precautionary savings channel balances the volatility of risk-free rate well. Yet, the level of the risk-free rate is not compatible with our empirical data. The model is, thus, affected by the risk-free rate puzzle described in Weil (1989). Chen (2017) reports a lower level for the simulated risk-free rate. However, this value cannot be replicated in neither his nor our code. Overall, we conclude from our simulations and that of Chen's (2017) that the model fares fairly well over the business cycle dimension, the consumption growth moments and for the equity premium, though it is not capable of matching the level of the empirical risk-free rate.

[6]This value is reported to be perfectly matched in Table 1 in Chen (2017), as he is reporting the empirical moment twice. We provide the corrected values in our Table 2.2.

Table 2.2: Calibration results

Moment		**Calibration**	**Chen (2017)**
	Data	**Simulations**	**Simulations**
Asset Prices			
90-Day T-bill Return (%)	0.17	0.65	0.35
Vol of R^f (%)	0.90	0.74	0.52
Persistence of Tobin's Q		0.96	0.96
Mean Sharpe Ratio of CRSP Index	0.22	0.23	0.16
Equity Premium R^e (%)	1.82	2.46	1.72
Vol of R^e (%)	8.24	10.70	11.04
Business Cycle			
Mean Output/Capital	0.143	0.089	0.142
Mean Investment Rate	0.025	0.021	0.021
Mean Output Growth (%)	0.48	0.45	0.45
Vol HP-filtered GDP (%)	1.72	1.52	1.53
Persistence of Output/Capital	0.997	0.986	0.983
Relative Volatility of Consumption Growth	0.52	0.51	0.46
Mean Adj Cost / Output (%)		0.11	0.11
Consumption Growth			
Mean of ln of Consumption Growth (%)	0.47	0.45	0.46
Std of ln of Consumption Growth (%)	0.52	0.61	0.56

Note: This table shows simulated moments implied by the calibrated values given in Table 2.1. The calibrated structural parameters of interest are given by $\beta = 0.995$ and $\overline{rra} = 28.57$. The column labeled Chen (2017) contains the published values in his Tables 1, 2 and Table 3. The data used is taken from the online appendix of Chen (2017). It is described in more details in Appendix 2.D.

The previous calibration exercise seeks confirmatory evidence for the model by matching model simulated moments to those observed empirically using economically plausible parameter values. Yet, what if economically implausible parameter values are able to achieve such a match? From a pure calibration point of view, those will be deemed acceptable, though economically inconceivable. This is where econometric analysis goes beyond the scope of calibration. With the aid of estimated

confidence intervals, we can assess the validity of the entire range of possible parameter values that are compatible with empirical data. In the next section, we lay out the partial indirect inference framework which we use to estimate the structural parameters of interest.

2.3 Returning to the econometrics fold

The indirect inference estimation philosophy is introduced and refined by Smith (1993), Gourieroux et al. (1993) and Gallant and Tauchen (1996). This approach is used in the presence of a nonlinear analytically intractable structural model, which implies that the parameters of such a model (known as the structural parameters), ξ, cannot be directly estimated. The underlying idea is to identify a binding function, $\theta(\xi)$, which relates the structural parameters ξ to the instrumental parameters θ which, in turn, are estimated from an instrumental model that is easily estimated. Indirect inference implies that two sets of instrumental parameters are estimated from the instrumental model; one using the simulated data from the structural model, and the other from empirical data. The structural parameters are, then, estimated such that the minimum of a quadratic loss function calculated between the two sets of instrumental parameters is achieved.

2.3.1 The partial indirect inference approach

Intuition and motivation

Even though the DSGE asset pricing model accommodates both asset pricing and macroeconomic dynamics, it cannot realistically represent all of the complexities of the economy. In spite of this, its stochastic discount factor may be able to price assets and convey some reasonable economic insights. As a result of this intrinsic

misspecification, the empirical data generating process and the simulated data from the structural model do not coincide. This renders any indirect estimation strategy in which all structural parameters are estimated based on a correctly specified structural model, infeasible.

Alternatively, Dridi et al. (2007) proposes an extension to the indirect inference theory to accommodate misspecified structural models. This approach is called partial indirect inference, and it focuses on the consistent estimation of only a subset of the structural parameters; those that are believed not to be misspecified, while the rest of the parameters remain calibrated. In this manner, calibration can be viewed as econometrics for misspecified models. In their terminology, we split the parameters $\xi = (\xi_1, \xi_2)^\top$, such that the only parameters of interest for the estimation process are ξ_1, while ξ_2 refers to nuisance parameters that will remain calibrated for the entire exercise. The aim is to obtain a consistent estimator of the true unknown value ξ_1^0 when solving the sample or simulation-based counterpart of the binding function

$$\theta^0 = \tilde{\theta}^0 \left(\xi_1^0, \xi_2^*\right) \tag{2.3.1}$$

with respect to ξ_1. In this context, ξ_2^* are the pseudo-true values of the nuisance parameters ξ_2. Equation (2.3.1) constitutes a necessary condition which implies that the structural model fully encompasses the instrumental one in the presence of misspecification. Thus, if we choose a convenient instrumental model, Equation (2.3.1) characterizes the true unknown parameters ξ_1^0 given the misspecification in ξ_2.

If, however, only a subset of the encompassing conditions in (2.3.1) are fulfilled, we are in a partial encompassing case. Hence, the identification of the structural parameters ξ is incomplete, but we achieve consistent estimation of the structural parameters of interest ξ_1, if the under-identification is only about a subset of the

pseudo-parameters ξ_2 that do not appear in the binding function. In this case, the necessary condition becomes

$$\theta_1^0 = \tilde{\theta}_1^0 \left(\xi_1^0, \xi_{21}^* \right). \tag{2.3.2}$$

This means that the structural model's nuisance parameters are now $\xi_2 = \left(\xi_{21}, \bar{\xi}_{22} \right)^\top$, where $\bar{\xi}_{22}$ do not interfere with the binding function, and thus are allowed to escape the encompassing condition (2.3.2). These parameters, in turn, remain calibrated during the estimation process (hence the usage of the over bar), while their counterparts, ξ_{21}, become part of the estimation process, i.e. they are identified from the instrumental parameters, θ_1, and are thus necessary for the consistent estimation of ξ_1.

PII estimator

In this subsection, we detail the construction of an indirect estimation strategy for the structural parameters of interest ξ_1. We denote the empirical time series as $\{y_t\}_{t=1}^T$, and the model-implied series obtained from simulations by $\{\tilde{y}_s(\xi_1, z_0)\}_{s=1}^S$, where z_0 refers to the initial value of the state variable.

The crucial step is to carefully choose an instrumental model which is capable of capturing the model-implied financial time series, and has a tractable estimation function for its parameters, i.e. the instrumental parameters. Similar to the recommendations of Dridi et al. (2007), we advocate the use of well-chosen moment restrictions that reflect the asset pricing implications of the DSGE asset pricing model rather than using a full parametric model as an instrumental model. We,

first, describe the estimation of the instrumental parameters based on empirical data.[7] The set of k moment restrictions is given by

$$\mathbb{E}\left[u_{1,t}\left(\{y_t\}_{t-l}^{t}, \theta_1^0\right)\right] = 0. \tag{2.3.3}$$

Moreover, the number of moment restrictions is at least as large as the number of structural parameters, i.e. $k = \dim \theta_1 \ \geq \ p_1 + p_{21} = \dim \xi_1 + \ \dim \xi_{21}$. To estimate the instrumental parameters θ_1, we maximize a GMM-type criterion function given by

$$\min_{\{\theta_1 \in \Theta_1\}} Q_{1,T}\left(\{y_t\}_{t=1}^{T}, \theta_1\right), \tag{2.3.4}$$

$$\text{where} \quad Q_{1,T}\left(\{y_t\}_{t=1}^{T}, \theta_1\right) = \frac{1}{2}\, g_{1,T}\left(\{y_t\}_{t=1}^{T}, \theta_1\right)^{\top} \cdot \widehat{W}_{1,T} \cdot g_{1,T}\left(\{y_t\}_{t=1}^{T}, \theta_1\right), \tag{2.3.5}$$

$$g_{1,T}\left(\{y_t\}_{t=1}^{T}, \theta_1\right) = \frac{1}{T}\sum_{t=1}^{T} u_{1,t}\left(\{y_t\}_{t-l}^{t}, \theta_1\right), \tag{2.3.6}$$

with $\widehat{W}_{1,T} \xrightarrow{a.s.} W_1$, a positive semi-definite weighting matrix.

$$\hat{\theta}_{1,T} = \underset{\{\theta_1 \in \Theta_1\}}{\operatorname{argmin}} \ Q_{1,T}\left(\{y_t\}_{t=1}^{T}, \theta_1\right)$$

is a consistent estimator of θ_1^0.

As the simulated data stems from a misspecified simulator, its probability limit is not the same as that of the observed data. For the consistency of the instrumental parameter estimates associated with the simulated time series, we impose an identification assumption for the simulated time series given by

$$\mathbb{E}^{*}\left[u_{1,t}\left(\{\tilde{y}_t^s(\xi)\}_{t-l}^{t}, \tilde{\theta}_1^0(\xi_1^0, \xi_{21}^*)\right)\right] = 0.$$

[7] We use the notation of the partial encompassing case in Dridi et al. (2007). All quantities are indexed by a 1. More elaboration is given in Section 3.2.3 in Chapter 3.

Under appropriate GMM assumptions given in Appendix 2.A,

$$\tilde{\theta}^s_{1,T}(\xi_1, \xi_{21}, \bar{\xi}_{22}) = \underset{\{\theta_1 \in \Theta_1\}}{\operatorname{argmin}} \; Q_{1,T}\left(\{\tilde{y}^s_T(\xi)\}^T_{t=1}, \theta^s_1\right) \tag{2.3.7}$$

and $\tilde{\theta}^s_{1,T}(\xi_1, \xi_{21}, \bar{\xi}_{22}) = \frac{1}{S}\sum_{s=1}^{S} \tilde{\theta}^s_{1,T}(\xi_1, \xi_{21}, \bar{\xi}_{22})$ is a consistent estimator of $\tilde{\theta}^0_1\left(\xi^0_1, \xi^*_{21}\right)$.

For the indirect estimator of the structural parameters, we require partial encompassing given by

$$\theta^0_1 = \tilde{\theta}^0_1(\xi^0_1, \xi^*_{21}), \tag{2.3.8}$$

where θ^0_1 is the probability limit of the instrumental parameters associated with the observed data and $\tilde{\theta}^0_1(\xi^0_1, \xi^*_{21})$ is the probability limit for the simulated time series. Equation (2.3.8) is the partial encompassing condition in Dridi et al. (2007) and the necessary condition in Equation (2.3.2) needed in the partial encompassing case. We refer to it as the partial encompassing null hypothesis $H^{(1)}_0\left(\bar{\xi}_{22}\right)$.

The partial indirect inference (PII) estimator is defined as

$$\begin{aligned}\begin{pmatrix} \hat{\xi}_{1,TS}(\bar{\xi}_{22}) \\ \hat{\xi}_{21,TS}(\bar{\xi}_{22}) \end{pmatrix} = \underset{\{(\xi_1,\xi_{21})\in \Xi_1 \times \Xi_{21}\}}{\operatorname{argmin}} & \left[\hat{\theta}_{1,T} - \frac{1}{S}\sum_{s=1}^{S} \tilde{\theta}^s_{1,T}(\xi_1, \xi_{21}, \bar{\xi}_{22})\right]^\top \cdot \widehat{\Omega}_{1,T} \\ & \cdot \left[\hat{\theta}_{1,T} - \frac{1}{S}\sum_{s=1}^{S} \tilde{\theta}^s_{1,T}(\xi_1, \xi_{21}, \bar{\xi}_{22})\right],\end{aligned} \tag{2.3.9}$$

$$\hat{\theta}_{1,T} = \underset{\{\theta_1 \in \Theta_1\}}{\operatorname{argmin}} \; Q_{1,T}\left(\{y_t\}^T_{t=1}, \theta_1\right), \tag{2.3.10}$$

$$\tilde{\theta}^s_{1,T}\left(\xi_1, \xi_{21}, \bar{\xi}_{22}\right) = \underset{\{\theta_1 \in \Theta_1\}}{\operatorname{argmin}} \; Q_{1,T}\left(\{\tilde{y}^s_T(\xi)\}^T_{t=1}, \theta^s_1\right), \tag{2.3.11}$$

and $\widehat{\Omega}_{1,T}$ is a positive definite weighting matrix that converges almost surely to the non-stochastic positive definite matrix Ω_1.

Given that $\hat{\xi}_{1,TS}\left(\bar{\xi}_{22}\right)$ is a consistent estimator of ξ_1^0, the structural parameters estimates of ξ_1 and ξ_{21} follow an asymptotic normal distribution

$$\sqrt{T}\begin{pmatrix}\hat{\xi}_{1,TS}\left(\bar{\xi}_{22}\right)-\xi_1^0\\ \hat{\xi}_{21,TS}\left(\bar{\xi}_{22}\right)-\xi_{21}^*\end{pmatrix}\xrightarrow{d}\mathcal{N}\left(0,\Sigma\left(S,\Omega_1\right)\right), \tag{2.3.12}$$

where the asymptotic covariance $\Sigma\left(S,\Omega_1\right)$ is given in Equation (2.B.1) in Appendix 2.B. This asymptotic covariance matrix can be used to construct confidence intervals of our parameters of interest. Using this technique, we can return calibration to the econometrics fold.

The underlying assumptions that ensure the consistency of the PII estimator under the partial encompassing case are discussed in Appendix 2.A and 2.B. We refer the reader to Dridi et al. (2007), as well as Smith (1993), Gourieroux et al. (1993) and Gallant and Tauchen (1996) for the assumptions governing the consistency of indirect inference estimation in general. A brief summary of how they are different than the assumptions needed for PII is provided in Appendix 3.A.

2.3.2 Specification of the instrumental model

The PII estimation methodology is adapted to the structural model at hand; the DSGE asset pricing model proposed by Chen (2017). Here, we conceive the asset pricing implications of the model, the implied SDF, to be the economic reality that we want to capture. Hence, the investor's preference parameters are of relevance, i.e. $\xi_1=(\beta,\overline{rra})^\top$ where $\overline{rra}=\gamma/\bar{S}$, while the remaining parameters are understood as caricatural aspects of the model perceived as the nuisance parameters, ξ_2. We investigate which informational content the empirical data has on the implied timing and risk preference. As the size of the relative risk aversion and the time preference rate carry economic meaning, this is crucial for the empirical assessment of the

model. These parameters play a key role in consumption-preference based asset pricing which determine the model-implied equilibrium risk-free rate and the market equity premium. If the parameter estimates are outside the range of economically plausible values, this is empirical evidence against the structural model. Moreover, if the estimated confidence intervals of the parameters include a wide range of plausible and implausible values, then the observed data are not informative for assessing the empirical performance of the model.

The structural nuisance parameters, ξ_2, are needed to specify a complete model, but they do not convey economic reality. The bridge between the theoretical model and the economic reality is fragile, hence, we rely on calibration for the macroeconomic part of the model. Section 3.2.3 elaborates on the reasoning behind the fragility of the macroeconomic dynamics in the DSGE asset pricing model. The nuisance parameters are thus given by $\bar{\xi}_2 = (\rho_s, \alpha, \delta, \phi, \mu, \rho_z, \sigma_z)^\top$ and are calibrated to the values specified in Section 2.2.3, i.e. $\bar{\xi}_2 = (0.98, 0.35, 0.016, 100, 0.0045, 0.98, 0.012)^\top$.

The choice of moment conditions for the instrumental parameters is guided by the model-implied equations for the risk-free rate and the conditional Sharpe ratio which are given in Equations (2.2.11) and (2.2.12). The dynamics of the risk-free rate is affected by the time preference parameter, β, as well as the intertemporal substitution and the precautionary savings motive. These, in turn, are driven by the steady state relative risk aversion $\overline{rra} = \gamma/\bar{S}$. In addition, the conditional Sharpe ratio is influenced by the steady state relative risk aversion. Thus, we make use of the unconditional time-series averages of the risk-free rate $\mathbb{E}(R_t^f) = \mu_{R_f}$. Moreover, we would like to use the Sharpe ratio given by $\frac{\mathbb{E}(R_{m,t}-R_t^f)}{\sigma(R_{m,t}-R_t^f)}$ to identify the risk aversion parameter. However, as no Law of Iterated Expectations exists for ratios of moments, the conditional Sharpe ratio cannot be transformed into an unconditional Sharpe ratio readily. Moreover, it is also unclear whether the ratio

of the empirical equivalents of the expectation and standard deviation converges in probability to the population equivalents. Hence instead of the Sharpe ratio, we propose to use the expected value of the equity premium $\mathbb{E}(R_{m,t} - R_t^f) = \mathbb{E}(R_{m,t}^e) = \mu_{R_m^e}$ and its second moment $\text{Var}(R_{m,t} - R_t^f) = \sigma^2(R_{m,t} - R_t^f) = \sigma^2(R_t^e) = \sigma_{R_m^e}^2$ separately. As a fourth moment, we use the variance of the risk-free rate $\text{Var}(R_t^f) = \sigma^2(R_t^f) = \sigma_{R_f}^2$.

Hence, the moment restrictions used to estimate the instrumental parameters $\theta_1 = \left(\mu_{R_f}, \mu_{R_m^e}, \sigma_{R_m^e}^2, \sigma_{R_f}^2\right)^\top$ are given by

$$\mathbb{E}\left[u_{1,t}\left(\{y_t\}_{t-l}^t, \theta_1\right)\right] = \mathbb{E}\begin{bmatrix} R_t^f - \mu_{R_f} \\ R_{m,t}^e - \mu_{R_m^e} \\ (R_{m,t}^e)^2 - (\mu_{R_m^e})^2 - \sigma_{R_m^e}^2 \\ (R_t^f)^2 - (\mu_{R_f})^2 - \sigma_{R_f}^2 \end{bmatrix} = 0. \tag{2.3.13}$$

Note that the moment conditions yield an exactly identified problem. Hence there is no need to numerically optimize the instrumental objective function given in Equation (2.3.5). Instead, we use the sample equivalents of the moments specified above.

The classification of the structural parameters at the beginning of this section raises the question of whether the partial encompassing condition holds for our parameters of interest $\xi_1 = (\beta, \overline{rra})$ and the chosen moment conditions. Equation (2.2.11) includes the persistence of habit, ρ_s, as a component of the intertemporal substitution, yet ρ_s is considered a nuisance parameter in our classification. A more refined classification is also plausible, where ρ_s qualifies as a ξ_{21} parameter. This choice would imply that the moment conditions in our instrumental model should identify ρ_s. Section 3.2.3 elaborates more on this possible extension as well as its implications on the estimation strategy.

2.4 Results

The econometric assessment of Chen's (2017) model is conducted in various steps. We start by estimating the structural parameters of interest, ξ_1. Then, we compute approximate confidence intervals around these estimates to evaluate which preference parameter values are compatible with the observed data. Finally, we implement a parametric bootstrap to assess the impact of the estimation uncertainty on the DSGE asset pricing-implied moments that are matched to the empirical data.

To find the estimates of ξ_1, we initially perform a grid search for the ξ_1 parameter combination that returns the minimum value of the PII objective function described in Equation (2.3.9) together with our choice of moment conditions given by Equation (2.3.13). Details of the grid are described in Appendix 2.C.[8] From the minimum value of the grid search, we start a numerical optimization of the objective function with respect to ξ_1. The optimization is based on the non-gradient based Neldor-Mead algorithm.[9] It yields an estimate of the time preference rate, $\hat{\beta}$, of 1.0008, hence, a time preference rate larger than one, and a relative risk aversion estimate, $\widehat{\overline{rra}}$, of 22.6621.

We, then, compute approximate confidence intervals based on the asymptotic distribution described in Appendix 2.B. The estimates, the standard errors and the 95% confidence interval are given in Table 2.3. Both confidence intervals are relatively tight around the estimated values, as the standard errors are small in magnitude. Hence, only a small range of preference parameters values are capable of matching the simulated moments to their empirical counterparts. This implies that these parameters are indeed identifiable from the data.

[8] The grid is minimized for values of $\beta = 1.001$ and $\overline{rra} = 22.5$. These parameter values are inner solutions of the specified grid, and the objective function is not flat around the minimum.

[9] As a robustness check, we also start the numerical optimization from different starting values and obtain similar results. This is unsurprising as the objective function has a clear minimum.

Table 2.3: Partial indirect inference estimation results

			Confidence Interval	
Parameter	**Estimate**	**Standard Error**	**2.5%**	**97.5%**
β	1.0008	0.0034	0.9941	1.0075
$\overline{rra}$	22.66	2.20	18.34	26.98

Note: This table reports the estimation results for the parameters of interest ξ_1, i.e. β and $\overline{rra}$. It also provides standard errors and 95% confidence intervals. The empirical data used are the real post-war quarterly data from 1948 to 2012 and are chosen as in Chen (2017).

The steady-state relative risk aversion estimate is given by $\widehat{\overline{rra}} = 22.66$, and its confidence interval ranges from around 18.3 to 27. The calibrated value of 28.57, the rra value also used by Campbell and Cochrane (1999) and Chen (2017), is not included in the confidence interval and, hence, it is not compatible with the empirical data. Another concern is that the model implied steady-state relative risk aversion is not within the microeconomic evidence based relative risk aversion range of 1 to 5 proposed by Mehra and Prescott (1985). Hence, risk aversion in our model is in fact not low, and the estimated parameter value, along with its confidence interval, is economically not plausible.[10] It is, however, smaller than in a pure consumption-based asset pricing model with power utility preferences, where astronomical risk aversion values, in a magnitude of 40 up to 200, are needed to resolve the equity premium puzzle (c.f. Weil (1989)). In the partial-equilibrium habit persistence model proposed by Campbell and Cochrane (1999) and the general equilibrium model evaluated here, the steady state value is given by $\overline{rra} = 28.57$. Hence, it is even larger than our $\overline{rra}$ estimate. The critique of a relatively high risk aversion coefficient value applies to all habit driven asset pricing models. Cochrane

[10]Note that the parameter of the utility function, γ, is set to 2 but risk aversion in our model is given by $rra_t = \frac{\gamma}{S_t}$.

(2016) and (2017) refers to this problem as the equity-premium risk-free rate puzzle. In a nutshell, habit persistence models yield plausible equity premia with a relatively low risk-free rate and sensible consumption growth moments, but the model-implied risk aversion is not low.[11] The results on the risk aversion coefficient are, thus, in line with the habit formation asset pricing literature.

The implications of the time preference rate, β, results are even more troubling. The parameter estimate is given by $\hat{\beta} = 1.0008$, and its confidence interval ranges from 0.994 to 1.0075. The calibrated time preference rate of $\beta = 0.995$ is included in the approximate confidence interval and it is compatible with the observed data. In the asset pricing literature, e.g. in Mehra and Prescott (1985), Weil (1989), Campbell and Cochrane (1999) and Cochrane (2009), we typically find values of the time preference rate, β, smaller than unity. Any value of the time preference rate above one implies that the representative agent prefers consumption tomorrow over consumption today; a fact that is not supported by microeconomic experiments. The confidence interval for the time preference rate includes many values that are in excess of unity and, hence, these values are economically implausible. This finding is linked to the risk-free rate puzzle described by Weil (1989). The large value of β can be explained by a model-implied risk-free rate that is too large in comparison to its empirical equivalent. The high model-implied risk-free rate is slightly mitigated by using a value of the time preference rate that is larger than one when we match empirical and simulated moments in the PII estimation. In this case, the first term governing the risk-free rate in Equation (2.2.11), $-\log(\beta)$, is negative and decreases the level of the risk-free rate.

[11] The puzzle is, hence, distilled in sensible asset pricing moments obtained without having low utility curvature and risk aversion. He concludes that no model so far has achieved a full solution of the equity premium puzzle.

In addition to the sensibility of the preference parameter estimates, we assess the economic plausibility of the model-implied moments using a parametric bootstrap. We achieve this by drawing randomly from the joint normal distribution of the estimates of the structural parameters of interest based on the asymptotic results, i.e. from

$$\xi_1^* \sim \mathcal{N}\left(\begin{pmatrix} 1.0008 \\ 22.6621 \end{pmatrix}, \begin{pmatrix} 0.0000116 & -0.0064 \\ -0.0064 & 4.8617 \end{pmatrix}\right). \tag{2.4.1}$$

We use $M = 1000$ draws of β and $\overline{rra}$ to solve and simulate the model at the respective values. Then, we compute the implied asset pricing and macroeconomic moments and calculate the mean over all M samples, as well as the 2.5% and 97.5% bootstrap quantiles. The bootstrap results are given in Table 2.4.

The table shows that the macroeconomic moments governing the business cycle and consumption growth do not change qualitatively with the change of β and $\overline{rra}$ as compared to Table 2.2. Moreover, the business cycle moments are not sensitive to our bootstrapping exercise. Most of those moments are not affected by different draws of the preference parameters; the bootstrap intervals are either just one value or their width is very small. Hence, the impact of estimation uncertainty on these model-implied moments is, thus, negligible.

The resulting asset pricing moments are impacted by the different choice of preference parameters in comparison to the calibration results in Table 2.2. The model-implied Sharpe ratio is slightly lower than that implied by US data. This result is due to the fact that the volatility of the excess return is slightly too high, and the level of expected excess return is slightly too low. Both of these quantities are, however, better matched to US data in comparison to the calibrated values. The simulated mean risk-free rate is higher than the one implied by US data, while its volatility is slightly lower. Furthermore, the asset pricing moments are impacted

Table 2.4: Estimation-implied economic plausibility check

Target Moment			**Bootstrap Quantiles**	
	Data	**Implied Estimate**	**2.5%**	**97.5%**
Asset Prices				
90-Day T-bill Return (%)	0.17	0.61	0.36	0.82
Vol of R^f (%)	0.90	0.67	0.59	0.76
Persistence of Tobin's Q		0.96	0.96	0.96
Mean Sharpe Ratio of CRSP Index	0.22	0.17	0.11	0.23
Equity Premium R^e (%)	1.82	1.64	1.04	2.35
Vol of R^e (%)	8.24	9.85	9.14	10.78
Business Cycle				
Mean Output/Capital	0.143	0.076	0.064	0.091
Mean Investment Rate	0.025	0.021	0.021	0.021
Mean Output Growth (%)	0.48	0.45	0.45	0.45
Vol HP-filtered GDP (%)	1.72	1.53	1.52	1.53
Persistence of Output/Capital	0.997	0.984	0.981	0.985
Relative Volatility of Consumption Growth	0.52	0.47	0.40	0.53
Mean Adj Cost / Output (%)		0.11	0.10	0.11
Consumption Growth				
Mean of ln of Consumption Growth (%)	0.47	0.45	0.45	0.45
Std of ln of Consumption Growth (%)	0.52	0.56	0.48	0.63

Note: This table shows the results of a parametric bootstrap using $M = 1000$ draws from the joint normal distribution of β and $\overline{rra}$ around the PII estimates $\hat{\beta} = 1.0008$ and $\widehat{\overline{rra}} = 22.6621$. It shows the selected bootstrap quantiles of asset prices, business cycle and consumption growth moments along with the estimate-implied and empirical means.

by the different bootstrap draws of the preference parameters and are, thus, affected by estimation uncertainty. The equity premium moments lie within the bootstrap interval bounds, and the empirical Sharpe ratio is approximately equivalent to the upper bound. The widths of the bootstrapped intervals for all three quantities are small and contain economically plausible values. Hence, the equity premium implied

by our model is economically sensible. This finding is in line with the habit formation literature summarized by Cochrane (2017).

Additionally, the bootstrapping results confirm that the DSGE asset pricing model is not able to match the risk-free rate moments. The mean as well as the 2.5% and the 97.5% bootstrapping interval bounds for the expected risk-free rate are larger than the empirical counterpart. Hence, the risk-free rate puzzle is also apparent here. The volatility of the risk-free rate implied by the bootstrap draws is slightly lower than the empirical one. Hence, the model-implied risk-free rate is not excessively volatile, but its level is too high.

Over all, the empirical performance of the DGSE extension to the asset pricing model should be taken with a grain of salt as it does not solve the asset pricing puzzles as well as implied in the calibration results of Chen (2017). We find that the equity premium puzzle is only resolved if we accept a value for the relative risk aversion that is around 20. This value is, however, above the range of risk aversion values conventionally found in the microeconomic evidence based literature (c.f. Mehra and Prescott, 1985). More problematic, however, is the unresolved risk-free rate puzzle, as we find that the model cannot match the risk-free rate level in the U.S. economy. This, in turn, is reflected in a time preference rate in excess of unity which is economically inconceivable.

2.5 Conclusion

Incorporating preference-based asset pricing in a DSGE framework holds the promise to resolve prominent puzzles of financial economics with a stochastic discount factor that is consistent with macroeconomic processes. However, the apparent empirical success of the DSGE asset pricing approaches, the most recent exponent of which is the model by Chen (2017), is predominantly based on calibration studies, which have

been criticized by Hansen and Heckman (1996) and Dridi et al. (2007) for lacking the discipline of econometric analysis. On the other hand, Kim and Pagan (1999; p. 328) argue that when dealing with such highly stylized models, "the specification errors being committed are of sufficient magnitude to make conventional estimation and testing of dubious value".

In the debate between proponents of calibration and econometricians, we concur with Dridi et al. (2007) that even if a model is misspecified, economic reality is captured by certain parameters of interest that one should aim to estimate consistently. Pursuing such a goal entails focusing on economically meaningful identifying restrictions that are associated with the parts of a DSGE asset pricing model that claim to capture economic reality. Moreover, empirical tests of the model should reach beyond the confirmatory nature of calibration practices. To implement these ideas, we employ the partial indirect inference (PII) framework proposed by Dridi et al. (2007). In line with the PII philosophy, we use binding functions that aim at the consistent estimation of some structural model parameters of interest (reflecting investor preferences), while treating others (associated with macroeconomic dynamics) as nuisance parameters.

Our results indicate that the very positive calibration results regarding the empirical performance of DSGE asset pricing models should not be overstated. The estimated model is able to match the equity premium and the Sharpe ratio, as well as the business cycle and the consumption growth moments. These moments remain economically plausible even when we take estimation uncertainty into consideration. The macroeconomic moments are mainly impacted by a sensible calibration choice and only slightly affected when varying the estimated preference parameters. However, although the equity premium and the Sharpe ratio implied by the estimated model are plausible, they are associated with a point estimate of relative risk aver-

sion that is generally considered as too high (as are the bounds of the 95% confidence interval). The estimated model only provides a solution to the equity premium puzzle, if one is willing to accept a risk aversion coefficient in the magnitude of around 20. This is a familiar caveat, which applies to partial equilibrium habit-based asset pricing models (e.g. Campbell and Cochrane (1999), Cochrane (2016), Cochrane (2017)). Our results suggest that it applies to DSGE asset pricing models with nonlinear habit preferences, too. The estimation also does not yield economically sensible model-implied values of the risk-free rate, neither in terms of the point estimate of the mean risk-free rate, nor in terms of the bounds of the 95% confidence interval. Whereas the model does not suffer from an excessively volatile risk-free rate, it fails to match its empirical level. The implausibly high value for the model-implied mean risk-free rate is associated with a point estimate of the time preference parameter greater than unity. Hence, the DSGE asset pricing model is unable to resolve the risk-free rate puzzle described in Weil (1989). Our econometric analysis, thus, suggests that empirical asset pricing within a DSGE framework, although it shows some potential, is not yet a panacea to resolve the prominent asset pricing puzzles.

Appendix

2.A The partial indirect inference estimator with instrumental parameters estimated by moment conditions

We construct an indirect estimation strategy for the structural parameters of interest ξ_1. In the following, we denote empirical time series as $\{y_t\}_{t=1}^T$ and we obtain the model-implied series through simulations from $\{\tilde{y}_T^s(\xi, z_0^s)\}_{s=1}^S$ where z_0^s contains the initial value of the state variables. As in Dridi et al. (2007), we assume that the observed data is a realization of a stochastic process with true unknown p.d.f. P_0 : $\{y_t, t \in \mathbb{Z}\}$

Assumption 1. *(i)* P_0 *belongs to a family* $\mathcal{P}$ *of p.d.f. on* $\mathcal{Y}^{\mathbb{Z}}$,

(ii) $\tilde{\xi}_1$ *is an application of* $\mathcal{P}$ *onto a part* $\Xi_1 = \tilde{\xi}_1(\mathcal{P})$ *of* $\mathbb{R}^{p_1}$,

(iii) $\tilde{\xi}_1(\mathcal{P}_0) = \xi_1^0$, *the true parameters of interest belong to the interior* Ξ_1^0 *of* Ξ_1.

These structural parameters of interest, ξ_1, are defined through a set of identifying moment conditions given by a partial parametric model

$$\mathbb{E}_{\mathcal{P}}\left[h(y_t, \ldots, y_{t-p}; \xi_1)\right] = 0 \quad \rightarrow \ \xi_1 = \tilde{\xi}_1(\mathcal{P}).$$

To obtain a fully parametric model, we have to make additional nominal assumptions. This model is likely inconsistent with the true data-generating process. The

partial parametric model defined by Assumption 1 is plugged into the structural model which is fully parametric but misspecified.

Assumption 2 (Nominal assumption)**.** $\{y_t, t \in \mathbb{Z}\}$ *follows a stationary and ergodic process conformable to the nonlinear simultaneous model*

(i) $r\left(y_t, y_{t-1}, v_t, \xi\right) = 0, \qquad \varphi\left(v_t, v_{t-1}, \tilde{\varepsilon}_t, \xi\right) = 0,$

$\xi = (\xi_1, \xi_2) \in (\Xi_1 \times \Xi_2) = \Xi$ *which is a compact subset of* $\mathbb{R}^{p_1+p_2}$,

(ii) $\{\tilde{\varepsilon}_t, t \in \mathbb{Z}\}$ *is white noise with known distribution* G_*,

where $r(\,\cdot\,)$ describes the evolution of the observable variables given the state variables, and $\varphi(\,\cdot\,)$ that of the state variables given the exogenous variables. This assumption is comparable to the fully parametric model described in Gourieroux et al. (1993) which they perceive to describe the true data-generating process. In case of our misspecified simulator, this only constitutes a nominal assumption. For given values of $\xi = (\xi_1, \xi_2)^\top$, we simulate values $\{\tilde{y}_1^s(\xi, z_0^s), \ldots, \tilde{y}_T^s(\xi, z_0^s)\}$ given the initial condition $z_0^s = (y_0^s, v_0^s)^\top$ from the simulated values $\{\tilde{\varepsilon}_1, \ldots, \tilde{\varepsilon}_T\}$ from G_*. P_* denotes the probability limit of the simulated processes.[12]

Indirect inference about the true value of the structural parameters of interest ξ_1^0 of ξ_1 builds on the misspecified structural model introduced in Assumption 2 and the instrumental model $\mathcal{N}_\theta$. The pseudo-true values of the instrumental parameters are defined as probability limits of an extremum estimator associated with the criterion function $Q_{1,T}(\{y_t\}_{t=1}^T, \theta_1)$.[13] Hence, the idea of PII is to use calibration as econometrics of a misspecified structural model and to use this misspecified model as a simulator.

[12]For brevity, we omit the dependence of the simulation on the initial values of the state variables in the following.

[13]Here, $\theta_1 \in \Theta_1$ which is a compact subset of $\mathbb{R}^k$ and $\{y_t\}_{t=1}^T$ denote lagged values of y_t for a fixed number of M lags. Note that the instrumental parameters are denoted by θ_1 in accordance with the partial encompassing case in Dridi et al. (2007). In this setting, there is no second set of instrumental parameters θ_{21}. This is expanded upon in Chapter 3.

The instrumental model has to be chosen carefully as the estimation of the instrumental variables must be tractable, and it should be capable of capturing the properties of the model-implied financial time series. Similar to the recommendations of Dridi et al. (2007), we make use of moment restrictions that reflect the asset pricing implications of the DSGE asset pricing model rather than using a full parametric model as an instrumental model. The set of k moment restrictions is given by

$$\mathbb{E}\left[u_{1,t}\left(\{y_t\}_{t-l}^{t}, \theta_1^0\right)\right] = 0.$$

The number of moment restrictions has to be at least as large as the number of structural parameters, i.e. $k = \dim\ \theta_1 \ \geq\ p_1 + p_{21} = \dim\ \xi_1 + \ \dim\ \xi_{21}$ and $\theta_1 \in \Theta_1 \subset \mathbb{R}^k$. We assume that the true parameter θ_1^0 is the only value within the parameter space that gives a solution to the moment condition. Hence, the identification assumption reads

Assumption 3.

$$\mathbb{E}\left[u_{1,t}\left(\{y_t\}_{t-l}^{t}, \theta_1\right)\right] \neq 0 \quad \textit{for all } \theta_1 \neq \theta_1^0 \in \Theta_1.$$

We minimize a GMM-type criterion function given below to estimate the instrumental parameters θ_1,

$$\underset{\{\theta_1 \in \Theta_1\}}{min}\ Q_{1,T}\left(\{y_t\}_{t=1}^{T}, \theta_1\right),$$

$$\text{where} \quad Q_{1,T}\left(\{y_t\}_{t=1}^{T}, \theta_1\right) = \frac{1}{2}\, g_{1,T}\left(\{y_t\}_{t=1}^{T}, \theta_1\right)^{\top} \cdot \widehat{W}_{1,T} \cdot g_{1,T}\left(\{y_t\}_{t=1}^{T}, \theta_1\right),$$

$$g_{1,T}\left(\{y_t\}_{t=1}^{T}, \theta_1\right) = \frac{1}{T}\sum_{t=1}^{T} u_{1,t}\left(\{y_t\}_{t-l}^{t}, \theta_1\right),$$

with $\widehat{W}_{1,T} \overset{a.s.}{\to} W_1$, a positive semi-definite weighting matrix.

Following Hansen (1982), we impose the following regularity conditions

Assumption 4. *(i)* Θ_1 *is a compact subset of* $\mathbb{R}^k$,

(ii) $u_{1,t}(\cdot, \theta_1)$ *is Borel measurable for each* $\theta_1 \in \Theta_1$,

(iii) $\mathbb{E}\left[u_{1,t}\left(\{y_t\}_{t-l}^{t}, \theta_1\right)\right]$ *exists and is finite for all* $\theta_1 \in \Theta_1$,

(iv) $u_{1,t}\left(\{y_t\}_{t-l}^{t}, \theta_1\right)$ *is first-moment continuous at all* $\theta_1 \in \Theta_1$.

Using Assumption 4 and the stationarity and ergodictiy assumption of the time series results in sufficient conditions that the GMM-type criterion in Equation (2.3.4) converges almost surely uniformly to a non-stochastic limit criterion

$$Q_{1,\infty}\left(G_*, \xi_1^0, \xi_{21}^*, \theta_1\right) = \frac{1}{2}\mathbb{E}\left[u_{1,t}\left(\{y_t\}_{t-l}^{t}, \theta_1\right)\right]^\top \cdot W_1 \cdot \mathbb{E}\left[u_{1,t}\left(\{y_t\}_{t-l}^{t}, \theta_1\right)\right].$$

Moreover, Assumption 3 implies that the limit criterion is uniquely minimized by

$$\theta_1^0 = \underset{\{\theta_1 \in \Theta_1\}}{\operatorname{argmin}} \; Q_{1,\infty}\left(G_*, \xi_1, \xi_{21}, \theta_1\right). \tag{2.A.1}$$

Hence, under the nominal assumption 2, the identification assumption 3, and the equicontinuity assumption 4,

$$\hat{\theta}_{1,T} = \underset{\{\theta_1 \in \Theta_1\}}{\operatorname{argmin}} \; Q_{1,T}\left(\{y_t\}_{t=1}^{T}, \theta_1\right)$$

is a consistent estimator of θ_1^0 (Singleton, 2009).

In case of a misspecified simulator, the probability limits of the simulated and observed time series are not the same. In addition to the assumptions for the data-generating process of the observed time series, we need assumptions for the misspecified simulator. As above, we impose an identification assumption for the simulated time series

Assumption 5.

$$\mathbb{E}^* \left[u_{1,t} \left(\{\tilde{y}_t^s(\xi)\}_{t-l}^t, \theta_1^s \right) \right] \neq 0 \quad \textit{for all } \theta_1^s \neq \tilde{\theta}_1^0(\xi_1^0, \xi_{21}^*) \in \Theta_1^s.$$

We also impose an equivalent GMM regularity conditions for the moment conditions evaluated at the simulated series, i.e.

Assumption 6. *(i)* Θ_1^s *is a compact subset of* $\mathbb{R}^k$,

(ii) $u_{1,t}(\cdot, \theta_1^s)$ *is Borel measurable for each* $\theta_1^s \in \Theta_1^s$,

(iii) $\mathbb{E}^* \left[u_{1,t} \left(\{\tilde{y}_t^s(\xi)\}_{t-l}^t, \theta_1^s \right) \right]$ *exists and is finite for all* $\theta_1^s \in \Theta_1^s$,

(iv) $u_{1,t} \left(\{\tilde{y}_t^s(\xi)\}_{t-l}^t, \theta_1^s \right)$ *is first-moment continuous at all* $\theta_1^s \in \Theta_1^s$.

Comparable to the observed time series case and under Assumption 6 for stationary and ergodic simulated series, the GMM-type criterion in Equation (2.3.4) evaluated at the simulated data, i.e. $Q_{1,T} \left(\{\tilde{y}_T^s(\xi)\}_{t=1}^T, \theta_1^s \right)$, converges almost surely uniformly to a non-stochastic limit criterion.[14] Given Assumption 5, the limit criterion is uniquely minimized by $\tilde{\theta}_1^0 (\xi_1^0, \xi_{21}^*)$. Hence, under the nominal assumption 2, the identification assumption 5, and the equicontinuity assumption 6 for the simulated time series,

$$\tilde{\theta}_{1,T}^s(\xi_1, \xi_{21}, \bar{\xi}_{22}) = \underset{\{\theta_1 \in \Theta_1\}}{\operatorname{argmin}} \; Q_{1,T} \left(\{\tilde{y}_T^s(\xi)\}_{t=1}^T, \theta_1^s \right)$$

is a consistent estimator of $\tilde{\theta}_1^0 (\xi_1^0, \xi_{21}^*)$.

[14] This limit criterion is given by

$$Q_{1,\infty}^* \left(G_*, \xi_1^0, \xi_{21}^*, \theta_1^s \right) = \frac{1}{2} \mathbb{E}^* \left[u_{1,t} \left(\{\tilde{y}_t^s(\xi)\}_{t-l}^t, \theta_1^s \right) \right]^\top \cdot W_1 \cdot \mathbb{E}^* \left[u_{1,t} \left(\{\tilde{y}_t^s(\xi)\}_{t-l}^t, \theta_1^s \right) \right].$$

For the indirect estimator of the structural parameters, we impose the following assumptions on the binding function

Assumption 7. *(i)* $\theta_1(\cdot,\cdot)$ *is one-to-one,*

$$\textit{(ii)}\ P_* \lim_{T\to\infty} \frac{\partial \tilde{\theta}^s_{1,T}}{\partial \begin{pmatrix} \xi_1 \\ \xi_{21} \end{pmatrix}} \left(\xi_1^0, \xi_{21}^*, \bar{\xi}_{22}\right)^\top = \frac{\partial \tilde{\theta}_1}{\partial \begin{pmatrix} \xi_1 \\ \xi_{21} \end{pmatrix}} \left(\xi_1^0, \xi_{21}^*\right)^\top \quad \textit{has rank } p_1 + p_{21}.$$

The one-to-one assumption in 7 *(i)* is comparable to assumption (A4) in Gourieroux et al. (1993) and the rank assumption in 7 *(ii)* is equivalent to assumption (A14) in Dridi et al. (2007). We further require partial encompassing given by

Assumption 8. $\theta_1^0 = \tilde{\theta}_1^0(\xi_1^0, \xi_{21}^*)$,

where θ_1^0 is the probability limit of the instrumental parameters associated with the observed data defined in Equation (2.A.1) and $\tilde{\theta}_1^0(\xi_1^0, \xi_{21}^*)$ is the probability limit for the simulated time series. Assumption 8 is the partial encompassing condition in Dridi et al. (2007). We refer to it as the partial encompassing null hypothesis $H_0^{(1)}\left(\bar{\xi}_{22}\right)$.

It follows that under Assumptions 3 to 8, the instrumental parameter estimators converge uniformly in (ξ_1, ξ_{21}) to

$$P_0 \lim_{T\to\infty} \hat{\theta}_{1,T} = \theta_1^0 \qquad \text{and} \qquad P_* \lim_{T\to\infty} \tilde{\theta}^s_{1,T}(\xi_1, \xi_{21}) = \tilde{\theta}_1^0(\xi_1^0, \xi_{21}^*),$$

where $P_0 \lim_{T\to\infty}$ and $P_* \lim_{T\to\infty}$ denote the limit with respect to the probability distributions P_0 and P_* for the observed and simulated series.

The partial indirect inference (PII) estimator is defined as

$$\begin{aligned}
\begin{pmatrix} \hat{\xi}_{1,TS}(\bar{\xi}_{22}) \\ \hat{\xi}_{21,TS}(\bar{\xi}_{22}) \end{pmatrix} = & \underset{\{(\xi_1,\xi_{21})\in\Xi_1\times\Xi_{21}\}}{\operatorname{argmin}} \left[\hat{\theta}_{1,T} - \frac{1}{S}\sum_{s=1}^{S}\tilde{\theta}^s_{1,T}(\xi_1,\xi_{21},\bar{\xi}_{22})\right]^{\top} \cdot \widehat{\Omega}_{1,T} \\
& \cdot \left[\hat{\theta}_{1,T} - \frac{1}{S}\sum_{s=1}^{S}\tilde{\theta}^s_{1,T}(\xi_1,\xi_{21},\bar{\xi}_{22})\right], \\
\hat{\theta}_{1,T} = & \underset{\{\theta_1\in\Theta_1\}}{\operatorname{argmin}} Q_{1,T}\left(\{y_t\}_{t=1}^{T},\theta_1\right), \\
\tilde{\theta}^s_{1,T}\left(\xi_1,\xi_{21},\bar{\xi}_{22}\right) = & \underset{\{\theta_1\in\Theta_1\}}{\operatorname{argmin}} Q_{1,T}\left(\{\tilde{y}^s_T(\xi)\}_{t=1}^{T},\theta^s_1\right),
\end{aligned}$$

and $\widehat{\Omega}_{1,T}$ is a positive definite weighting matrix that converges almost surely to the non-stochastic positive definite matrix Ω_1.

Proposition 1 (Consistency)**.** *Under assumptions 1, 3 - 8,* $\hat{\xi}_{1,TS}\left(\bar{\xi}_{22}\right)$ *is a consistent estimator of* ξ_1^0.

The misspecified model defined in Assumption 2 endowed with the pseudo-true value $\begin{pmatrix} \xi_1^0 \\ \xi_{21}^* \end{pmatrix}$ partially encompasses $\mathcal{N}_\theta$ under assumptions 7 and 8. This partial encompassing provides a sufficient condition for the consistency of the partial indirect inference estimator of the parameter of interest $\hat{\xi}_{1,TS}\left(\bar{\xi}_{22}\right)$ as described in Proposition 3.3. in Dridi et al. (2007). The proof of the proposition is an adapted version of those found in Dridi and Renault (2000) and Dridi et al. (2007). In our case, we use a GMM-type instrumental model rather than a general extremum estimator. This difference features in the identification assumptions 3 and 5 and the regularity conditions 4 and 6 which are specific to the GMM-type instrumental model. Assumptions 1, 2 and 7 are comparable to those in Dridi et al. (2007) for the partial encompassing case in the absence of exogenous variables.

Asymptotic distribution of the partial indirect inference estimator

To derive the asymptotic distribution of the structural parameters, we follow a sequential approach. In a first step, we derive the asymptotic distribution of the instrumental parameters θ_1 for the GMM-type instrumental model. We impose additional assumptions on the moment conditions. More specifically, we assume that a central limit theorem applies to appropriately scaled moment conditions evaluated at the observed data $\{y_t\}_{t=1}^T$ and the simulated data $\{\tilde{y}_t^s(\xi)\}_{t=1}^T$.

Assumption 9. *A multivariate central limit theorem applies, such that under Assumption 3*

$$\sqrt{T}\left[\frac{1}{T}\sum_{t=1}^{T} u_{1,t}\left(\{y_t\}_{t-l}^{t}, \theta_1^0\right)\right] \underset{d}{\to} \mathcal{N}(0, V_1)$$

with

$$V_1 = \Gamma_{1,0} + \sum_{j=1}^{\infty}\left(\Gamma_{1,j} + \Gamma_{1,j}^{\top}\right)$$
$$\Gamma_{1,j} = \mathbb{E}\left[u_{1,t}\left(\{y_t\}_{t-l}^{t}, \theta_1^0\right) u_{1,t-j}\left(\{y_t\}_{t-l-j}^{t}, \theta_1^0\right)^{\top}\right]$$

and

Assumption 10. *A multivariate central limit theorem applies, such that under Assumption 5*

$$\sqrt{T}\left[\frac{1}{T}\sum_{t=1}^{T} u_{1,t}\left(\{\tilde{y}_T^s(\xi)\}_{t-l}^{t}, \tilde{\theta}_1^0\left(\bar{\xi}_{22}\right)\right)\right] \underset{d}{\to} \mathcal{N}(0, V_1^*)$$

with

$$V_1^* = \Gamma_{1,0}^* + \sum_{j=1}^{\infty} \left(\Gamma_{1,j}^* + \Gamma_{1,j}^{*\top} \right)$$
$$\Gamma_{1,j}^* = \mathbb{E}^* \left[u_{1,t} \left(\{\tilde{y}_T^s(\xi)\}_{t-l}^t, \tilde{\theta}_1^0 \left(\bar{\xi}_{22} \right) \right) u_{1,t-j} \left(\{\tilde{y}_T^s(\xi)\}_{t-l-j}^t, \tilde{\theta}_1^0 \left(\bar{\xi}_{22} \right) \right)^\top \right].$$

Under the null hypothesis of partial encompassing $H_0^{(1)} \left(\bar{\xi}_{22} \right) : \theta_1^0 = \tilde{\theta}_1^0 \left(\bar{\xi}_{22} \right)$ given in Assumption 8, the following result holds.

Proposition 2 (Asymptotic distribution of the instrumental parameters)**.** *Under Assumptions 3, 5, 9, 10 and partial encompassing given in 8, the instrumental parameters are asymptotically distributed as*

$$\sqrt{T} \left(\hat{\theta}_{1,T} - \frac{1}{S} \sum_{s=1}^{S} \tilde{\theta}_{1,T}^s \left(\xi_1^0, \xi_{21}^* \right) \right) \xrightarrow{d} \mathcal{N} \left(0, \Phi_1^0 \left(S, W_1 \right) \right) \tag{2.A.2}$$

where the asymptotic covariance matrix is given by

$$\Phi_1^0 \left(S, W_1 \right) = C_1^0 V_1 C_1^{0\top} + \frac{1}{S} C_1^{*0} V_1^* C_1^{*0\top} \tag{2.A.3}$$

and

$$C_1^0 = \left\{ \mathbb{E} \left[\frac{\partial u_{1,t}^\top}{\partial \theta_1} \left(y, \theta_1^0 \right) \right] W_1 \mathbb{E} \left[\frac{\partial u_{1,t}}{\partial \theta_1^\top} \left(y, \theta_1^0 \right) \right] \right\}^{-1} \mathbb{E} \left[\frac{\partial u_{1,t}^\top}{\partial \theta_1} \left(y, \theta_1^0 \right) \right] W_1, \tag{2.A.4}$$
$$C_1^{*0} = \left\{ \mathbb{E}^* \left[\frac{\partial u_{1,t}^\top}{\partial \theta_1} \left(\tilde{y}, \theta_1^0 \right) \right] W_1 \mathbb{E}^* \left[\frac{\partial u_{1,t}}{\partial \theta_1^\top} \left(\tilde{y}, \theta_1^0 \right) \right] \right\}^{-1} \mathbb{E}^* \left[\frac{\partial u_{1,t}^\top}{\partial \theta_1} \left(\tilde{y}, \theta_1^0 \right) \right] W_1, \tag{2.A.5}$$
$$\Gamma_{1,j}^* = \mathbb{E}^* \left[u_{1,t} \left(\tilde{y}, \theta_1^0 \right) u_{1,t-j} \left(\tilde{y}, \theta_1^0 \right)^\top \right]. \tag{2.A.6}$$

where y and $\tilde{y}$ are short-hand notations for $\{y_t\}_{t=1}^T$ and $\{\tilde{y}_T^s(\xi)\}_{t=1}^T$, respectively.

The asymptotic distribution of the estimated structural parameters is described in the following proposition.

Proposition 3 (Asymptotic distribution of the structural parameters)**.** *Under assumptions 1 - 7, 8, 9 and 10, the structural parameters estimates of* ξ_1 *and* ξ_{21} *follow an asymptotic normal distribution*

$$\sqrt{T}\begin{pmatrix} \hat{\xi}_{1,TS}\left(\bar{\xi}_{22}\right) - \xi_1^0 \\ \hat{\xi}_{21,TS}\left(\bar{\xi}_{22}\right) - \xi_{21}^* \end{pmatrix} \xrightarrow{d} \mathcal{N}\left(0, \Sigma\left(S, \Omega_1\right)\right) \tag{2.A.7}$$

where the asymptotic covariance matrix $\Sigma\left(S, \Omega_1\right)$ *is given in Equations* (2.B.1) *in Appendix 2.B, Equations* (2.A.3)*, and* (2.A.4) - (2.A.6)*.*

The proof of this proposition and the assumptions needed for the asymptotic distribution are provided in Appendix 2.B.

2.B Derivation of the asymptotic distribution

In this section, we derive the asymptotic distribution of the parameters of interest ξ_1 (and of ξ_{21}). The objective function of a partial encompassing indirect inference estimator is given by the following quadratic form

$$\min_{\{(\xi_1,\xi_{21})\in(\Xi_1\times\Xi_{21})\}} \left[\hat{\theta}_{1,T} - \frac{1}{S}\sum_{s=1}^{S}\tilde{\theta}_{1,T}^{s}\left(\xi_1, \xi_{21}, \bar{\xi}_{22}\right)\right]^{\top} \widehat{\Omega}_{1,T} \left[\hat{\theta}_{1,T} - \frac{1}{S}\sum_{s=1}^{S}\tilde{\theta}_{1,T}^{s}\left(\xi_1, \xi_{21}, \bar{\xi}_{22}\right)\right].$$

The first order condition (FOC) to this minimization problem with respect to the estimated structural parameters reads

$$\frac{1}{S}\sum_{s=1}^{S}\frac{\partial\tilde{\theta}_{1,T}^{s}}{\partial\begin{pmatrix}\xi_1\\ \xi_{21}\end{pmatrix}}\left(\hat{\xi}_{1,TS}\left(\bar{\xi}_{22}\right),\hat{\xi}_{21,TS}\left(\bar{\xi}_{22}\right),\bar{\xi}_{22}\right)^{\top}\widehat{\Omega}_{1,T}$$
$$\cdot\left[\hat{\theta}_{1,T}-\frac{1}{S}\sum_{s=1}^{S}\tilde{\theta}_{1,T}^{s}\left(\hat{\xi}_{1,TS}\left(\bar{\xi}_{22}\right),\hat{\xi}_{21,TS}\left(\bar{\xi}_{22}\right),\bar{\xi}_{22}\right)\right]=0.$$

We evaluate the FOC around the limit values ξ_1^0 and ξ_{21}^*. We need the following two results from before; first that the derivative of the instrumental parameters with respect to the structural parameters of interest follows a uniform convergence in the neighborhood of θ_0, i.e.

$$\frac{\partial\tilde{\theta}_{1,T}^{s}}{\partial\begin{pmatrix}\xi_1\\ \xi_{21}\end{pmatrix}}\left(\hat{\xi}_{1,TS}\left(\bar{\xi}_{22}\right),\hat{\xi}_{21,TS}\left(\bar{\xi}_{22}\right),\bar{\xi}_{22}\right)^{\top}\underset{a.s.}{\to}\frac{\partial\tilde{\theta}_{1}}{\partial\begin{pmatrix}\xi_1\\ \xi_{21}\end{pmatrix}}\left(\xi_1^0,\xi_{21}^*\right)^{\top},$$

and second, the partial encompassing assumption 7 *(ii)* given by

$$P_*\lim_{T\to\infty}\frac{\partial\tilde{\theta}_{1,T}^{s}}{\partial\begin{pmatrix}\xi_1\\ \xi_{21}\end{pmatrix}}\left(\xi_1^0,\xi_{21}^*,\bar{\xi}_{22}\right)^{\top}=\frac{\partial\tilde{\theta}_{1}}{\partial\begin{pmatrix}\xi_1\\ \xi_{21}\end{pmatrix}}\left(\xi_1^0,\xi_{21}^*\right)^{\top}\quad\text{has rank } p_1+p_{21}.$$

The expansion is given by

$$\frac{1}{S}\sum_{s=1}^{S}\frac{\partial\tilde{\theta}_{1,T}^{s}}{\partial\begin{pmatrix}\xi_1\\ \xi_{21}\end{pmatrix}}\left(\hat{\xi}_{1,TS}\left(\bar{\xi}_{22}\right),\hat{\xi}_{21,TS}\left(\bar{\xi}_{22}\right),\bar{\xi}_{22}\right)^{\top}\widehat{\Omega}_{1,T}\sqrt{T}\left[\hat{\theta}_{1,T}-\left(\frac{1}{S}\sum_{s=1}^{S}\tilde{\theta}_{1,T}^{s}\left(\xi_1^0,\xi_{21}^*\right)\right.\right.$$
$$\left.\left.+\frac{1}{S}\sum_{s=1}^{S}\frac{\partial\tilde{\theta}_{1,T}^{s}}{\partial\begin{pmatrix}\xi_1\\ \xi_{21}\end{pmatrix}^{\top}}\left(\xi_1^0,\xi_{21}^*\right)\begin{pmatrix}\hat{\xi}_{1,TS}\left(\bar{\xi}_{22}\right)-\xi_1^0\\ \hat{\xi}_{21,TS}\left(\bar{\xi}_{22}\right)-\xi_{21}^*\end{pmatrix}\right)\right].$$

We rearrange the equation for the structural parameters. Asymptotically, they can be represented as

$$\sqrt{T}\begin{pmatrix}\hat{\xi}_{1,TS}\left(\bar{\xi}_{22}\right)-\xi_1^0\\ \hat{\xi}_{21,TS}\left(\bar{\xi}_{22}\right)-\xi_{21}^*\end{pmatrix}\simeq\left\{\frac{\partial\tilde{\theta}_1}{\partial\begin{pmatrix}\xi_1\\ \xi_{21}\end{pmatrix}}\left(\xi_1^0,\xi_{21}^*\right)^{\top}\Omega_1\frac{\partial\tilde{\theta}_1}{\partial\begin{pmatrix}\xi_1\\ \xi_{21}\end{pmatrix}^{\top}}\left(\xi_1^0,\xi_{21}^*\right)\right\}^{-1}$$
$$\cdot\frac{\partial\tilde{\theta}_1}{\partial\begin{pmatrix}\xi_1\\ \xi_{21}\end{pmatrix}}\left(\xi_1^0,\xi_{21}^*\right)^{\top}\Omega_1\cdot\sqrt{T}\left[\hat{\theta}_{1,T}-\frac{1}{S}\sum_{s=1}^{S}\tilde{\theta}_{1,T}^{s}\left(\xi_1^0,\xi_{21}^*\right)\right]$$

Asymptotic distribution of the instrumental parameters

As moment conditions in a GMM-type manner are used to estimate the instrumental parameters θ_1, the objective function evaluated at the observed time series $\{y_t\}_{t=1}^{T}$ is given by

$$Q_{1,T}\left(\{y_t\}_{t=1}^{T},\theta_1\right)=\frac{1}{2}\,g_{1,T}\left(\{y_t\}_{t=1}^{T},\theta_1\right)^{\top}\cdot\widehat{W}_{1,T}\cdot g_{1,T}\left(\{y_t\}_{t=1}^{T},\theta_1\right),$$

where $g_{1,T}\left(\{y_t\}_{t=1}^T, \theta_1\right) = \frac{1}{T}\sum_{t=1}^T u_{1,t}\left(\{y_t\}_{t-l}^t, \theta_1\right)$ is the sample average of the moment condition whose limit is given as $\mathbb{E}\left[u_{1,t}\left(\{y_t\}_{t-l}^t, \theta_1\right)\right] \neq 0$ for all $\theta_1 \neq \theta_1^0$.

First, we show how $\sqrt{T}\left(\hat{\theta}_{1,T} - \theta_1^0\right)$ is distributed. We apply a strategy similar to that of the quadratic form above. We take the FOC of the objective function

$$\frac{\partial g_{1,T}^\top}{\partial \theta_1}\left(\{y_t\}_{t=1}^T, \hat{\theta}_{1,T}\right) \cdot \widehat{W}_{1,T} \cdot g_{1,T}\left(\{y_t\}_{t=1}^T, \hat{\theta}_{1,T}\right)$$

and use a mean value expansions of $g_{1,T}(\,\cdot\,)$ around the limit value θ_1^0

$$g_{1,T}\left(\{y_t\}_{t=1}^T, \hat{\theta}_{1,T}\right) \simeq g_{1,T}\left(\{y_t\}_{t=1}^T, \theta_1^0\right) + \frac{\partial g_{1,T}}{\partial \theta_1^\top}\left(\{y_t\}_{t=1}^T, \theta_1^0\right)\left(\hat{\theta}_{1,T} - \theta_1^0\right).$$

Then, we plug this expansion into the FOC and rearrange the equation for the instrumental parameters

$$\begin{aligned}\left(\hat{\theta}_{1,T} - \theta_1^0\right) = -&\left\{\frac{\partial g_{1,T}^\top}{\partial \theta_1}\left(\{y_t\}_{t=1}^T, \hat{\theta}_{1,T}\right)\widehat{W}_{1,T}\frac{\partial g_{1,T}}{\partial \theta_1^\top}\left(\{y_t\}_{t=1}^T, \theta_1^0\right)\right\}^{-1}\frac{\partial g_{1,T}^\top}{\partial \theta_1}\left(\{y_t\}_{t=1}^T, \hat{\theta}_{1,T}\right)\widehat{W}_{1,T} \\ &\cdot g_{1,T}\left(\{y_t\}_{t=1}^T, \theta_1^0\right).\end{aligned}$$

Asymptotically the equation above can be written as

$$\begin{aligned}&\sqrt{T}\left(\hat{\theta}_{1,T} - \theta_1^0\right) \\ \simeq &-\left\{\mathbb{E}\left[\frac{\partial u_{1,t}^\top}{\partial \theta_1}\left(\theta_1^0\right)\right] W_1 \mathbb{E}\left[\frac{\partial u_{1,t}}{\partial \theta_1^\top}\left(\theta_1^0\right)\right]\right\}^{-1}\mathbb{E}\left[\frac{\partial u_{1,t}^\top}{\partial \theta_1}\left(\theta_1^0\right)\right] W_1 \cdot \sqrt{T} g_{1,T}\left(\{y_t\}_{t=1}^T, \theta_1^0\right) \\ \simeq &-C_1^0 \cdot \sqrt{T} g_{1,T}\left(\{y_t\}_{t=1}^T, \theta_1^0\right),\end{aligned}$$

where $g_{1,T}\left(\{y_t\}_{t=1}^T, \theta_1^0\right) = \frac{1}{T}\sum_{t=1}^T u_{1,t}\left(\{y_t\}_{t-l}^t, \theta_1^0\right)$.

Under the CLT in Assumption 9, the instrumental parameters evaluated at the observed data are distributed as

$$\sqrt{T}\left(\hat{\theta}_{1,T}-\theta_1^0\right)\underset{d}{\to}\mathcal{N}\left(0,C_1^0V_1C_1^{0\top}\right).$$

Second, we elaborate on how the instrumental parameters for the simulated time series $\sqrt{T}\left(\tilde{\theta}^s_{1,T}\left(\xi_1^0,\xi_{21}^*\right)-\tilde{\theta}_1^0\left(\xi_1^0,\xi_{21}^*\right)\right)$ are distributed. For simplicity, define $\tilde{\theta}^s_{1,T}\left(\xi_1^0,\xi_{21}^*\right)\equiv\tilde{\theta}^s_{1,T}\left(\bar{\xi}_{22}\right)$ and $\tilde{\theta}_1^0\left(\bar{\xi}_{22}\right)\equiv\tilde{\theta}_1^0\left(\xi_1^0,\xi_{21}^*\right)$. Following the same steps for the simulated series as for the objective function evaluated at the observed data, we calculate the FOC

$$\frac{\partial g_{1,T}^\top}{\partial\theta_1}\left(\{\tilde{y}_T^s(\xi)\}_{t=1}^T,\tilde{\theta}^s_{1,T}\left(\bar{\xi}_{22}\right)\right)\cdot\widehat{W}_{1,T}\cdot g_{1,T}\left(\{\tilde{y}_T^s(\xi)\}_{t=1}^T,\tilde{\theta}^s_{1,T}\left(\bar{\xi}_{22}\right)\right)$$

and use a mean value expansions of $g_{1,T}(\,\cdot\,)$ around the limit value $\tilde{\theta}_1^0\left(\bar{\xi}_{22}\right)$

$$g_{1,T}\left(\tilde{\theta}^s_{1,T}\left(\bar{\xi}_{22}\right)\right)\simeq g_{1,T}\left(\{\tilde{y}_T^s(\xi)\}_{t=1}^T,\tilde{\theta}_1^0\left(\bar{\xi}_{22}\right)\right)+\frac{\partial g_{1,T}}{\partial\theta_1^\top}\left(\tilde{\theta}_1^0\left(\bar{\xi}_{22}\right)\right)\left(\tilde{\theta}^s_{1,T}\left(\bar{\xi}_{22}\right)-\tilde{\theta}_1^0\left(\bar{\xi}_{22}\right)\right).$$

Then, we plug this expansion into the FOC and rearrange the equation for the instrumental parameters

$$\begin{aligned}&\left(\tilde{\theta}^s_{1,T}\left(\bar{\xi}_{22}\right)-\tilde{\theta}_1^0\left(\bar{\xi}_{22}\right)\right)\\&=-\left\{\frac{\partial g_{1,T}^\top}{\partial\theta_1}\left(\tilde{\theta}^s_{1,T}\left(\bar{\xi}_{22}\right)\right)\widehat{W}_{1,T}\frac{\partial g_{1,T}}{\partial\theta_1^\top}\left(\tilde{\theta}_1^0\left(\bar{\xi}_{22}\right)\right)\right\}^{-1}\frac{\partial g_{1,T}^\top}{\partial\theta_1}\left(\tilde{\theta}^s_{1,T}\left(\bar{\xi}_{22}\right)\right)\widehat{W}_{1,T}\\&\quad\cdot g_{1,T}\left(\{\tilde{y}_T^s(\xi)\}_{t=1}^T,\tilde{\theta}_1^0\left(\bar{\xi}_{22}\right)\right).\end{aligned}$$

Based on the simulated time series $\{\tilde{y}_T^s(\xi)\}_{t=1}^T$, the instrumental parameters can be asymptotically written as

$$\begin{aligned}
&\sqrt{T}\left(\tilde{\theta}_{1,T}^s\left(\bar{\xi}_{22}\right)-\tilde{\theta}_1^0\left(\bar{\xi}_{22}\right)\right)\\
\simeq &-\left\{\mathbb{E}^*\left[\frac{\partial u_{1,t}^\top}{\partial\theta_1}\left(\{\tilde{y}_T^s(\xi)\}_{t-l}^t,\tilde{\theta}_1^0\left(\bar{\xi}_{22}\right)\right)\right]W_1\mathbb{E}^*\left[\frac{\partial u_{1,t}}{\partial\theta_1^\top}\left(\{\tilde{y}_T^s(\xi)\}_{t-l}^t,\tilde{\theta}_1^0\left(\bar{\xi}_{22}\right)\right)\right]\right\}^{-1}\\
&\cdot\mathbb{E}^*\left[\frac{\partial u_{1,t}^\top}{\partial\theta_1}\left(\{\tilde{y}_T^s(\xi)\}_{t-l}^t,\tilde{\theta}_1^0\left(\bar{\xi}_{22}\right)\right)\right]W_1\cdot\sqrt{T}g_{1,T}\left(\{\tilde{y}_T^s(\xi)\}_{t=1}^T,\tilde{\theta}_1^0\left(\bar{\xi}_{22}\right)\right),
\end{aligned}$$

where $g_{1,T}\left(\{\tilde{y}_T^s(\xi)\}_{t=1}^T,\tilde{\theta}_1^0\left(\bar{\xi}_{22}\right)\right)=\frac{1}{T}\sum_{t=1}^T u_{1,t}\left(\{\tilde{y}_T^s(\xi)\}_{t-l}^t,\tilde{\theta}_1^0\left(\bar{\xi}_{22}\right)\right)$.
Under the null hypothesis of partial encompassing $H_0^{(1)}\left(\bar{\xi}_{22}\right):\ \theta_1^0=\tilde{\theta}_1^0\left(\bar{\xi}_{22}\right)$ given in Assumption 8 and the CLT in Assumption 10, it follows that

$$\begin{aligned}
\sqrt{T}\left(\tilde{\theta}_{1,T}^s\left(\bar{\xi}_{22}\right)-\tilde{\theta}_1^0\right)\simeq &-\left\{\mathbb{E}^*\left[\frac{\partial u_{1,t}^\top}{\partial\theta_1}\left(\{\tilde{y}_T^s(\xi)\}_{t-l}^t,\theta_1^0\right)\right]W_1\mathbb{E}^*\left[\frac{\partial u_{1,t}}{\partial\theta_1^\top}\left(\{\tilde{y}_T^s(\xi)\}_{t-l}^t,\theta_1^0\right)\right]\right\}^{-1}\\
&\cdot\mathbb{E}^*\left[\frac{\partial u_{1,t}^\top}{\partial\theta_1}\left(\{\tilde{y}_T^s(\xi)\}_{t-l}^t,\theta_1^0\right)\right]W_1\cdot\sqrt{T}g_{1,T}\left(\{\tilde{y}_T^s(\xi)\}_{t=1}^T,\theta_1^0\right)\\
\simeq &-C_1^{*0}\cdot\sqrt{T}g_{1,T}\left(\{\tilde{y}_T^s(\xi)\}_{t=1}^T,\theta_1^0\right),
\end{aligned}$$

where $\sqrt{T}g_{1,T}\left(\{\tilde{y}_T^s(\xi)\}_{t=1}^T,\theta_1^0\right)=\sqrt{T}\frac{1}{T}\sum_{t=1}^T u_{1,t}\left(\{\tilde{y}_T^s(\xi)\}_{t-l}^t,\theta_1^0\right)\underset{d}{\to}\mathcal{N}(0,V_1^*)$.
Under the null hypothesis of partial encompassing, the instrumental parameters evaluated at the simulated series are distributed as

$$\sqrt{T}\left(\tilde{\theta}_{1,T}^s\left(\bar{\xi}_{22}\right)-\theta_1^0\right)\underset{d}{\to}\mathcal{N}\left(0,C_1^{*0}V_1^*C_1^{*0\top}\right).$$

Third, we investigate the distribution of $\sqrt{T}\left(\frac{1}{S}\sum_{s=1}^{S}\tilde{\theta}_{1,T}^{s}\left(\xi_1^0,\xi_{21}^*\right)-\theta_1^0\right)$. Under the null hypothesis of partial encompassing, the instrumental parameters evaluated at the simulated series are distributed as

$$\sqrt{T}\left(\tilde{\theta}_{1,T}^{s}\left(\bar{\xi}_{22}\right)-\theta_1^0\right)\underset{d}{\to}\mathcal{N}\left(0,\frac{1}{S}C_1^{*0}V_1^*C_1^{*0^\top}\right).$$

Finally, the previous results are combined to show the distribution of $\sqrt{T}\left(\hat{\theta}_{1,T}-\frac{1}{S}\sum_{s=1}^{S}\tilde{\theta}_{1,T}^{s}\left(\xi_1^0,\xi_{21}^*\right)\right)$. Based on the results above, the expression can asymptotically be written as

$$\sqrt{T}\left(\hat{\theta}_{1,T}-\frac{1}{S}\sum_{s=1}^{S}\tilde{\theta}_{1,T}^{s}\left(\xi_1^0,\xi_{21}^*\right)\right)\simeq -C_1^0\cdot\sqrt{T}g_{1,T}\left(\{y_t\}_{t=1}^{T},\theta_1^0\right)+C_1^{*0}\sqrt{T}g_{1,T}\left(\{\tilde{y}_T^s(\xi)\}_{t=1}^{T},\theta_1^0\right)$$

and is asymptotically normally distributed with asymptotic covariance matrix $\Phi_1^0\left(S,W_1\right)$:

$$\Phi_1^0\left(S,W_1\right)=C_1^0V_1C_1^{0^\top}-C_1^0K_1C_1^{*0^\top}-C_1^{*0}K_1'C_1^{0^\top}+\frac{1}{S}C_1^{*0}V_1^*C_1^{*0^\top}+\left(1-\frac{1}{S}\right)C_1^{*0}K_1^*C_1^{*0^\top},$$

where K_1 and K_1^* are asymptotic covariance matrices of the observed and simulated data which are non-zero if exogenous variables exist in the model. If there are no exogenous variables in the model, the asymptotic covariance is given by

$$\Phi_1^0\left(S,W_1\right)=C_1^0V_1C_1^{0^\top}+\frac{1}{S}C_1^{*0}V_1^*C_1^{*0^\top}.$$

Given the results above, we can show the asymptotic distribution of the instrumental parameters. Under Assumptions 3, 5, 9, 10 and 8, the instrumental parameters are asymptotically distributed as

$$\sqrt{T}\left(\hat{\theta}_{1,T}-\frac{1}{S}\sum_{s=1}^{S}\tilde{\theta}_{1,T}^{s}\left(\xi_1^0,\xi_{21}^*\right)\right)\overset{d}{\to}\mathcal{N}\left(0,\Phi_1^0\left(S,W_1\right)\right),$$

where the asymptotic covariance matrix is given by

$$\Phi_1^0(S, W_1) = C_1^0 V_1 C_1^{0\top} + \frac{1}{S} C_1^{*0} V_1^* C_1^{*0\top},$$

and

$$\begin{aligned}
C_1^0 &= \left\{ \mathbb{E}\left[\frac{\partial u_{1,t}^\top}{\partial \theta_1}\left(y, \theta_1^0\right) \right] W_1 \mathbb{E}\left[\frac{\partial u_{1,t}}{\partial \theta_1^\top}\left(y, \theta_1^0\right) \right] \right\}^{-1} \mathbb{E}\left[\frac{\partial u_{1,t}^\top}{\partial \theta_1}\left(y, \theta_1^0\right) \right] W_1, \\
C_1^{*0} &= \left\{ \mathbb{E}^*\left[\frac{\partial u_{1,t}^\top}{\partial \theta_1}\left(\tilde{y}, \theta_1^0\right) \right] W_1 \mathbb{E}^*\left[\frac{\partial u_{1,t}}{\partial \theta_1^\top}\left(\tilde{y}, \theta_1^0\right) \right] \right\}^{-1} \mathbb{E}^*\left[\frac{\partial u_{1,t}^\top}{\partial \theta_1}\left(\tilde{y}, \theta_1^0\right) \right] W_1, \\
\Gamma_{1,j}^* &= \mathbb{E}^*\left[u_{1,t}\left(\tilde{y}, \theta_1^0\right) u_{1,t-j}\left(\tilde{y}, \theta_1^0\right)^\top \right].
\end{aligned}$$

where y and $\tilde{y}$ are short-hand notations for $\{y_t\}_{t=1}^T$ and $\{\tilde{y}_T^s(\xi)\}_{t=1}^T$, respectively.

Asymptotic distribution of the structural parameters

Overall the estimated structural parameters are distributed as follows: Under assumptions 1 - 8, 9 and 10, the structural parameters estimates of ξ_1 and ξ_{21} follow an asymptotic normal distribution

$$\sqrt{T}\begin{pmatrix} \hat{\xi}_{1,TS}\left(\bar{\xi}_{22}\right) - \xi_1^0 \\ \hat{\xi}_{21,TS}\left(\bar{\xi}_{22}\right) - \xi_{21}^* \end{pmatrix} \xrightarrow{d} \mathcal{N}\left(0, \Sigma\left(S, \Omega_1\right)\right)$$

where the asymptotic covariance matrix is given by

$$\Sigma\left(S,\Omega_1\right)=\left\{\frac{\partial\tilde{\theta}_1}{\partial\begin{pmatrix}\xi_1\\ \xi_{21}\end{pmatrix}}\left(\xi_1^0,\xi_{21}^*\right)^\top\Omega_1\frac{\partial\tilde{\theta}_1}{\partial\begin{pmatrix}\xi_1\\ \xi_{21}\end{pmatrix}}^\top\left(\xi_1^0,\xi_{21}^*\right)\right\}^{-1}\frac{\partial\tilde{\theta}_1}{\partial\begin{pmatrix}\xi_1\\ \xi_{21}\end{pmatrix}}\left(\xi_1^0,\xi_{21}^*\right)^\top\Omega_1$$
$$\cdot\,\Phi_1^0\left(S,W_1\right)\Omega_1\frac{\partial\tilde{\theta}_1}{\partial\begin{pmatrix}\xi_1\\ \xi_{21}\end{pmatrix}}^\top\left(\xi_1^0,\xi_{21}^*\right)\left\{\frac{\partial\tilde{\theta}_1}{\partial\begin{pmatrix}\xi_1\\ \xi_{21}\end{pmatrix}}\left(\xi_1^0,\xi_{21}^*\right)^\top\Omega_1\frac{\partial\tilde{\theta}_1}{\partial\begin{pmatrix}\xi_1\\ \xi_{21}\end{pmatrix}}^\top\left(\xi_1^0,\xi_{21}^*\right)\right\}^{-1}. \tag{2.B.1}$$

The asymptotic covariance matrix of the auxiliary parameters is given by

$$\Phi_1^0\left(S,W_1\right)=C_1^0V_1{C_1^0}^\top+\frac{1}{S}C_1^{*0}V_1^*{C_1^{*0}}^\top,$$

where the components read

$$C_1^0=\left\{\mathbb{E}\left[\frac{\partial u_{1,t}^\top}{\partial\theta_1}\left(y,\theta_1^0\right)\right]W_1\mathbb{E}\left[\frac{\partial u_{1,t}}{\partial\theta_1^\top}\left(y,\theta_1^0\right)\right]\right\}^{-1}\mathbb{E}\left[\frac{\partial u_{1,t}^\top}{\partial\theta_1}\left(y,\theta_1^0\right)\right]W_1,$$
$$C_1^{*0}=\left\{\mathbb{E}^*\left[\frac{\partial u_{1,t}^\top}{\partial\theta_1}\left(\tilde{y},\theta_1^0\right)\right]W_1\mathbb{E}^*\left[\frac{\partial u_{1,t}}{\partial\theta_1^\top}\left(\tilde{y},\theta_1^0\right)\right]\right\}^{-1}\mathbb{E}^*\left[\frac{\partial u_{1,t}^\top}{\partial\theta_1}\left(\tilde{y},\theta_1^0\right)\right]W_1,$$
$$\Gamma_{1,j}^*=\mathbb{E}^*\left[u_{1,t}\left(\tilde{y},\theta_1^0\right)u_{1,t-j}\left(\tilde{y},\theta_1^0\right)^\top\right].$$

where y and $\tilde{y}$ are short-hand notations for $\{y_t\}_{t=1}^T$ and $\{\tilde{y}_T^s(\xi)\}_{t=1}^T$, respectively.

Efficient weighting matrix

Proposition 4 (Asymptotic distribution of the optimal structural parameters)**.** *Under assumptions 1 - 7, 8, 9 and 10, and using the optimal weighting matrix*

$\Omega_1^*\left(\bar{\xi}_{22}\right) = \Phi_1^0(S, W_1)^{-1}$, *the optimal structural parameters estimates of* ξ_1^{**} *and* ξ_{21}^{**} *follow an asymptotic normal distribution*

$$\sqrt{T}\begin{pmatrix} \hat{\xi}_{1,TS}^{**}\left(\bar{\xi}_{22}\right) - \xi_1^0 \\ \hat{\xi}_{21,TS}^{**}\left(\bar{\xi}_{22}\right) - \xi_{21}^* \end{pmatrix} \xrightarrow{d} \mathcal{N}\left(0, \Sigma\left(S, \Omega_1^*\left(\bar{\xi}_{22}\right)\right)\right)$$

where the asymptotic covariance matrix is given by

$$\Sigma\left(S, \Omega_1^*\left(\bar{\xi}_{22}\right)\right) = \left\{ \frac{\partial \tilde{\theta}_1}{\partial \begin{pmatrix} \xi_1 \\ \xi_{21} \end{pmatrix}} \left(\xi_1^0, \xi_{21}^*\right)^\top \Phi_1^0\left(S, W_1\right)^{-1} \frac{\partial \tilde{\theta}_1}{\partial \begin{pmatrix} \xi_1 \\ \xi_{21} \end{pmatrix}^\top} \left(\xi_1^0, \xi_{21}^*\right) \right\}^{-1}.$$

Estimation of the asymptotic covariance matrix

For the calculation of $\Sigma\left(S, \Omega_1\right)$, we rely on Equations (2.B.1), (2.A.3), and (2.A.4) - (2.A.6) in Appendix 2.A.

The first building block is calculating V_1 and V_1^*, the variance-covariance matrices of the moment conditions in Equation (2.3.13) evaluated using the empirical data and the model simulated data, respectively. These are computed using the Newey and West (1987) method to account for serial correlation, up to the 10th order, between the moment conditions.

The next step is calculating C_1^0 and C_1^{*0} shown in Equations (2.A.4) and (2.A.5) for the empirical and simulated data, respectively. In our implementation, W_1 is chosen to be an identity matrix. Given all the necessary inputs, $\Phi_1^0\left(S, W_1\right)$ can now be calculated.

As 500 ensembles are simulated from the DSGE model for each parameter value, the second part of Equation (2.A.3) is evaluated 500 times for each of the ensembles, and the average is used to compute Φ_1^0.

Finally, $\Sigma(S, \Omega_1)$ is calculated using Equation (2.B.1). Again, Ω_1 is chosen to be an identity matrix to assign identical weights to the sensitivity of each instrumental parameter to changes in each of the structural parameters.

2.C Grid Search

To find the estimates of ξ_1, we initially perform a grid search for the ξ_1 parameter combination that returns the minimum value of the PII objective function described in Equation (2.3.9) and our choice of moment conditions given by Equation (2.3.13). The β grid ranges from 0.98 to 1.01 in increments of 0.001, and the $\overline{rra}$ grid is spanned between 15.5 and 39.5 in unit increments. As values of β close to 1 are reasonable, we allow for time preference rates larger than one to find a minimum within the grid. As for the $\overline{rra}$, we base our specification of the grid on the steady-state values reported in Campbell and Cochrane (1999) and Chen (2017). We use their steady-state relative risk aversion value, $\overline{rra} = 28.6$, in the middle of the grid and vary around it. Note that we fix the utility parameter $\gamma = 2$ and vary the steady state surplus consumption from 0.068 to 0.129.

The grid is minimized for values of $\beta = 1.001$ and $\overline{rra} = 22.5$ and the objective function is not flat around the minimum.

2.D Data

The empirical data used for the analysis of this study and shown in Tables 2.1, 2.2 and 2.4 are real U.S. post-war quarterly data from 1948 to 2012 and are chosen similar to Chen (2017). The data, together with their sources, are summarized in Table 2.D.1. The macroeconomic data are publicly available and can be easily retrieved. Output, consumption, investment, wages and capital are calculated from

quantities available in the National Income and Product Accounts (NIPA) with the exception of private fixed assets which is retrieved from Fixed Asset Tables (FAT). All the quantities are deflated using their price indices and divided by the population to get their real per capita values. Productivity, however, is mimicked by total factor productivity (TFP) which is retrieved from Fernald (2014).

Unlike the macroeconomic data, the financial time series are not publicly available. The risk-free rate is calculated as the forecast of the ex-post real return of the 90-day Treasury bill. The data needed for this forecast is the current treasury bill yield and the inflation rate for the past 12 months. The earlier is retrieved from the Center for Research in Security Prices (CRSP) while the latter is retrieved from the Bureau of Labor Statistics (BLS). Firm returns are calculated as the weighted average of the CRSP index and the Barclays U.S. corporate investment grade index. The latter is retrieved from Lehman Bond indices and is weighted by the firm value. Firm value, in turn, is calculated as debt plus market equity, both of which are retrieved from Compustat. Finally, Tobin's Q time series can be retrieved from FRED.

Table 2.D.1: Data sources

Variable	Data	Source	URL
Output	GDP	NIPA table 1.1.4	https://apps.bea.gov/iTable/iTable.cfm?reqid=19&step=4&isuri=1&categories=flatfiles
Consumption	Non durable goods	NIPA table 1.1.4	same as before
	Services	NIPA table 1.1.4	same as before
Investment	Private fixed investments	NIPA table 1.1.4	same as before
	Durable goods	NIPA table 1.1.4	same as before
Wages	Compensation of Employees	NIPA table 3.9.4	same as before
Capital	Durable goods	NIPA table 1.1.4	same as before
	Government fixed assets	NIPA table 1.1.4	same as before
	Private fixed assets	FAT table 1.1	https://apps.bea.gov/iTable/iTable.cfm?reqid=10&step=2&isuri=1
Productivity	Total Factor Productivity (TFP)	Fernald (2014)	http://www.johnfernald.net/TFP
Risk-free rate	Forecast of the 90-day Treasury bill	CRSP	Not available
Firm returns	Weighted average of CRSP	CRSP	Not available
	Barclays U.S. corporate investment grade index	Lehman Bond Indices from Datastream	Not available
CPI	Seasonally adjusted inflation	BLS	https://fred.stlouisfed.org/series/CPIAUCSL
Firm value	Debt and Market Equity	Compustat	Not available
Tobin's Q	Tobin's Q	FRED	Not available

Note: This table summarizes the U.S. post war empirical data used in the paper.

2.E Numerical solution of the model

To numerically solve the DSGE model, we rely on the projection method developed by Chen (2017).[15] The projection method entails a homotopy method, whereby the surplus consumption growth is added to the SDF in increments. This is done by including a parameter in the SDF that is an exponent, ν, to the surplus consumption growth, and thus controls its effect. This parameter ranges from zero to 1 in 11 incremental steps. At $\nu = 0$, the SDF is merely that of a power utility model, while at $\nu = 1$, the full extent of the external habit persistence model is included in the SDF. At each of these 11 steps, the model is solved, and the new solution is the starting point for the next step. The homotopy method helps stabilize the nonlinear solver.

At each of these incremental steps, the model is solved by discretizing the productivity process into 13 states using a 13-point Markov chain via the Rouwenhorst (1995) method. The laws of motion for capital and surplus consumption are approximated by two-dimensional cubic splines of 6th order and 8th order, respectively. Broyden's method is used to calculate the cubic spline coefficients that satisfy the firm's Euler equation given in Equation (2.2.9). Given the productivity states today and tomorrow as well as tomorrow's values for capital and surplus consumption that follow from their laws of motion, the remaining endogenous variables in the model can be simulated.

[15] Some of the MATLAB code is provided on his website `https://sites.google.com/site/chenandrewy/`. Our model solution is based on the code in the RFS folder.

2.F Details on the model solution

The firm's Euler equation

Chen (2017) claims that the habit in consumption leads to a consumption distortion. Due to that, the welfare theorems are no longer valid, and we cannot solve for an equilibrium using a social planner problem. A valid alternative in this setting is a recursive equilibrium which amounts to transforming the infinite-time problem into a recursive problem. Thus, we solve the problem via value functions which only depend on the value at time t and $t+1$

$$\begin{aligned} V(K';K,S,Z) = \max_{\{I,N,K'\}} & \left[\Pi(K,Z,N) - W(K,S,Z)N - \Phi(I,K) - I \right. \\ & \left. + \mathbb{E}_Z \left(M(K,S,Z;Z')V(K';K',S',Z')\right)\right], \\ \text{s.t.} \quad & K' = (1-\delta)K + I, \end{aligned}$$

where $V(\cdot)$ is the value function, K, S and Z are state variables that we can observe at time t which describe the state of the economy, and K'[16], I and N are called control variables which have to be chosen optimally at time t. The intuition is that given the optimal decision of these variables in $t+1$, what is the optimal choice at time t?

In order to make the optimization problem computationally less demanding, Chen (2017) discretizes the productivity process to a 13 point Markov-chain with a transition matrix $\pi_Z(Z_i, Z_j)$ which gives the probability of moving from state i in period t to state j in period $t+1$. Thus, the expected value and the optimization

[16] variables with ' denote values at time $t+1$

problem can be written in terms of a discrete random variable Z. When the economy is at state i in period t, its Bellman equation can be written as

$$V(K';K,S,Z_i) = \max_{\{I,N,K'\}} \Big[\Pi(K,Z_i,N) - W(K,S,Z_i)N - \Phi(I,K) - I + \sum_{Z_j} \pi_Z(Z_i,Z_j)M(K,S,Z_i;Z_j)V(K';K',S',Z_j)\Big],$$

$$\text{s.t.} \quad K' = (1-\delta)K + I.$$

A solution to this optimization problem consists of the F.O.C. w.r.t. labor which gives the equilibrium wage, the F.O.C. w.r.t. investment and the Envelope and firm's Euler equation. Equation (2.F.1) shows the equilibrium condition that sets the marginal productivity of labor equivalent to the wage:

$$\frac{\partial V}{\partial N} = \Pi_N(K,Z_i,N) - W(K,S,Z_i) \stackrel{!}{=} 0, \tag{2.F.1}$$

where Π_N denotes the derivative of the production function w.r.t. labor N.

Equation (2.F.2), in turn, denotes the F.O.C. w.r.t investment.

$$\begin{aligned} &\frac{\partial V}{\partial I} = -1 - \Phi_I(I,K) + \sum_{Z_j} \pi_Z(Z_i,Z_j)M(\cdot)\frac{\partial V}{\partial K'}\frac{\partial K'}{\partial I} \stackrel{!}{=} 0, \\ &\text{or} \quad 1 + \Phi_I(I,K) = \sum_{Z_j} \pi_Z(Z_i,Z_j)M(\cdot)V_{K'}(\cdot), \end{aligned} \tag{2.F.2}$$

where $V_{K'}(\cdot)$ is

$$\frac{\partial V}{\partial K'} = -\frac{\partial \Phi}{\partial I}\frac{\partial I}{\partial K'} - \frac{\partial I}{\partial K'} + \sum_{Z_j} \pi_Z(Z_i,Z_j)M(\cdot)\frac{\partial V}{\partial K'} \stackrel{!}{=} 0. \tag{2.F.3}$$

In order to solve the F.O.C. seen in Equation (2.F.3), we have to find the partial derivative of the value function w.r.t. K'. This can be done using the following trick

1. plug the optimal K' into the value function
2. take the partial derivative of the value function w.r.t. K

$$\frac{\partial V}{\partial K} = \Pi_K(K, Z_i, N) - \Phi_K(I, K) - \frac{\partial \Phi}{\partial I}\frac{\partial I}{\partial K} - \frac{\partial I}{\partial K}$$
$$V_K(\cdot) = \Pi_K(\cdot) + (1-\delta)(1 + \Phi_I(I, K)) - \Phi_K(I, K)$$

3. Envelope theorem: as in equilibrium K and K' are almost the same, we omit the partial derivative of K' w.r.t. K and the partial derivative of the value function w.r.t. K' can be obtained by iterating the derivative above one period forward:

$$V_{K'}(\cdot; Z_j) = \Pi_{K'}(K', Z_j, N') + (1-\delta)(1 + \Phi_{I'}(I_j, K')) - \Phi_{K'}(I_j, K')$$

4. Plug this partial derivative into the F.O.C. w.r.t. investment above and obtain the firm's Euler equation.

$$\begin{aligned}
\Phi_I(I, K) + 1 &= \sum_{Z_j} \pi_Z(Z_i, Z_j) M(\cdot) \left[\Pi_{K'}(K', Z_j, N') + (1-\delta)(1 + \Phi_{I'}(I_j, K')) - \Phi_{K'}(I_j, K')\right] \\
1 &= \sum_{Z_j} \pi_Z(Z_i, Z_j) M(\cdot) \frac{\Pi_{K'}(K', Z_j, N') + (1-\delta)(1 + \Phi_{I'}(I_j, K')) - \Phi_{K'}(I_j, K')}{\Phi_I(I, K) + 1} \\
1 &= \mathbb{E}_Z \left[M(\cdot) \frac{\Pi_{K'}(K', Z_j, N') + (1-\delta)(1 + \Phi_{I'}(I_j, K')) - \Phi_{K'}(I_j, K')}{\Phi_I(I, K) + 1} \right]
\end{aligned}$$

Household's Euler equation

Based on the intertemporal consumption and savings decision of the household, we obtain the usual Euler equation which holds for returns. The risky asset in this setting is investment and the Euler equation in terms of the return to investment R_I reads

$$\mathbb{E}_Z \left[M(K, S, Z_i; Z_j) R_I(K, S, Z_i; Z_j) \right] = 1,$$

or with the discretized productivity process we have

$$\sum_{Z_j} \pi_Z(Z_i, Z_j) M(K, S, Z_i; Z_j) R_I(K, S, Z_i; Z_j) = 1.$$

Equilibrium

The household does not value labor, i.e., $N = 1$ and we can obtain the return of investment by equating the two Euler equations which yields a state dependent return on investment

$$R_I(K, S, Z_i; Z_j) = \frac{\Pi_{K'}(K', Z_j, 1) + (1 - \delta)(1 + \Phi_{I'}(I_j, K')) - \Phi_{K'}(I_j, K')}{\Phi_I(I, K) + 1},$$

as the capital, labor and investment chosen by the firms and the households are the same in equilibrium.

We obtain the following equilibrium conditions:

$$1 = \mathbb{E}_Z \left[M(K, S, Z_i; Z_j) R_I(K, S, Z_i; Z_j) \right],$$

$$\text{with} \qquad R_I(K, S, Z_i; Z_j) = \frac{\Pi_{K'}(K', Z_j, 1) + (1-\delta)(1 + \Phi_{I'}(I_j, K')) - \Phi_{K'}(I_j, K')}{\Phi_I(I, K) + 1},$$

$$\text{where} \quad M = M(K, S, Z_i; Z_j) = \beta \left(\frac{C_j}{C} \frac{S_j}{S} \right)^{-\gamma}, \qquad \text{from household optimization,}$$

$$C_j = \Pi(K', Z_j, 1) - \Phi(I_j, K') - I_j, \qquad \text{from accounting identity,}$$

$$C = \Pi(K, Z_i, 1) - \Phi(I, K) - I,$$

$$K' = G(K, S, Z_i), \qquad \text{time-invariant policy function, solution to the Bellman equation,}$$

$$I = G(K, S, Z_i) - (1-\delta)K,$$

$$I_j = G(K', S', Z_j) - (1-\delta)K'$$

$$= G(G(K, S, Z_i), S', Z_j) - (1-\delta)G(K, S, Z_i),$$

and the evolution of surplus consumption satisfies

$$s_j = (1 - \rho_s)\bar{s} + \rho_s s + \lambda(c_j - c).$$

Chapter 3

The "Price" of Misspecification in DSGE Asset Pricing Models

3.1 Introduction

The econometric approach studied in Chapter 2 has relayed the concept of enclosing calibration within the folds of formal econometric methodology via the partial indirect inference (PII) estimation method from Dridi et al. (2007). Its main purpose is to circumvent the inaccuracies in statistical inference caused by potential, yet very likely, misspecification in the DSGE asset pricing model. The aim of the current chapter is to highlight, as well as to gauge against, the effect of such misspecification on the estimation quality of the models' parameter estimates and its statistically inferred key implications.

In order to achieve this aim, the PII method and its results are compared with two other estimation strategies; the classical Indirect Inference (II) method à la Gourieroux et al. (1993) that does not account for misspecification at all, and the full encompassing partial indirect inference (FII) method, also from Dridi et al. (2007), that allows for a certain degree of misspecification in the model. This chapter also

makes use of the recently developed "dark matter" measure in Chen et al. (2019) to quantify the degree of fragility entailed by each of the three different methodologies. The measure is used to challenge the findings of the previous chapter. These are primarily founded on the assumption that the source of potential misspecification in the DSGE asset prcing model is its representation of the macroeconomic dynamics. To provide an even field, the DSGE asset pricing model presented in Chen (2017) and discussed in Chapter 2 is used as the playground for the three estimation methodologies.

The concept of misspecification in the context of structural asset pricing models is well established in the literature. Ludvigson (2013) elegantly articulates the fact that misspecification is an inherent feature of asset pricing models, as the models are merely "abstractions and therefore by definition misspecified". The Hansen-Jaganathan distance, developed by Hansen and Jagannathan (1997), has long been used as a measure to compare between misspecified asset pricing models, see for example Hodrick and Zhang (2001), Chen and Ludvigson (2009), Kan and Robotti (2008), Almeida and Garcia (2012) and Antoine, Proulx and Renault (2020), among others. Other prominent examples such as Kan and Zhang (1999) and Gospodinov, Kan and Robotti (2014) construct misspecification-robust inference in the context of linear factor asset pricing models.

More recently, Chen et al. (2019) developed their dark matter measure to assess the fragility of asset pricing models towards their potentially misspecified moment conditions in the context of GMM estimation. Their empirical application demonstrates how the measure works in the context of two potentially misspecified models; a rare-disaster risk model and a long-run risk model with endowment economies. This chapter extends their study by applying this dark matter measure to a DSGE asset pricing model with external habit preferences. To the best of this author's

knowledge, this is the first study that attempts to assess the effects of misspecfication in the context of DSGE asset pricing models.

As discussed in the previous chapter, DSGE asset pricing models have been rather infamous since their introduction by Jermann (1998). They attempt to resolve the famous asset pricing puzzles while maintaining the macroeconomic business cycle dynamics. Their appeal also stems from the fact that they represent a more realistic portrayal of reality in comparison to the endowment economy setup that has thus far been considered in asset pricing models. In those endowment economies, the consumption process that generates the stochastic discount factor (SDF) responsible for pricing assets is assumed to be an exogenous process. DSGE asset pricing models, on the other hand, offer an endogenous consumption process that is generated from the macroeconomic dynamics embedded in the model.

It should be acknowledged that however complex the dynamics in the DSGE asset pricing model are, they cannot feasibly capture all the relevant aspects of economic reality. From an asset pricing perspective, there is more faith that the asset pricing part of the model is tailored to correctly reflect economic reality, as we rely on its SDF specification to price assets. On the other hand, the macroeconomic part of the model is only seen as a mimic of the economy that is necessary to fully parameterize the model and allow for simulations.

Given the source of the potential misspecification in the model, the econometrician needs to be aware of the drawbacks to the inferenctial statistics incurred by this particular misspecification. Additionally and as highlighted in the preceding chapter, DSGE asset pricing models are quite cumbersome when it comes to estimating their parameters and conducting econometric analysis. They often have intractable likelihood functions which halts any attempt towards their direct estimation. As will be shown in this chapter, this is where indirect inference estimation methods

come into play, as they are capable of accounting for these two obstacles in their econometric methodology.

The chapter starts by incorrectly assuming that there is no misspecification at all in the DSGE asset pricing model. In this case, Indirect Inference (II) estimation from Gourieroux et al. (1993) is used with a GMM model (Hansen, 1982) as its instrumental model to estimate all of the structural parameters (i.e. both asset pricing and macroeconomic parameters). Next, misspecification is accounted for by using the full encompassing indirect inference (FII) estimation strategy from Dridi et al. (2007). In this step, it is assumed that the instrumental GMM model fully encompasses the structural DSGE asset pricing model. This means that the set of moment restrictions provided in the GMM estimation are potentially able to identify all the parameters of the structural model.

In a further step, the GMM instrumental model is shrunk to only the set of moment constraints that identify the asset pricing parameters of interest. This means that it only partially encompasses the structural model, and only the parameters of interest will be estimated while the remaining (macroeconomic) nuisance parameters will be pinned down by calibration. This latter strategy is essentially the partial encompassing indirect inference (PII) estimation strategy from Dridi et al. (2007) that has been utilized in Chapter 2.

As previously explained, GMM estimation is used as the instrumental model with different sets of moment constraints that either fully or partially encompass the DSGE asset pricing model. Therefore, the dark matter measure developed by Chen et al. (2019) arises as a suitable metric to determine the degree of fragility that the full set of moment conditions impose on the estimation of the parameters of interest. Hypothetically, adding more informative moment constraints to the GMM estimation should result in reasonable point estimates with adequately tight and

economically reasonable confidence bounds, i.e., the parameters of interest should be better identified. However, if adding more moments to the GMM estimation results in having wider confidence bounds that span unreasonable values, then those additional moment constraints are introducing noise rather than information to the estimation process. Thus, examining the point estimates and confidence bounds that result from II, FII and PII estimations should serve as a means to determine whether the macroeconomic part of the model is indeed misspecified.

However, in a GMM context, tight confidence intervals are a result of smaller standard errors that come from asymptotic covariance matrices that have highly sensitive moment conditions to the estimated parameters. This is a desirable feature provided that the moment conditions come from a correctly specified model, as this is the basis of econometric estimation (see for example Andrews, Gentzkow and Shapiro, 2017). Yet, if there is potential misspecification, then this indicates that those moment conditions are susceptible to considerable change when the values of the parameters are changed. Thus, the key implications arising from the structural model are excessively sensitive to small changes in the data generating process (DGP). This is what is deemed by Chen et al. (2019) as model fragility and is accounted for using their dark matter measure.

In this paper, the dark matter measure is thus used to investigate the fragility of the macroeconomic moment conditions used in the GMM instrumental model. The measure is thought of as a second-layer filter to rule out the inclusion of macroeconomic moment conditions that suspiciously improve the identification of the asset pricing parameters of interest. Had the information from the dark matter measure not been considered, some macroeconomic parameters would have been mistakenly included in the estimation process as pseudo-parameters of interest. This is due to

the fact that the moment conditions necessary for their identification improve the overall identification of the parameters of interest as well.

Our findings confirm that the macroeconomic dynamics in the DSGE asset pricing model presented in Chen (2017) are indeed misspecified. The PII results from Chapter 2 yield the most economically reasonable point estimates with adequately tight confidence bounds. Adding the macroeconomic restrictions and attempting to estimate the entire model's parameters adds unnecessarily more noise rather than information to the process of identifying the parameters of interest. This results in unrealistically huge confidence bounds. The dark matter measure further confirms that the baseline moment restrictions in the GMM instrumental model are far more superior in identifying the asset pricing parameters of interest relative to the full moment constraints even when misspecification is accounted for using FII.

The only exception to this conclusion is the finding obtained from incrementally adding the macroeconomic moment conditions (and thus the macroeconomic parameters) to the estimation process to examine their individual effect. The results indicate that adding the second moment of the Gross Domestic Product (GDP) results in comparable point estimates and tight bounds for the asset pricing parameters. The dark matter measure further confirms that this additional moment condition has a negligible effect on the fragility of the model. It also slightly improves the asset pricing implications derived from the model. Therefore, it is worthwhile to expand the PII strategy from Chapter 2 to include this macroeconomic moment to the set of baseline moment restrictions in the instrumental GMM model.

The remainder of this chapter is organized as follows; Section 3.2 highlights the econometric methodology of this study. Specifically, Sections 3.2.1 and 3.2.2 outline the difference between the three different indirect inference methodologies utilized in this study, as well as their specific estimators and asymptotic distributions, respec-

tively. Section 3.2.3 tailors the specifications of the instrumental model underlying the three estimators to the DSGE asset pricing model used in the study, while Section 3.2.4 discusses the dark matter measure and adapts it also to this study. Section 3.3 presents the findings of the study as well as an in-depth analysis and critique of the results. Finally, Section 3.4 concludes.

3.2 Misspecification in estimation and inference

As previously highlighted, estimating the parameters of DSGE asset pricing models in general and the model in Chen (2017) specifically is a challenging undertaking. The complex dynamics depicted in those models render their likelihood functions intractable. A possible solution is to use II estimation as proposed by Smith (1993), Gourieroux et al. (1993) and Gallant and Tauchen (1996). Section 2.3 briefly explained the rationale behind the indirect inference methodology and how it provides a workaround for intractable likelihood functions via the use of an instrumental model whose parameters are easily estimated. The estimation of the DSGE structural parameters is then achieved by minimizing a quadratic loss function constructed using the instrumental parameters that are estimated twice; once using empirical data and once using simulated data from the DSGE asset pricing model that is dependent on the values of the structural parameters.

The main pillar, thus, of II estimation is the assumption that the data generating process (DGP) of the simulated data correctly mimics reality, i.e., that the DSGE asset pricing model is correctly specified. Yet, this is a very restrictive assumption. Dridi et al. (2007) offer a tailored II estimation methodology for DSGE models that accounts for potential misspecification in parts of the model. The authors have two methodological strategies depending on whether the instrumental model fully or partially encompasses the dynamics of the DSGE model; the FII estimation and the

PII estimation, respectively. The methodological strategy implemented in Chapter 2 is one possible application of PII estimation.

The binding function, as defined by Gourieroux et al. (1993) is what links the instrumental parameters estimated using simulated data to the structural parameters of the DSGE asset pricing model. The assumption governing how this binding function is formulated is the key difference between the three different estimation methodologies. In this section, I focus on where exactly the three methodologies, II, FII and PII, diverge in their formulation of the binding function and the resulting asymptotic distribution of their estimates. Appendix 3.A provides a summary of how the underlying assumptions governing the II and FII estimation differ from the outlined assumptions for PII given in Appendix 2.A. Similarly, Appendix 3.B provides an abridged version of how the derivation of the asymptotic distributions of II and FII estimation can be generalized from the detailed derivation given in Appendix 2.B.

The notation used follows closely that of Section 2.3 where the PII estimation strategy was first introduced and explained. This current section expands on this explanation to engulf the II and FII estimation strategies, thus making the methodologies governing the three strategies directly comparable.

3.2.1 The indirect inference methodology

Since the three methodologies have an underlying GMM instrumental model, I begin by examining how its k moment restrictions are represented using observable data

$$\mathbb{E}\left[u_t\left(\{y_t\}_{t-l}^{t},\theta\right)\right]=\mathbb{E}\begin{bmatrix}u_{1,t}\left(\{y_t\}_{t-l}^{t},\theta_1^0\right)\\ u_{2,t}\left(\{y_t\}_{t-l}^{t},\theta_2^0\right)\end{bmatrix}=0. \tag{3.2.1}$$

It is assumed in Equation (3.2.1) that the moment restrictions can be divided into two sets of separable moment conditions k_1 and k_2. The k_1 moment conditions $u_{1,t}\left(\{y_t\}_{t-l}^{t}, \theta_1\right)$ encompass the true part of the structural model, i.e., the part of the model that contains the structural parameters of interest ξ_1. The k_2 moment conditions $u_{2,t}\left(\{y_t\}_{t-l}^{t}, \theta_2\right)$ encompass the potentially misspecified part of the structural model, and thus should identify the nuisance structural parameters ξ_2.

It could be the case that the separability between the two sets of moment conditions is not quite clear cut. Therefore, the set of nuisance parameters ξ_2 is better defined as $\xi_2 = (\xi_{21}, \xi_{22})^\top$, where ξ_{21} represents a subset of the nuisance parameters that are identified by $u_{1,t}\left(\{y_t\}_{t-l}^{t}, \theta_1\right)$ as a by-product of identifying ξ_1. ξ_{22}, in this case, represents the subset of the nuisance structural parameters that are only identified from $u_{2,t}\left(\{y_t\}_{t-l}^{t}, \theta_2\right)$.

For identification, the number of moment restrictions has to be at least greater than the number of structural parameters, i.e. $k_1 = \dim \theta_1 \geq p_1 + p_{21} = \dim \xi_1 + \dim \xi_{21}$, and $k_2 = \dim \theta_2 \geq p_{22} = \dim \xi_{22}$. Next comes the GMM criterion function that would enable the instrumental parameters $\theta = (\theta_1, \theta_2)^\top$ to be estimated

$$\min_{\{\theta \in \Theta\}} \; Q_T\left(\{y_t\}_{t=1}^{T}, \theta\right), \tag{3.2.2}$$

$$\text{where} \quad Q_T\left(\{y_t\}_{t=1}^{T}, \theta\right) = \frac{1}{2}\, g_T\left(\{y_t\}_{t=1}^{T}, \theta\right)^\top \cdot \widehat{W}_T \cdot g_T\left(\{y_t\}_{t=1}^{T}, \theta\right), \tag{3.2.3}$$

$$g_T\left(\{y_t\}_{t=1}^{T}, \theta\right) = \frac{1}{T}\sum_{t=1}^{T} u_t\left(\{y_t\}_{t-l}^{t}, \theta\right), \tag{3.2.4}$$

with $\widehat{W}_T \xrightarrow{a.s.} W$, a positive semi-definite weighting matrix.

In II and FII estimation,

$$\hat{\theta}_T = \left(\hat{\theta}_1, \hat{\theta}_2\right)^\top = \underset{\{\theta \in \Theta\}}{\operatorname{argmin}} \; Q_T\left(\{y_t\}_{t=1}^{T}, \theta\right)$$

is a consistent estimator of $\theta^0 = (\theta_1^0, \theta_2^0)^\top$ which is the true value achieved at the probability limit using the observed data.

In PII estimation, as seen in Section 2.3.1, the econometrician considers calibrating the set of nuisance parameters ξ_{22}, as she believes that their estimation would only introduce noise to the estimation process since their value lacks any economic meaning. As such, the k_2 moment conditions $u_{2,t}\left(\{y_t\}_{t-l}^t, \theta_2\right)$ are removed from the set of moment restrictions. This is how the GMM criterion function in Equations (2.3.4) - (2.3.6) arise[1]. They are repeated here for convenience.

$$\min_{\{\theta_1 \in \Theta_1\}} \; Q_{1,T}\left(\{y_t\}_{t=1}^T, \theta_1\right), \tag{3.2.5}$$

$$\text{where} \quad Q_{1,T}\left(\{y_t\}_{t=1}^T, \theta_1\right) = \frac{1}{2}\, g_{1,T}\left(\{y_t\}_{t=1}^T, \theta_1\right)^\top \cdot \widehat{W}_{1,T} \cdot g_{1,T}\left(\{y_t\}_{t=1}^T, \theta_1\right), \tag{3.2.6}$$

$$g_{1,T}\left(\{y_t\}_{t=1}^T, \theta_1\right) = \frac{1}{T}\sum_{t=1}^{T} u_{1,t}\left(\{y_t\}_{t-l}^t, \theta_1\right), \tag{3.2.7}$$

with $\widehat{W}_{1,T} \xrightarrow{a.s.} W_1$, a positive semi-definite weighting matrix.

$$\hat{\theta}_{1,T} = \underset{\{\theta_1 \in \Theta_1\}}{\operatorname{argmin}} \; Q_{1,T}\left(\{y_t\}_{t=1}^T, \theta_1\right)$$

is a consistent estimator of θ_1^0.

Similarly, for the simulated data, the set of k moment restrictions can be represented as

$$\mathbb{E}\left[u_t\left(\{\tilde{y}_t^s(\xi)\}_{t-l}^t, \tilde{\theta}^0\left(\xi_1^0, \xi_{21}^*, \xi_{22}^*\right)\right)\right] = \mathbb{E}\begin{bmatrix} u_{1,t}\left(\{\tilde{y}_t^s(\xi)\}_{t-l}^t, \tilde{\theta}_1^0(\xi_1^0, \xi_{21}^*)\right) \\ u_{2,t}\left(\{\tilde{y}_t^s(\xi)\}_{t-l}^t, \theta_2^0(\xi_{22}^*)\right) \end{bmatrix} = 0, \tag{3.2.8}$$

[1]It also explains why all the quantites are indexed by 1, as the estimation is only dependent on the k_1 set of moment restrictions.

and a similar GMM criterion function is minimized to get the simulated instrumental parameters. Under II and FII estimation this is

$$\tilde{\theta}_T^s(\xi_1, \xi_{21}, \xi_{22}) = \underset{\{\theta \in \Theta\}}{\operatorname{argmin}} \; Q_T \left(\{\tilde{y}_T^s(\xi)\}_{t=1}^T, \theta^s \right).$$

Under the assumptions governing II estimation which do not account for misspecification in the structural model, $\tilde{\theta}_T^s(\xi_1, \xi_{21}, \xi_{22})$ is a consistent estimator of θ^0, as the DGP of the simulated data is assumed not to differ from that of the observed data. To account for misspecification, FII estimation considers that $\tilde{\theta}_T^s(\xi_1, \xi_{21}, \xi_{22})$ is a consistent estimator of $\tilde{\theta}^0\left(\xi_1^0, \xi_{21}^*, \xi_{22}^*\right)$, which is in turn the true value achieved at the probability limit using the simulated data.

In PII estimation, misspecification in the DGP of the simulated data as well as calibration of ξ_{22} parameters takes place. This is shown in the GMM criterion function in Equation (2.3.7), and is repeated here for convenience,

$$\tilde{\theta}_{1,T}^s(\xi_1, \xi_{21}, \bar{\xi}_{22}) = \underset{\{\theta_1 \in \Theta_1\}}{\operatorname{argmin}} \; Q_{1,T} \left(\{\tilde{y}_T^s(\xi)\}_{t=1}^T, \theta_1^s \right). \tag{3.2.9}$$

In this case, only $\tilde{\theta}_{1,T}^s(\xi_1, \xi_{21}, \bar{\xi}_{22})$ is a consistent estimator of $\tilde{\theta}_1^0\left(\xi_1^0, \xi_{21}^*\right)$.

The instrumental moment conditions in the GMM functions of the II and the FII estimators fully encompass the structural DSGE asset pricing model. The two estimators, however, differ in their formulation of the binding function. For II estimation, as no misspecification is handled here, the mapping at the probability limit between the instrumental parameters from the observed and the simulated data is assumed to be achieved at the true values of all the structural parameters, as shown below

$$\theta^0 = \tilde{\theta}^0(\xi_1^0, \xi_{21}^0, \xi_{22}^0). \tag{3.2.10}$$

Conversly in FII estimation, this mapping happens at the true values of the structural parameters of interest ξ_1, but only at pseudo-true values of the nuisance parameters $\xi_2 = (\xi_{21}, \xi_{22})^\top$, as misspecification is assumed in the dynamics governing those parameters. To show this, these parameters are denoted with an asterisk in the binding function

$$\theta^0 = \tilde{\theta}^0(\xi_1^0, \xi_{21}^*, \xi_{22}^*). \tag{3.2.11}$$

PII estimation requires that the instrumental model only partially encompasses the structural model, as the ξ_{22} parameters are calibrated in the estimation. Similar to the FII estimation, misspecification in the dynamics governing ξ_{21} is taken into consideration. The mapping in the binding function is assumed to be at the true values of the parameters of interest ξ_1 and only at pseudo-true values of ξ_{21}. Accordingly, the binding function can be stated as in Equation (2.3.8) which is repeated here for ease of comparison

$$\theta_1^0 = \tilde{\theta}_1^0(\xi_1^0, \xi_{21}^*). \tag{3.2.12}$$

The methodology implemented in Chapter 2 is thus an instance of PII estimation where there are no ξ_{21} nuisance parameters.

3.2.2 Estimators and asymptotic distributions

Given the explanation of the underlying instrumental GMM model and the binding functions of the three different indirect inference estimators, this subsection specifies the quadratic forms of the estimators as well as their asymptotic distributions. It starts with the FII estimator, as the two other methodologies can be specified as special cases from it. Through this formulation, it can be immediately recognized whether the different methodologies will result in different point estimates or whether the differences only impact the standard errors of the estimates.

Fully encompassing partial Indirect Inference (FII) estimation

The FII estimator can be defined as

$$\begin{pmatrix} \hat{\xi}_{1,TS} \\ \hat{\xi}_{21,TS} \\ \hat{\xi}_{22,TS} \end{pmatrix} = \underset{\{(\xi_1,\xi_{21},\xi_{22})\in\Xi_1\times\Xi_{21}\times\Xi_{22}\}}{\operatorname{argmin}} \left[\hat{\theta}_T - \frac{1}{S}\sum_{s=1}^{S}\tilde{\theta}_T^s(\xi_1,\xi_{21},\xi_{22})\right]^\top \cdot \widehat{\Omega}_T \cdot \left[\hat{\theta}_T - \frac{1}{S}\sum_{s=1}^{S}\tilde{\theta}_T^s(\xi_1,\xi_{21},\xi_{22})\right], \tag{3.2.13}$$

$$\hat{\theta}_T = \underset{\{\theta\in\Theta\}}{\operatorname{argmin}}\ Q_T\left(\{y_t\}_{t=1}^T,\theta\right), \tag{3.2.14}$$

$$\tilde{\theta}_T^s\left(\xi_1,\xi_{21},\xi_{22}\right) = \underset{\{\theta\in\Theta\}}{\operatorname{argmin}}\ Q_T\left(\{\tilde{y}_T^s(\xi)\}_{t=1}^T,\theta^s\right), \tag{3.2.15}$$

$$\widehat{\Omega}_T \xrightarrow{a.s.} \Omega. \tag{3.2.16}$$

Under the assumption of misspecification in the DGP and the other assumptions detailed in Appendix 3.A following Dridi et al. (2007), $\hat{\xi}_{1,TS}$ is a consistent estimate of ξ_1^0. Simultaneously $\hat{\xi}_{21,TS}$ and $\hat{\xi}_{22,TS}$ converge in the probability limit to the pseudo-true values ξ_{21}^* and ξ_{22}^*, respectively. The asymptotic distribution can, thus, be depicted as

$$\sqrt{T}\begin{pmatrix} \hat{\xi}_{1,TS} - \xi_1^0 \\ \hat{\xi}_{21,TS} - \xi_{21}^* \\ \hat{\xi}_{22,TS} - \xi_{22}^* \end{pmatrix} \xrightarrow{d} \mathcal{N}\left(0, \Sigma_{FII}\left(S,\Omega\right)\right). \tag{3.2.17}$$

Following the derivations in Appendix 3.B, $\Sigma_{FII}(S,\Omega)$ can then be formulated as

$$\begin{aligned}\Sigma_{FII}(S,\Omega) =& \left\{ \frac{\partial\tilde{\theta}}{\partial\begin{pmatrix}\xi_1\\ \xi_{21}\\ \xi_{22}\end{pmatrix}} \left(\xi_1^0,\xi_{21}^*,\xi_{22}^*\right)^\top \Omega \frac{\partial\tilde{\theta}}{\partial\begin{pmatrix}\xi_1\\ \xi_{21}\\ \xi_{22}\end{pmatrix}}^\top \left(\xi_1^0,\xi_{21}^*,\xi_{22}^*\right) \right\}^{-1} \\ & \cdot \frac{\partial\tilde{\theta}}{\partial\begin{pmatrix}\xi_1\\ \xi_{21}\\ \xi_{22}\end{pmatrix}} \left(\xi_1^0,\xi_{21}^*,\xi_{22}^*\right)^\top \Omega \quad \Phi_{FII}^0(S,W) \quad \Omega \frac{\partial\tilde{\theta}}{\partial\begin{pmatrix}\xi_1\\ \xi_{21}\\ \xi_{22}\end{pmatrix}}^\top \left(\xi_1^0,\xi_{21}^*,\xi_{22}^*\right) \\ & \cdot \left\{ \frac{\partial\tilde{\theta}}{\partial\begin{pmatrix}\xi_1\\ \xi_{21}\\ \xi_{22}\end{pmatrix}} \left(\xi_1^0,\xi_{21}^*,\xi_{22}^*\right)^\top \Omega \frac{\partial\tilde{\theta}}{\partial\begin{pmatrix}\xi_1\\ \xi_{21}\\ \xi_{22}\end{pmatrix}}^\top \left(\xi_1^0,\xi_{21}^*,\xi_{22}^*\right) \right\}^{-1}.\end{aligned} \tag{3.2.18}$$

$\Phi_{FII}^0(S,W)$ here represents the asymptotic covariance matrix resulting from the underlying instrumental GMM model. This can be written explicitly as

$$\Phi_{FII}^0(S,W) = C^0 V C^{0\top} + \frac{1}{S} C^{*0} V^* C^{*0\top}, \tag{3.2.19}$$

and its separate constituents are[2]

$$C^0 = \left\{ \mathbb{E}\left[\frac{\partial u_t^\top}{\partial \theta} \left(y, \theta^0 \right) \right] W \mathbb{E}\left[\frac{\partial u_1}{\partial \theta^\top} \left(y, \theta^0 \right) \right] \right\}^{-1} \mathbb{E}\left[\frac{\partial u_t^\top}{\partial \theta} \left(y, \theta^0 \right) \right] W, \tag{3.2.20}$$

$$V = \Gamma_0 + \sum_{j=1}^{\infty} \left(\Gamma_j + \Gamma_j^\top \right), \tag{3.2.21}$$

$$\Gamma_j = \mathbb{E}\left[u_t \left(y, \theta^0 \right) u_{t-j} \left(y, \theta^0 \right)^\top \right], \tag{3.2.22}$$

$$C^{*0} = \left\{ \mathbb{E}^*\left[\frac{\partial u_t^\top}{\partial \theta} \left(\tilde{y}, \theta^0 \right) \right] W \mathbb{E}^*\left[\frac{\partial u_t}{\partial \theta^\top} \left(\tilde{y}, \theta^0 \right) \right] \right\}^{-1} \mathbb{E}^*\left[\frac{\partial u_t^\top}{\partial \theta} \left(\tilde{y}, \theta^0 \right) \right] W, \tag{3.2.23}$$

$$V^* = \Gamma_0^* + \sum_{j=1}^{\infty} \left(\Gamma_j^* + \Gamma_j^{*\top} \right), \tag{3.2.24}$$

$$\Gamma_j^* = \mathbb{E}^*\left[u_t \left(\tilde{y}, \theta^0 \right) u_{t-j} \left(\tilde{y}, \theta^0 \right)^\top \right]. \tag{3.2.25}$$

Indirect Inference (II) estimation

The II estimator is similar to Equations (3.2.13) to (3.2.16). This is not surprising, as the underlying instrumental GMM model is specified in the same way for both sets of estimates such that it fully encompass the structural DSGE model. Therefore, the point estimates obtained using both FII and II methodologies are identical. The main difference between the two methodologies, thus, lies in their inference. II estimation does not allow for misspecification in the structural DSGE model, and hence assumes that the DGP of the simulated series is identical to that of the observed data. Following Gourieroux et al. (1993), the assumptions detailed in Appendix 3.A entail that the entire set of $\hat{\xi}_{TS} = \left(\hat{\xi}_{1,TS}, \hat{\xi}_{21,TS}, \hat{\xi}_{22,TS} \right)$ is a consistent estimate of $\xi^0 = \left(\xi_1^0, \xi_{21}^0, \xi_{22}^0 \right)$.

[2]For ease of notation, $\{y_t\}_{t=1}^T$, representing the observed series, and $\{\tilde{y}_T^s(\xi)\}_{t=1}^T$, representing the simulated series, are replaced by y and $\tilde{y}$, respectively.

The asymptotic distribution can be depicted as

$$\sqrt{T}\begin{pmatrix}\hat{\xi}_{1,TS}-\xi_1^0\\ \hat{\xi}_{21,TS}-\xi_{21}^0\\ \hat{\xi}_{22,TS}-\xi_{22}^0\end{pmatrix}\xrightarrow{d}\mathcal{N}\left(0,\Sigma_{II}\left(S,\Omega\right)\right). \tag{3.2.26}$$

Following the derivations in Appendix 3.B, $\Sigma_{II}\left(S,\Omega\right)$ can be formulated as

$$\begin{aligned}\Sigma_{II}\left(S,\Omega\right)=&\left\{\frac{\partial\tilde{\theta}}{\partial\begin{pmatrix}\xi_1\\ \xi_{21}\\ \xi_{22}\end{pmatrix}}\left(\xi_1^0,\xi_{21}^0,\xi_{22}^0\right)^\top\Omega\frac{\partial\tilde{\theta}}{\partial\begin{pmatrix}\xi_1\\ \xi_{21}\\ \xi_{22}\end{pmatrix}}^\top\left(\xi_1^0,\xi_{21}^0,\xi_{22}^0\right)\right\}^{-1}\\ &\cdot\frac{\partial\tilde{\theta}}{\partial\begin{pmatrix}\xi_1\\ \xi_{21}\\ \xi_{22}\end{pmatrix}}\left(\xi_1^0,\xi_{21}^0,\xi_{22}^0\right)^\top\Omega\quad\Phi_{II}^0\left(S,W\right)\quad\Omega\frac{\partial\tilde{\theta}}{\partial\begin{pmatrix}\xi_1\\ \xi_{21}\\ \xi_{22}\end{pmatrix}}^\top\left(\xi_1^0,\xi_{21}^0,\xi_{22}^0\right)\\ &\cdot\left\{\frac{\partial\tilde{\theta}_1}{\partial\begin{pmatrix}\xi_1\\ \xi_{21}\\ \xi_{22}\end{pmatrix}}\left(\xi_1^0,\xi_{21}^0,\xi_{22}^0\right)^\top\Omega\frac{\partial\tilde{\theta}}{\partial\begin{pmatrix}\xi_1\\ \xi_{21}\\ \xi_{22}\end{pmatrix}}^\top\left(\xi_1^0,\xi_{21}^0,\xi_{22}^0\right)\right\}^{-1}.\end{aligned} \tag{3.2.27}$$

Note that the two Equations (3.2.18) and (3.2.27) are formulated very similarly. Notation-wise, the only difference between them comes from the superscript notation differences in ξ_{21} and ξ_{22}. The former equation indicates that the derivatives are evaluated at the true values of the parameters, while in the latter the pseudo-true values are used. Yet, a substantial difference comes from the way $\Phi^0\left(S,W\right)$ is specified. In II estimaton, since the DGP of the simulated series is assumed to be identical to that of the observed data,

C^0 and C^{*0} from Equations (3.2.20) and (3.2.23) are assumed to be identical. Thus, $\Phi^0_{II}(S,W)$ can be specifed as

$$\Phi^0(S,W) = \left(1 + \frac{1}{S}\right) C^0 V {C^0}^\top, \tag{3.2.28}$$

where its constituents are defined similar to Equations (3.2.20) - (3.2.22).

Partial encompassing partial Indirect Inference (PII) estimator

In PII estimation, calibration is formally incorporated into the estimation strategy. As explained previously, the set of structural nuisance parameters, ξ_{22}, are not estimated in this setting, but rather remain fixed at appropriate values required for the structural model to deliver sensible economic implications. The estimator is defined as in Equation (2.3.9), and is repeated here for convenience

$$\begin{aligned}\begin{pmatrix} \hat{\xi}_{1,TS}(\bar{\xi}_{22}) \\ \hat{\xi}_{21,TS}(\bar{\xi}_{22}) \end{pmatrix} = \underset{\{(\xi_1,\xi_{21})\in\Xi_1\times\Xi_{21}\}}{\operatorname{argmin}} & \left[\hat{\theta}_{1,T} - \frac{1}{S}\sum_{s=1}^{S}\tilde{\theta}^s_{1,T}(\xi_1,\xi_{21},\bar{\xi}_{22})\right]^\top \cdot \widehat{\Omega}_{1,T} \\ & \cdot \left[\hat{\theta}_{1,T} - \frac{1}{S}\sum_{s=1}^{S}\tilde{\theta}^s_{1,T}(\xi_1,\xi_{21},\bar{\xi}_{22})\right],\end{aligned} \tag{3.2.29}$$

$$\hat{\theta}_{1,T} = \underset{\{\theta_1\in\Theta_1\}}{\operatorname{argmin}}\ Q_{1,T}\left(\{y_t\}_{t=1}^T, \theta_1\right), \tag{3.2.30}$$

$$\tilde{\theta}^s_{1,T}\left(\xi_1,\xi_{21},\bar{\xi}_{22}\right) = \underset{\{\theta_1\in\Theta_1\}}{\operatorname{argmin}}\ Q_{1,T}\left(\{\tilde{y}^s_T(\xi)\}_{t=1}^T, \theta^s_1\right), \tag{3.2.31}$$

$$\widehat{\Omega}_{1,T} \xrightarrow{a.s.} \Omega_1. \tag{3.2.32}$$

It can be seen here that the estimates for $\hat{\xi}_{1,TS}(\bar{\xi}_{22})$ and $\hat{\xi}_{21,TS}(\bar{\xi}_{22})$ are expected to be different than the ones provided by FII and II, as the underlying instrumental GMM model is reduced to only the baseline moment restrictions $u_{1,t}(y,\theta_1)$. The loss of the information provided by $u_{2,t}(y,\theta_2)$ is expected to affect the point estimates of $\hat{\xi}_{1,TS}(\bar{\xi}_{22})$ and $\hat{\xi}_{21,TS}(\bar{\xi}_{22})$.[3]

[3]This is true as long as $\frac{1}{T}\sum_{t=1}^{T}\frac{\partial u^\top_{2,t}}{\partial\theta_1}\left(\{y_t\}_{t=1}^T,\theta_2\right) \neq 0$

The partial encompassing hypothesis in Dridi et al. (2007) along with the necessary assumptions, as highlighted in Appendix 2.A, stipulate that only $\hat{\xi}_{1,TS}(\bar{\xi}_{22})$ is a consistent estimator of ξ_1^0, while $\hat{\xi}_{21,TS}(\bar{\xi}_{22})$ converges to a pseudo-true value ξ_{21}^* in the limit. The asymptotic distribution is then

$$\sqrt{T}\begin{pmatrix}\hat{\xi}_{1,TS}\left(\bar{\xi}_{22}\right)-\xi_1^0\\ \hat{\xi}_{21,TS}\left(\bar{\xi}_{22}\right)-\xi_{21}^*\end{pmatrix}\xrightarrow{d}\mathcal{N}\left(0,\Sigma_{PII}\left(S,\Omega_1\right)\right) \tag{3.2.33}$$

where $\Sigma_{PII}\left(S,\Omega_1\right)$ is depicted as

$$\begin{aligned}\Sigma_{PII}\left(S,\Omega_1\right)=&\left\{\frac{\partial\tilde{\theta}_1}{\partial\begin{pmatrix}\xi_1\\ \xi_{21}\end{pmatrix}}\left(\xi_1^0,\xi_{21}^*\right)^\top\Omega_1\frac{\partial\tilde{\theta}_1}{\partial\begin{pmatrix}\xi_1\\ \xi_{21}\end{pmatrix}^\top}\left(\xi_1^0,\xi_{21}^*\right)\right\}^{-1}\frac{\partial\tilde{\theta}_1}{\partial\begin{pmatrix}\xi_1\\ \xi_{21}\end{pmatrix}}\left(\xi_1^0,\xi_{21}^*\right)^\top\Omega_1\\ &\cdot\Phi_1^0\left(S,W_1\right)\Omega_1\frac{\partial\tilde{\theta}_1}{\partial\begin{pmatrix}\xi_1\\ \xi_{21}\end{pmatrix}^\top}\left(\xi_1^0,\xi_{21}^*\right)\left\{\frac{\partial\tilde{\theta}_1}{\partial\begin{pmatrix}\xi_1\\ \xi_{21}\end{pmatrix}}\left(\xi_1^0,\xi_{21}^*\right)^\top\Omega_1\frac{\partial\tilde{\theta}_1}{\partial\begin{pmatrix}\xi_1\\ \xi_{21}\end{pmatrix}^\top}\left(\xi_1^0,\xi_{21}^*\right)\right\}^{-1}.\end{aligned} \tag{3.2.34}$$

Similar to FII estimation, misspecification in the DGP of the simulated series is taken into consideration. Accordingly, $\Phi_1^0\left(S,W_1\right)$ can be viewed as the upper left quadrant of the FII matrix $\Phi_{FII}^0\left(S,W\right)$ and is presented as follows

$$\Phi_1^0\left(S,W_1\right)=C_1^0V_1{C_1^0}^\top+\frac{1}{S}C_1^{*0}V_1^*{C_1^{*0}}^\top, \tag{3.2.35}$$

with its constituents being

$$
\begin{aligned}
C_1^0 &= \left\{ \mathbb{E}\left[\frac{\partial u_{1,t}^\top}{\partial \theta_1}\left(y, \theta_1^0\right) \right] W_1 \mathbb{E}\left[\frac{\partial u_{1,t}}{\partial \theta_1^\top}\left(y, \theta_1^0\right) \right] \right\}^{-1} \mathbb{E}\left[\frac{\partial u_{1,t}^\top}{\partial \theta_1}\left(y, \theta_1^0\right) \right] W_1, \\
V_1 &= \Gamma_{1,0} + \sum_{j=1}^{\infty} \left(\Gamma_{1,j} + \Gamma_{1,j}^\top \right), \\
\Gamma_{1,j} &= \mathbb{E}\left[u_{1,t}\left(\tilde{y}, \theta_1^0\right) u_{1,t-j}\left(\tilde{y}, \theta_1^0\right)^\top \right], \\
C_1^{*0} &= \left\{ \mathbb{E}^*\left[\frac{\partial u_{1,t}^\top}{\partial \theta_1}\left(\tilde{y}, \theta_1^0\right) \right] W_1 \mathbb{E}^*\left[\frac{\partial u_{1,t}}{\partial \theta_1^\top}\left(\tilde{y}, \theta_1^0\right) \right] \right\}^{-1} \mathbb{E}^*\left[\frac{\partial u_{1,t}^\top}{\partial \theta_1}\left(\tilde{y}, \theta_1^0\right) \right] W_1, \\
V_1^* &= \Gamma_{1,0}^* + \sum_{j=1}^{\infty} \left(\Gamma_{1,j}^* + \Gamma_{1,j}^{*\top} \right), \\
\Gamma_{1,j}^* &= \mathbb{E}^*\left[u_{1,t}\left(\tilde{y}, \theta_1^0\right) u_{1,t-j}\left(\tilde{y}, \theta_1^0\right)^\top \right].
\end{aligned}
$$

Now that the asymptotic distributions of the different estimators have been defined, the next step is to tailor their specification to the DSGE asset pricing model developed in Chen (2017) and discussed in details in Section 2.2. Since the specification of the PII estimator has been previously discussed in Section 2.3.2, the next section follows along the same lines to explain how this specification can be expanded to accommodate both the II and FII estimators as well.

3.2.3 Specifying the instrumental model - an expanded version

The natural beginning is to classify the structural parameters into those of interest, ξ_1, and those which are considered nuisance, $\xi_2 = (\xi_{21}, \xi_{22})^\top$. The same lines of argument used in Section 2.3.2 are followed; specifically, that the asset pricing part of the model is seen to correctly reflect economic reality, while the macroeconomic part of the model only abstractedly mimics the economy. This argument was briefly commented on in Section 2.3.2, and this section fully elaborates on why this is considered sensible.

Two arguments support this view; first, the asset pricing dynamics represented in the model are characterized by two structural parameters; the time preference rate, β, and

the steady-state relative risk aversion parameter, $\overline{rra} = \gamma/\bar{S}$. The time preference rate reflects the representative agent's intuitive preference for consumption today rather than tomorrow. Microeconomic experiments have indeed confirmed that this value should be smaller than unity (see for example, Samuelson, 1938 and Ainslie, 1992). The steady-state relative risk aversion parameter is linked to the curvature of the utility function and its value has been determined in the literature using Arrow-Debreu pricing experiments. Mehra and Prescott (1985) presume that an appropriate range is between 1 and 5. The second argument is that, as result of those parameter values, real financial quantities can be determined; namely, the risk-free rate and the market equity premium. The latter is a traded quantity whose value can be checked, and the former is regularly reported by central banks.

The macroeconomic part of the model, on the contrary, contains quantities and parameters that are more difficult to pinpoint either by experiments or by examining the economy. For example, the capital adjustment costs parameter, ϕ, is arbitrarily set at a certain value to constrain the quantity of capital generated by the model. Additionally, the Cobb-Douglas production function in the DSGE model does not have an empirical equivalent. Furthermore, there is still an on-going prominent debate among macroeconomic theorists on how to adequately measure aggregate capital in the first place.

Therefore, and similar to Section 2.3.2, the asset pricing parameters of interest that should be consistently estimated using the different estimation methodologies are $\xi_1 = (\beta, \overline{rra})^\top$, while all the other parameters in the model should be considered nuisance parameters $\xi_2 = \xi_{22} = (\rho_s, \alpha, \delta, \phi, \mu, \rho_z, \sigma_z)^\top$. In this setup, no ξ_{21} parameters are defined. However, it turns out, that for FII and II estimation strategies, the estimation of the entire set of structural parameters is quite cumbersome. In spite of having moments that allegedly should identify all the parameters in ξ_{22}, as specified in Table 2.1, the quadratic function in Equation (3.2.13) did not converge using the none gradient-based Nelder-Mead optimizer. A series of trial and error experiments lead to a shrinkage in the set of nuisance parameters to $\xi_{22} = (\rho_s, \phi, \sigma_z)^\top$. The rest of the parameters $(\alpha, \delta, \mu, \rho_z)^\top$ are

then considered as auxiliary parameters and are left calibrated at the values proposed in Table 2.1. In this context, the FII and II estimation strategies entail an instrumental model that does not truly fully encompass the structural DSGE asset pricing model as presumed. However, they still provide a fuller encompassing representation of the structural model than the PII strategy. Thus, the premise of the study remains intact.

To identify the structural parameters of interest, ξ_1, the scheme presented in Section 2.3.2 is again followed, as it is derived by the model-implied Equations (2.2.11) and (2.2.12) where those parameters appear. Therefore, the time preference rate, β, is identified by the first two moments of the risk-free rate $\mathbb{E}(R_t^f)$ and $\sigma^2(R_t^f)$, while the steady-state relative risk aversion, $\overline{rra}$ is identified via the first two moments of the equity premium; $\mathbb{E}(R_{m,t}^e)$ and $\sigma^2(R_{m,t}^e)$, respectively.

To identify the set of nuisance parameters $\xi_{22} = (\rho_s, \phi, \sigma_z)^\top$, the moment conditions considered in Chen (2013)[4] in his simulated methods of moments (SMM) estimation are followed. In this case, the volatility of productivity, σ_z, is identified from the volatility of GDP. Therefore, the first two moments of GDP are considered, $\mathbb{E}(Y_t)$ and $\sigma^2(Y_t)$, respectively. The adjustment cost parameter ϕ is identified from the relative volatility of consumption to GDP. Since this is a ratio, it cannot be ensured that its sample counterpart converges in probability to its population value.[5] Therefore, the paper opts to just add the first two moments of consumption, $\mathbb{E}(C_t)$ and $\sigma^2(C_t)$, respectively, to the set of moment conditions, as the first two moments of GDP are already considered.

The most troublesome parameter to identify is the persistence of surplus consumption, ρ_s. Chen (2013) identifies it from the volatility of the equity premium which is inherently its second moment and is already used in the identification of ξ_1. Additionally, the parameter also appears in Equation (2.2.11) as an integral part of the model-implied risk-free rate. The question then arises whether ρ_s should be considered as a parameter in ξ_{21}. It turns out that the objective function under this variant does not converge, which makes

[4]This is the working paper version of the DSGE asset pricing model in Chen (2017).

[5]This is similar to the argument in Section 2.3.2 about why the Sharpe ratio could not be used in the set of moment restrictions in Equation (2.3.13).

this identification scheme for ρ_s rather doubtful. Other possibilities from the literature include using the first order autocorrelation of the price-dividend ratio. This is, however, left for future research.

The set of k moment conditions can then be written specifically for the DSGE asset pricing model as follows

$$\mathbb{E}\left[u_t\left(\{y_t\}_{t-l}^{t},\theta\right)\right]=\mathbb{E}\begin{bmatrix}u_{1,t}\left(\{y_t\}_{t-l}^{t},\theta_1^0\right)\\ \hdashline u_{2,t}\left(\{y_t\}_{t-l}^{t},\theta_2^0\right)\end{bmatrix}=\mathbb{E}\left[\begin{array}{c}R_t^f-\mu_{R_f}\\ R_{m,t}^e-\mu_{R_m^e}\\ (R_{m,t}^e)^2-(\mu_{R_m^e})^2-\sigma_{R_m^e}^2\\ (R_t^f)^2-(\mu_{R_f})^2-\sigma_{R_f}^2\\ \hdashline Y_t-\mu_Y\\ (Y_t)^2-(\mu_Y)^2-\sigma_Y^2\\ C_t-\mu_C\\ (C_t)^2-(\mu_C)^2-\sigma_C^2\end{array}\right]=0, \tag{3.2.36}$$

and the set of instrumental parameters for the PII estimation is $\theta_1=\left(\mu_{R_f},\mu_{R_m^e},\sigma_{R_m^e}^2,\sigma_{R_f}^2\right)^\top$, while for FII and II estimation, $\theta=\left(\mu_{R_f},\mu_{R_m^e},\sigma_{R_m^e}^2,\sigma_{R_f}^2,\mu_Y,\sigma_Y^2,\mu_C,\sigma_C^2\right)^\top$.

After explicitly detailing the three different indirect inference estimation methodologies that will be used as well as specifying their underlying instrumental GMM model, the next step is to formulate a quantifiable comparison between them. Towards this end, the dark matter measure developed in Chen et al. (2019) is utilized. This is explained in the next section.

3.2.4 The dark matter measure

The dark matter measure, as pioneered by Chen et al. (2019), is a metric used to quantify the extent of model fragility in potentially misspecified models that have a GMM setup. Model fragility, as defined by the authors, refers to the extent to which the moment conditions used in the GMM estimation are excessively sensitive to small changes

in the parameter values that they are supposed to identify. The authors argue that such sensitivity, while perceived as highly desirable in a correctly specified model, may render potentially misspecified models fragile, as it implies that a small change in the DGP can considerably distort the key implications of the model. The measure goes beyond regular statistical inference to convey that achieving economically meaningful and tight confidence bounds for parameter estimates is a desirable goal. Yet, it should be achieved by moment conditions that are not excessively fragile.

Fragility of the moment conditions has dire consequences, as shown by the authors. It manifests in the loss of power of the specification tests, which means that the model cannot be rejected by the empirical data. It, also, causes the model to have poor out-of-sample performance. Those two consequences of model fragility are however not investigated here and are left for future research. This study rather uses the dark matter measure as a tool of comparison between the different asymptotic variance-covariance matrices resulting from the three different estimation methodologies described in Section 3.2.2. This is because it is essentially a ratio between two asymptotic variance-covariance matrices; one computed using the baseline moment conditions, which are assumed to be correctly specified, and the other using the full set of moment conditions which may be misspecified.

This study adapts the authors' ratio to accommodate the setup of the indirect inference methodologies. Here, it is perceived that the baseline model is the PII estimation strategy with only the set of $\mathbb{E}\left[u_{1,t}(\{y_t\}_{t=1}^{T}, \theta_1)\right]$ as the moment conditions in the underlying GMM instrumental model. The full model is alternatively considered to be: once the FII estimation strategy, and once the II estimation strategy. This will ultimately provide further confirmation that the source of potential misspecification in the model comes from the part of the model that is concerned with the macroeconomic dynamics. It will, also, serve as a means towards identifying the best set of moment conditions to be put in the GMM instrumental model. This should then help in achieving the best possible identification scheme for the structural parameters of interest. The notation in Chen et al. (2019)

is followed as closely as possible while maintaining consistency with the notation that has thus far been used.

Setup

The asymptotic variance-covariance matrices for the full model, i.e. the FII and the II estimation strategies in Section 3.2.2 can be re-written as

$$\Sigma_F^m = D \cdot \Phi_m^0 \cdot D^\top \tag{3.2.37}$$

where $m = \{\text{FII, II}\}$ depending on the estimation strategy considered[6], and

$$D = \left\{ \frac{\partial \tilde{\theta}}{\partial \begin{pmatrix} \xi_1 \\ \xi_{21} \\ \xi_{22} \end{pmatrix}} \left(\xi_1^0, \xi_{21}^*, \xi_{22}^*\right)^\top \cdot \Omega \cdot \frac{\partial \tilde{\theta}}{\partial \begin{pmatrix} \xi_1 \\ \xi_{21} \\ \xi_{22} \end{pmatrix}^\top} \left(\xi_1^0, \xi_{21}^*, \xi_{22}^*\right) \right\}^{-1} \cdot \frac{\partial \tilde{\theta}}{\partial \begin{pmatrix} \xi_1 \\ \xi_{21} \\ \xi_{22} \end{pmatrix}} \left(\xi_1^0, \xi_{21}^*, \xi_{22}^*\right)^\top \cdot \Omega.$$

Similarly, for the baseline model, the asymptotic variance-covariance matrix can be visualized as

$$\Sigma_B = \Sigma_{PII} = D_1 \cdot \Phi_1^0 \cdot D_1^\top \tag{3.2.38}$$

where

$$D_1 = \left\{ \frac{\partial \tilde{\theta}_1}{\partial \begin{pmatrix} \xi_1 \\ \xi_{21} \end{pmatrix}} \left(\xi_1^0, \xi_{21}^*\right)^\top \cdot \Omega_1 \cdot \frac{\partial \tilde{\theta}_1}{\partial \begin{pmatrix} \xi_1 \\ \xi_{21} \end{pmatrix}^\top} \left(\xi_1^0, \xi_{21}^*\right) \right\}^{-1} \cdot \frac{\partial \tilde{\theta}_1}{\partial \begin{pmatrix} \xi_1 \\ \xi_{21} \end{pmatrix}} \left(\xi_1^0, \xi_{21}^*\right)^\top \cdot \Omega_1.$$

[6]Note that ξ_{21} is denoted with $*$ here. This is because it can be considered a true value, ξ_{21}^0, or a pseudo-true value, ξ_{21}^*, depending on whether the estimation strategy is II or FII, respectively. The same argument is followed for ξ_{22}.

Note that Σ_{PII} is the upper-left quadrant of Σ_{FII}. Hence, the usage of the subscript 1 in the notation. It is, however, not true for II, as Φ^0_{II} does not allow for misspecification in the DGP. Nevertheless, the subscript notation is maintained for convenience.

Chen et al. (2019) formulate the dark matter measure in terms of the information matrices computed from using the full GMM moment conditions relative to only the baseline moment conditions. This argument is also followed here, and thus

$$\mathbf{I}_F = (\Sigma^m_F)^{-1} = \left(D \cdot \Phi^0_m \cdot D^\top\right)^{-1}, \tag{3.2.39}$$

$$\mathbf{I}_B = (\Sigma_B)^{-1} = \left(D_1 \cdot \Phi^0_1 \cdot D_1^\top\right)^{-1}. \tag{3.2.40}$$

It should be noted, however, that in this study unlike that of Chen et al. (2019), all of the weighting matrices used are chosen to be identity matrices rather than the efficient weighting matrices. This choice enables a direct comparison between the three different estimators, as the minimization problem across all of the instrumental parameters is given equal weights. Accordingly, W and W_1, necessary for the development of Φ^0_m and Φ^0_1, respectively, as well as Ω and Ω_1 are all identity matrices. As such, the inverse of Σ^m_F and Σ_B in Equations (3.2.39) and (3.2.40) are accurately described as precision matrices rather than information matrices. The notation $\mathbf{I}_F$ and $\mathbf{I}_B$ is however maintained to match the notation in Chen et al. (2019).

This study is interested in investigating how much the full encompassing models, FII and II, impact the inferences of the parameters of interest, ξ_1, relative to the baseline partial encompassing model, PII. As such, we depict the marginal precision matrix

$$\mathbf{I}_{mF} = \Lambda \cdot \mathbf{I}_F^{-1} \cdot \Lambda^T \quad \text{with} \quad \Lambda = \left[I_{p_1} \mathbf{0}_{p_1 \times (p_{21}+p_{22})}\right], \tag{3.2.41}$$

which conveys the additional information (or noise?) imposed on the inference of the asset pricing parameters $\xi_1 = (\beta, \overline{rra})^\top$ by adding the macroeconomic moment conditions to the

underlying GMM model. The additional information imparted by this marginal precision matrix relative to the baseline precision matrix can be depicted as

$$\Pi = \mathbf{I}_{mF}^{1/2}\mathbf{I}_{B}^{-1}\mathbf{I}_{mF}^{1/2} - I_{p_1}. \tag{3.2.42}$$

Had we been interested in only one structural parameter, the value of Π would have been sufficient as the dark matter measure. However, since this is a multidimensional problem, the dark matter measure is then computed as the largest eigenvalue value of Π. This is formally defined by Chen et al. (2019) as

$$\vartheta(\xi_1) = \max v^{\top}\Pi v, \tag{3.2.43}$$

where v represents the matrix of eigenvectors of Π. This number then represents the maximum degree of fragility inherent in the model along all linear dimensions.

It is important to understand what this resulting number represents. The size of this measure indicates how much more information the marginal precision matrix of the full model adds that is relevant to the estimation of the ξ_1 parameters. As previously explained, this marginal precision matrix results from the information obtained from the set of instrumental parameters, θ_2, which in turn are identified from the potentially misspecified moment conditions. Therefore, the higher the size of $\vartheta(\xi_1)$, the more fragile the estimation of ξ_1, as it is excessively dependent on potentially misspecifed information.

Beyond the analysis provided in Chen et al. (2019), this study considers the case when the resulting maximum eigenvalue from Equation (3.2.43) has a negative sign. This would indicate that the marginal precision matrix of the full model is adding noise rather than information to the estimation strategy of ξ_1. In this case, the identification scheme of those parameters is better achieved using the baseline model. In terms of the "effective sample size" interpretation in Chen et al. (2019), this would mean that the empirical sample should be shortened in order for the full models to be able to match the inferential precision of the baseline model. The study uses this argument to determine how detrimen-

tal misspecification in the macroeconomic dynamics is to the inferential precision of the structural asset pricing parameters of interest. The results of such analyses are detailed in the next section.

3.3 Results

The main aim of this section is to compare the results of the FII and II estimation strategies with those achieved from the PII estimation in Section 2.4. The target is no longer, thus, to analyze the plausibility of the DSGE asset pricing model, proposed by Chen (2017), in solving the prominent asset pricing puzzles, which has been extensively dealt with in the aforementioned section. Rather, the target is to examine whether better inferential statistics for the parameters, and the asset pricing target moments of the model, can be achieved by explicitly investigating the effect of the underlying misspecification inherent in the model.

The task is to challenge the PII estimation results, repeated again in panel A of Table 3.1 for convenience, by including the information from the macroeconomic dynamics into the estimation strategy. I start by assuming that there is no misspecification in the structural DSGE asset pricing moment and perform II estimation. The results are displayed in panel B of Table 3.1. It is shown that even though the point estimates for the different parameters are somewhat reasonable, the standard errors are unreasonably large. This, in turn, translates into very wide confidence bounds that span unrealistic values; $\hat{\beta}$ is shown to accept values that are more economically reasonable, but also more values that are in excess of 1. The value for $\widehat{\overline{rra}}$ encompasses negative and positive values that are close to 100 which indicates that the model cannot reject the assumptions that the representative agent can be both risk neutral and excessively risk-averse. The confidence bounds for $\hat{\rho}_s$ accommodates values that are greater than 1 indicating a non-stationary habit process.

Table 3.1: Estimation results using the different methods

			Confidence Interval	
Parameter	**Estimate**	**Standard Error**	**2.5%**	**97.5%**
Panel A: PII results from Section 2.4				
β	1.0008	0.0034	0.9941	1.0075
$\overline{rra}$	22.66	2.20	18.34	26.98
Panel B: II results				ϑ = -0.4031
β	1.0039	0.0141	0.9763	1.0315
$\overline{rra}$	16.66	55.75	-92.61	125.93
ρ_s	0.9772	0.0693	0.8413	1.1130
ϕ	104.07	125.22	-141.36	349.49
σ_z	0.0135	0.0009	0.0118	0.0152
Panel C: FII results				ϑ = -0.4035
β	1.0039	0.0141	0.9763	1.0315
$\overline{rra}$	16.66	55.70	-92.52	125.84
ρ_s	0.9772	0.0693	0.8414	1.1129
ϕ	104.07	125.13	-141.19	349.33
σ_z	0.0135	0.0009	0.0118	0.0162

Note: This table reports the estimation results for the structural parameters. Panel A replicates the results from Section 2.4 using partial encompassing indirect inference (PII) estimation. Panels B and C report results using Indirect Inference (II) estimation and full encompassing indirect inference (FII) estimation, respectively. The standard errors and 95% confidence intervals of all the parameters are provided. The dark matter measure for FII and PII is provided as the value of ϑ in the respective panel with panel A considered as the baseline model.

Even more problematic is the value of $\hat{\phi}$ which spans a wide range of positive and negative values in three digits. The value of zero is thus included in this wide confidence

interval. This in turn implies that there are no convex capital adjustment costs incurred by the representative firm and consequently the capital stream K_t produced by the model is detrimentally destabilized. The only parameter that seems to have a reasonable point estimate as well as tight confidence bounds is the volatility of the technology process $\hat{\sigma}_z$.

Misspecification in the DGP is then accounted for by using the FII estimation strategy. The results are displayed in panel C of Table 3.1. As expected, the point estimates of the parameters are identical to those obtained from II estimation, since the quadratic function minimized to obtain those parameters remains unaltered as explained previously. The results, however, show that the statistical inference of the parameters is only very slightly improved. This indicates that $\Phi_{II} \approx \Phi_{FII}$, as this is the only difference between Equations (3.2.19) and (3.2.28). Consequently, it is concluded that the DGP governing the instrumental moment conditions resulting from both the observed and the simulated data is very close.

Would this finding negate misspecification in this DSGE asset pricing model? Technically, this finding indicates that the first two moments of R_t^f, R_t^e, Y_t and C_t, which comprise the set of instrumental GMM moment conditions, are not very different between the observed and the simulated data. Yet, there are other quantities in the model that have not been examined, such as I_t, K_t and W_t. Those macroeconomic quantities should have been able to identify the remaining structural parameters of the model that have remained calibrated, namely the set $(\alpha, \delta, \mu, \rho_z)^\top$. It has been previously mentioned in Section 3.2.3 that attempting to identify those parameters resulted in an unstable function that could not be successfully optimized. Therefore, misspecification in the macroeconomic dynamics of the DSGE asset pricing model cannot be ruled out.

The dark matter measure displayed in panels B and C in Table 3.1 further confirms the statistical inference findings. The negative values of ϑ indicates the inferiority of both the II and the FII estimation strategies relative to the baseline model represented by the PII estimation strategy. The size of the measure implies that the FII results are only slightly more precise than that of the II results. In terms of the "effective sample

size" interpretation, the dark matter measure specifies that the data set used in the full encompassing estimation strategies, FII and II, should be reduced by around 40% to match the inferential precision of the PII estimates. This indicates that the additional $u_{2,t}(y, \theta_2)$[7] moment conditions introduce noise rather than information into the identification process of the structural parameters of interest, $\xi_1 = (\beta, \overline{rra})$. They are, thus, disruptive to the estimation process, and the econometrician would do well by excluding them from the estimation and have them as calibrated values.

Yet, note that the estimation of $\hat{\sigma}_z$ in both FII and II estimation is rather precise. It might be the case that the instrumental GMM moments used for identifying this parameter carry some truths with regards to ξ_1. To investigate this issue, a new PII estimation is considered where only the first two moments of GDP are augmented to the $u_{1,t}(y, \theta_1)$ from before. In this instance, the presence of a ξ_{21} parameter is envisioned and is set equal to σ_z. The result of this compromise estimation strategy is presented in panel A of Table 3.2.

It is seen that the point estimates as well as the precision of the structural parameters considered are vastly improved relative to the ones seen in the FII and II estimation strategies in Table 3.1. In fact, the estimates are very much comparable to the PII results that were originally obtained; $\hat{\beta}$ remains slightly larger than unity, but its standard error is slightly improved. The estimated steady-state relative risk aversion parameter seems to indicate that the representative agent is less risk averse than indicated by the original PII results, as the $\widehat{\overline{rra}}$ is somewhat lower than in panel A of Table 3.1. Its confidence bounds are reasonably tight and encompasses the value from the original PII results. The estimation of $\hat{\sigma}_z$ is also precisely executed using this strategy. However, no economic meaning is attached to this value as it seen as a pseudo-true value under this estimation strategy, as explained previously. To confirm that the remaining first two moments of consumption is what is indeed troublesome in the II and FII results, a second PII estimation strategy is

[7] y here does not have any superscripts or subscripts to indicate that it can come from either the observed or the simulated data.

Table 3.2: PII estimation results using alternative specifications

Parameter	Estimate	Standard Error	Confidence Interval 2.5%	Confidence Interval 97.5%
Panel A: PII results with $\xi_{21} = \sigma_z$				$\vartheta = 0.29103$
β	1.0013	0.0033	0.9949	1.0077
$\overline{rra}$	17.19	4.02	9.32	25.07
σ_z	0.0135	0.0011	0.0114	0.0156
Panel B: PII results with $\xi_{21} = \phi$				ϑ = -0.2252
β	1.0001	0.0041	0.9921	1.0080
$\overline{rra}$	21.65	90.32	-155.37	198.67
ϕ	101.66	259.27	-406.49	609.82

Note: This table reports the partial encompassing indirect inference (PII) estimation results for different alternative specifications of ξ_{21}. The dark matter measure is provided as the value ϑ in the respective panel. The baseline model is the PII estimation in Panel A of Table 3.1.

considered with $\xi_{21} = \phi$. The results in panel B of Table 3.2 are quite comparable to the imprecise results previously found.

The question then becomes whether the original PII results from Section 2.4 should be denounced in favor of the modified estimation strategy with $\xi_{21} = \sigma_z$. The dark matter measure should shed some light on this issue. Again, the original PII estimation strategy is considered as the baseline model. The value of ϑ in panel A of Table 3.2 is found to be around 0.29. The positive value indicates that the overall precision of the new modified PII strategy is better in the estimation of the asset pricing parameters of interest. Additionally, the size of the measure is not large enough to indicate that there should be any concerns with regards to fragility, as the data set has to be stretched by only 30% for the baseline model to match the precision of the new modified strategy.

These results are further confirmed by the economic plausibility analysis in Table 3.3 which is conducted in a similar fashion to Table 2.4 for ease of comparison. The results show that the volatility of the risk-free rate is better matched in the modified PII strategy, though the level is still unreasonably high even with the slightly lower 95% confidence bound in the modified strategy. This implies that the risk-free rate puzzle remains thus far unresolved. The equity premium moments are comparable to those obtained from the original PII strategy; they still encompass the empirical values within the 95% confidence bounds. Therefore, the conclusion from Section 2.4 remains intact; namely that the equity premium puzzle is resolved provided that a higher than usual relative risk aversion parameter is accepted.

The main difference between Tables 2.4 and 3.3 lies in their matching of the business cycle moments. The modified PII strategy achieves a better match for the volatility of the HP-filtered GDP than its counterpart. This is unsurprising, as the second moment of the GDP is one of the moment restrictions used to identify σ_z in the modified PII estimation. It follows that most of the business cycle moments that are dependent on output are slightly more volatile than before, but the confidence bounds still encompass the value of the empirical data. Additionally, the relative volatility of consumption growth is better matched, with the empirical value lying conveniently in the midst of the confidence interval instead of on the upper bound.

Overall the empirical findings suggest that the modified PII strategy with $\xi_{21} = \sigma_z$ is capable of fairly enhancing the results of the original PII strategy in Section 2.4. Although the risk-free rate puzzle remains unresolved, the second moment of the risk-free rate is better matched while still retaining the favorable equity premium results. Additionally, many of the business cycle moments are better matched. The inclusion of the first two moments of GDP in the underlying GMM instrumental model, necessary to identify σ_z, instead of just calibrating its value creates more variation in the simulated business cycle moments which allows for a better match with the empirical equivalents.

Table 3.3: Implied economic plausibility check using modified PII results

Target Moment	Data	Implied Estimate	Bootstrap Quantiles 2.5%	97.5%
Asset Prices				
90-Day T-bill Return (%)	0.17	0.63	0.31	0.99
Vol of R^f (%)	0.90	0.73	0.62	0.84
Persistence of Tobin's Q		0.96	0.96	0.96
Mean Sharpe Ratio of CRSP Index	0.22	0.16	0.11	0.21
Equity Premium R^e (%)	1.82	1.57	1.04	2.05
Vol of R^e (%)	8.24	9.86	8.70	10.50
Business Cycle				
Mean Output/Capital	0.143	0.076	0.062	0.090
Mean Investment Rate	0.025	0.021	0.021	0.021
Mean Output Growth (%)	0.48	0.45	0.45	0.45
Vol HP-filtered GDP (%)	1.72	1.73	1.45	1.99
Persistence of Output/Capital	0.997	0.979	0.970	0.985
Relative Volatility of Consumption Growth	0.52	0.53	0.42	0.68
Mean Adj Cost / Output (%)		0.11	0.08	0.12
Consumption Growth				
Mean of ln of Consumption Growth (%)	0.47	0.45	0.45	0.45
Std of ln of Consumption Growth (%)	0.52	0.56	0.48	0.63

Note: This table shows the results of a parametric bootstrap using $M = 1000$ draws from the joint normal distribution of β, $\overline{rra}$ and σ_z around the PII estimates $\hat{\beta} = 1.0013$, $\widehat{\overline{rra}} = 17.19$ and $\hat{\sigma}_z = 0.0135$. It shows the selected bootstrap quantiles of asset prices, business cycle and consumption growth moments along with the estimate-implied and empirical means.

3.4 Conclusion

Formally enclosing calibration within the folds of econometric methodology via PII estimation (Dridi et al., 2007) provides a convenient way of dealing with DSGE asset pricing models that are inherently misspecified. It enables the calibration of all the nuisance parameters of the models that are responsible for the allegedly misspecified dynamics, while allowing the parameters of interest to be consistently estimated. Section 3.2.3 elaborates

extensively on why it is believed that the macroeconomic dynamics put forth by DSGE asset pricing models is believed to be potentially misspecified, while the asset pricing dynamics indeed convey true economic processes.

The natural question that follows then is whether those macroeconomic dynamics are indeed misspecified. If this is the case, then their inclusion in the estimation strategy would only introduce noise rather than meaningful information to the estimation of the asset pricing parameters of interest. This, consequently, translates into point estimates with very wide confidence bounds that span economically unreasonable values. To examine whether this is indeed the case, this study compares the results of the PII estimation in Section 2.4 with two other variants of the indirect inference methodology; namely, the classic II estimation, as proposed in Gourieroux et al. (1993) and the FII estimation as put forth by Dridi et al. (2007). The former does not account for misspecification at all, and thus claims to consistently estimate all the parameters of the model, while the latter allows for misspecification, but still estimates all the parameters of the model albeit with consistency claims for only the parameters of interest. The DSGE asset pricing model proposed by Chen (2017) and discussed in Section 2.2 is used as the underlying structural model for all three methodologies.

To quantitatively compare between the different estimation methods, the newly developed dark matter measure, proposed by Chen et al. (2019), is utilized. This measure uses the PII estimation as the baseline model and effectively relays how much the sample size used in the two other estimation methods should be lengthened (or shortened) to match the precision of the PII estimation. However, an excessively high positive value for the measure is viewed unfavorably, as it implies that the model is excessively sensitive/fragile to small changes in the DGP, even though its parameter estimates have tight confidence bounds. In this way, the dark matter measure is a second-line of defense against potential misspecification in the dynamics of the DSGE asset pricing moments.

The findings indicate that not all of the macroeconomic dynamics in the DSGE asset pricing model should be hastily dismissed from the estimation process via calibrating

their parameters. Although neither II nor FII can surpass the performance of the original PII estimation results in Section 2.4, a modified PII estimation, which includes the GDP dynamics as well as the asset pricing dynamics in the underlying instrumental model, is a worthwhile rival. The additionally included macroeconomic dynamics result in comparative point estimates with adequately tight confidence bounds for the asset pricing parameters as well as for the volatility of total factor productivity (TFP) parameter that arises as a by-product of this modified estimation strategy. Additionally, the dark matter measure confirms that there is little fragility in this modified estimation methodology.

The economic plausibility analysis conducted with this modified variant of the PII estimation results in modestly better asset pricing dynamics, but a remarkably better match to the business cycle moments. From an asset pricing perspective, the equity premium moments remain matched albeit with a relative risk aversion aversion that is slightly lower than the original PII results but still higher than conventionally accepted values. The risk-free rate puzzle continues to be troublesome, as the level of the risk-free rate is still unattainable, although its volatility is moderately approached. The business cycle moments, on the other hand, are noticeably better matched with their empirical equivalents, as the estimation strategy inherently grants the best possible fit for the GDP moments. As a result, all the business cycle moments that are dependent on the GDP dynamics conform better to their empirical counterparts.

Overall, this econometric analysis suggests that incorporating calibration within an econometric framework is the road map towards tackling misspecification issues that arise in DSGE asset pricing models. Yet, calibration should not be prematurely used to fix all of the allegedly nuisance parameters. Rather, careful analysis should be conducted to determine whether possibly some secondary dynamics could be included in the estimation process that will improve the overall precision of the estimates without incurring excessive fragility. In light of this conclusion, the possibilities for further improvements are endless, especially with regards to the persistence of habit parameter, ρ_s. This is left for future research.

Appendix

3.A The assumptions for the different estimators

This appendix section can be viewed as a road map describing how Appendix 2.A, which is explicitly written for PII estimation, can be tailored to fit the two other estimators discussed in Section 3.2. This section, thus, follows closely the assumptions in Gourieroux et al. (1993) for the II estimation as well as the assumptions in Dridi et al. (2007) for the FII and PII estimation strategies. The main aim here is to explicitly highlight where the two sets of assumptions differ and where they conform.

As mentioned in Section 3.2, the main difference between II estimation and FII and PII estimation strategies is the assumption of misspecification in the DGP in the latter two strategies regarding the dynamics governing the ξ_2 parameters. In II estimation, the DGP is assumed to be correctly specified for the entire structural model. Accordingly, there is no need to distinguish between the parameters that are of interest and which form part of the model that portrays a correctly specified DGP, ξ_1, and those which are not, ξ_2. As such, in II estimation, Assumption 1 is not needed and the nominal assumption, Assumption 2, provides the functional form of the true DGP for the entire set of structural parameters. For FII and PII estimation methodologies both Assumption 1 and Assumption 2 are needed.

The main difference between PII estimation and FII and II estimation is the fact that PII is only concerned with estimating the set of ξ_1 parameters. As such, the instrumental model, $\mathcal{N}_\theta$, only focuses on the k_1 moment restrictions that should be able to identify

the ξ_1 parameters, as explained in Section 3.2.1. Therefore, to generalize Assumption 3 in order to fit FII and II estimation, Equation (3.2.1) is followed. Assumption 3, which provides the GMM moment conditions using the empirical data, can thus be re-written as

$$\mathbb{E}\left[u_t\left(\{y_t\}_{t-l}^{t},\theta\right)\right] = \mathbb{E}\begin{bmatrix} u_{1,t}\left(\{y_t\}_{t-l}^{t},\theta_1\right) \\ u_{2,t}\left(\{y_t\}_{t-l}^{t},\theta_2\right) \end{bmatrix} \neq 0 \quad \text{for all } \theta_1 \neq \theta_1^0 \in \Theta_1 \quad \text{and } \theta_2 \neq \theta_2^0 \in \Theta_2.$$

The required GMM criterion function is then formulated as in Equations (3.2.2) - (3.2.4).

Assumption 4, which describes the regularity conditions imposed on the GMM estimation of the instrumental parameters, is maintained for both FII and II estimation. It is merely altered to include the entire set of $k_1 + k_2$ moment conditions and the entire set of instrumental parameters $\theta = (\theta_1, \theta_2)^\top$. The stationarity and ergodicity assumption of the time series as well as the altered Assumption 4 are then sufficient conditions for the GMM criterion function in Equation (3.2.2) to converge almost surely to a non-stochastic limit criterion function. For II estimation, this is

$$Q_\infty\left(G_*, \xi_1^0, \xi_{21}^0, \xi_{22}^0, \theta\right) = \frac{1}{2}\mathbb{E}\left[u_t\left(\{y_t\}_{t-l}^{t},\theta\right)\right]^\top \cdot W \cdot \mathbb{E}\left[u_t\left(\{y_t\}_{t-l}^{t},\theta\right)\right],$$

and for FII estimation, it is

$$Q_\infty\left(G_*, \xi_1^0, \xi_{21}^*, \xi_{22}^*, \theta\right) = \frac{1}{2}\mathbb{E}\left[u_t\left(\{y_t\}_{t-l}^{t},\theta\right)\right]^\top \cdot W \cdot \mathbb{E}\left[u_t\left(\{y_t\}_{t-l}^{t},\theta\right)\right].$$

Notice that the difference between the previous two criteria functions pertains only to the difference in the notation given to the ξ_{21} and ξ_{22} parameters. The former indicates that they are true values while in the latter, they are only pseudo-true values due to the assumption of misspecification. However, the l.h.s of both functions are exactly the same. Therefore, $Q_\infty\left(G_*, \xi_1^0, \xi_{21}^0, \xi_{22}^0, \theta\right) = Q_\infty\left(G_*, \xi_1^0, \xi_{21}^*, \xi_{22}^*, \theta\right)$. It is only that FII estimation

cautions against the misspecified DGP generated by ξ_{21} and ξ_{22}. Accordingly, the limit criterion function for both II and FII estimation is the same and is uniquely minimized by

$$\theta^0 = \underset{\{\theta \in \Theta\}}{\operatorname{argmin}} \; Q_\infty \left(G_*, \xi_1^0, \xi_{21}^*, \xi_{22}^*, \theta \right). \tag{3.A.1}$$

To maintain due diligence, the superscript given to ξ_{21} and ξ_{22} in Equation (3.A.1) is kept similar to the FII notation even though the equation conforms with II estimation too.

For II estimation, Assumption 2, and the altered Assumptions 3 and 4 provide that

$$\hat{\theta}_T = \underset{\{\theta \in \Theta\}}{\operatorname{argmin}} \; Q_T \left(\{y_t\}_{t=1}^T, \theta \right)$$

is a consistent estimator of θ^0. For FII estimation, Assumption 1 is also needed for the prior statement to hold.

Assumptions 5 and 6 are the simulated data counterparts to Assumptions 3 and 4. They are thus altered in a similar manner. Following Equation (3.2.8), Assumption 5 becomes

$$\mathbb{E}\left[u_t \left(\{\tilde{y}_t^s(\xi)\}_{t-l}^t, \theta^s \left(\xi_1, \xi_{21}, \xi_{22} \right) \right) \right] = \mathbb{E} \begin{bmatrix} u_{1,t} \left(\{\tilde{y}_t^s(\xi)\}_{t-l}^t, \theta_1^s(\xi_1, \xi_{21}) \right) \\ u_{2,t} \left(\{\tilde{y}_t^s(\xi)\}_{t-l}^t, \theta_2^s(\xi_{22}) \right) \end{bmatrix} \neq 0$$

$$\text{for all } \; \theta_1^s(\xi_1, \xi_{21}) \neq \tilde{\theta}_1^0(\xi_1^0, \xi_{21}^*) \in \Theta_1 \quad \text{and } \; \theta_2^s(\xi_{22}) \neq \tilde{\theta}_2^0(\xi_{22}^*) \in \Theta_2.$$

Assumption 7 is twofold. The first part maintains that the binding function is one-to-one, and this holds for FII and II estimation. The second part pertains to the rank assumption of the derivative of the instrumental parameters with respect to the structural parameters. In both FII and II estimation strategies, the structural nuisance parameters

ξ_{22} are estimated and not calibrated unlike PII. Therefore, for FII and II estimation, the second part of Assumption 7 becomes

$$P_* \lim_{T\to\infty} \frac{\partial \tilde{\theta}_T^s}{\partial \begin{pmatrix} \xi_1 \\ \xi_{21} \\ \xi_{22} \end{pmatrix}} \left(\xi_1^0, \xi_{21}^*, \xi_{22}^*\right)^\top \quad \text{has full rank } p_1 + p_{21} + p_{22}.$$

Note that for II estimation, ξ_{21}^* and ξ_{22}^* would be considered true values instead of the pseudo-true values, as no misspecification is assumed.

Assumption 8 explicitly denotes the binding function for partial encompassing. The counterparts for the full encompassing conditions required for II and FII estimaton are provided in Equations (3.2.10) and (3.2.11), respectively. As explained in Section 3.2.2 and highlighted in the altered Assumptions 3 to 7, both FII and II estimation have the same underlying instrumental model. They thus have the same estimator which is given in Equations (3.2.13) to (3.2.16).

Proposition 1 can also be altered to clarify the assumptions under which consistency is maintained for the two other estimators. For FII, Assumptions 1, 2 and the altered Assumptions 3 to 8 provide that $\hat{\xi}_{1,TS}$ is a consistent estimator of ξ_1^0 while $\hat{\xi}_{21,TS}$ and $\hat{\xi}_{22,TS}$ converge in the probability limit to the pseudo-true values ξ_{21}^* and ξ_{22}^*, respectively. Conversely, in II estimation, Assumption 2 and the altered Assumptions 3 to 8 provide that the entire set of $\hat{\xi}_{TS} = \left(\hat{\xi}_{1,TS}, \hat{\xi}_{21,TS}, \hat{\xi}_{22,TS}\right)^\top$ is a consistent estimate of $\xi^0 = \left(\xi_1^0, \xi_{21}^0, \xi_{22}^0\right)^\top$.

As previously explained in Section 3.2.2, the asymptotic distribution is what is truly different between the FII and II estimation methodologies. For both methodologies, Assumption 9 providing the central limit theorem necessary for the distribution of the em-

pirical moments is similar. It is slightly altered from Appendix 2.A to match the altered Assumption 3. It thus becomes

$$\sqrt{T}\left[\frac{1}{T}\sum_{t=1}^{T} u_{1,t}\left(\{y_t\}_{t-l}^{t}, \theta^0\right)\right] \underset{d}{\to} \mathcal{N}(0, V),$$

with V and Γ_j formulated as in Equations (3.2.21) and (3.2.22).

For II estimation, the DGP of the simulated series is assumed to be identical to that of the empirical series. As such, the altered Assumption 9 along with the assumptions in Proposition 1 are sufficient to put forth an altered Proposition 2 which provides the asymptotic distribution of the instrumental parameters under the II estimation

$$\sqrt{T}\left(\hat{\theta}_T - \frac{1}{S}\sum_{s=1}^{S} \tilde{\theta}_T^s\left(\xi_1^0, \xi_{21}^0, \xi_{22}^0\right)\right) \xrightarrow{d} \mathcal{N}\left(0, \Phi_{II}^0\left(S, W\right)\right), \tag{3.A.2}$$

where $\Phi_{II}^0\left(S, W\right)$ is provided in Equation (3.2.28).

For FII estimation, the allowance for misspecification materializes in the fact that the DGP for the simulated series is allowed to be different than that of the empirical series. As such, and following the altered Assumption 5, an altered Assumption 10 is needed for the simulated moments

$$\sqrt{T}\left[\frac{1}{T}\sum_{t=1}^{T} u_t\left(\{\tilde{y}_T^s(\xi)\}_{t-l}^{t}, \tilde{\theta}^0\left(\xi_1^0, \xi_{21}^*, \xi_{22}^*\right)\right)\right] \underset{d}{\to} \mathcal{N}(0, V^*),$$

where V^* and Γ_j^* are formulated as in Equations (3.2.24) and (3.2.25), respectively. Accordingly, FII estimation has a different Proposition 2 than II:

$$\sqrt{T}\left(\hat{\theta}_T - \frac{1}{S}\sum_{s=1}^{S} \tilde{\theta}_T^s\left(\xi_1^0, \xi_{21}^*, \xi_{22}^*\right)\right) \xrightarrow{d} \mathcal{N}\left(0, \Phi_{FII}^0\left(S, W\right)\right), \tag{3.A.3}$$

where $\Phi_{FII}^0\left(S, W\right)$ is provided in Equation (3.2.19).

Finally, an altered Proposition 3 is needed to provide the asymptotic distribution of the structural parameters under both FII and II estimation. In FII estimation, under

Assumptions 1 to 10, the structural parameter estimates $\hat{\xi}_{TS} = \left(\hat{\xi}_{1,TS}, \hat{\xi}_{21,TS}, \hat{\xi}_{22,TS}\right)^{\top}$ are asymptotically distributed as in Equation (3.2.17). In II estimation, only Assumptions 2 to 9 are required for the asymptotic distribution in Equation (3.2.26) to take place.

3.B Derivation of the different asymptotic distributions

The main aim of this appendix section is to show how the asymptotic distributions of the different estimators shown in Section 3.2.2 can be derived. The appendix section follows along the same lines of the derivation of the asymptotic distribution of the PII estimator presented in Appendix 2.B. The only difference is that the current appendix section shows how the derivation can be generalized to include the II and FII estimators too.

As usual, the starting point is to minimize the objective function of the estimator under analysis. As previously mentioned, the FII and II estimators have the same objective function which is presented in Equation (3.2.13). It is repeated here for convenience

$$\min_{\{(\xi_1,\xi_{21},\xi_{22})\in\Xi_1\times\Xi_{21}\times\Xi_{22}\}} \left[\hat{\theta}_T - \frac{1}{S}\sum_{s=1}^{S}\tilde{\theta}_T^s(\xi_1,\xi_{21},\xi_{22})\right]^{\top} \cdot \widehat{\Omega}_T \cdot \left[\hat{\theta}_T - \frac{1}{S}\sum_{s=1}^{S}\tilde{\theta}_T^s(\xi_1,\xi_{21},\xi_{22})\right].$$

Note that unlike the PII estimation, ξ_{22} is part of the estimation process and is not calibrated. As such, the first order condition (FOC) of this objective function with respect to the estimated structural parameters will include the set of ξ_{22} parameters as follows

$$\frac{1}{S}\sum_{s=1}^{S}\frac{\partial\tilde{\theta}_T^s}{\partial\begin{pmatrix}\xi_1\\ \xi_{21}\\ \xi_{22}\end{pmatrix}}\left(\hat{\xi}_{1,TS},\hat{\xi}_{21,TS},\hat{\xi}_{22,TS}\right)^{\top}\cdot\widehat{\Omega}_T \cdot\left[\hat{\theta}_T - \frac{1}{S}\sum_{s=1}^{S}\tilde{\theta}_T^s\left(\hat{\xi}_{1,TS},\hat{\xi}_{21,TS},\hat{\xi}_{22,TS}\right)\right] = 0.$$

The next step is to expand this FOC around the limit values of the structural parameters. For II estimation, these are $\left(\xi_1^0,\xi_{21}^0,\xi_{22}^0\right)$. For FII estimation, given the misspecifi-

cation assumption in the dynamics governed by the nuisance parameters, the limit values are $\left(\xi_1^0, \xi_{21}^*, \xi_{22}^*\right)$. For brevity, the notation here is expressed in terms of the FII estimation.

$$\frac{1}{S}\sum_{s=1}^{S}\frac{\partial\tilde{\theta}_T^s}{\partial\begin{pmatrix}\xi_1\\ \xi_{21}\\ \xi_{22}\end{pmatrix}}\left(\xi_1^0,\xi_{21}^*,\xi_{22}^*\right)^\top\widehat{\Omega}_T\sqrt{T}\left[\hat{\theta}_T-\left(\frac{1}{S}\sum_{s=1}^{S}\tilde{\theta}_T^s\left(\xi_1^0,\xi_{21}^*,\xi_{22}^*\right)\right.\right.$$

$$\left.\left.+\ \frac{1}{S}\sum_{s=1}^{S}\frac{\partial\tilde{\theta}_T^s}{\partial\begin{pmatrix}\xi_1\\ \xi_{21}\\ \xi_{22}\end{pmatrix}^\top}\left(\xi_1^0,\xi_{21}^*,\xi_{22}^*\right)\begin{pmatrix}\hat{\xi}_{1,TS}-\xi_1^0\\ \hat{\xi}_{21,TS}-\xi_{21}^*\\ \hat{\xi}_{22,TS}-\xi_{22}^*\end{pmatrix}\right)\right].$$

Rearranging to have the structural parameters on the l.h.s, the following equation results

$$\sqrt{T}\begin{pmatrix}\hat{\xi}_{1,TS}-\xi_1^0\\ \hat{\xi}_{21,TS}-\xi_{21}^*\\ \hat{\xi}_{22,TS}-\xi_{22}^*\end{pmatrix}\simeq\left\{\frac{\partial\tilde{\theta}}{\partial\begin{pmatrix}\xi_1\\ \xi_{21}\\ \xi_{22}\end{pmatrix}}\left(\xi_1^0,\xi_{21}^*,\xi_{22}^*\right)^\top\Omega\frac{\partial\tilde{\theta}}{\partial\begin{pmatrix}\xi_1\\ \xi_{21}\\ \xi_{22}\end{pmatrix}^\top}\left(\xi_1^0,\xi_{21}^*,\xi_{22}^*\right)\right\}^{-1} \tag{3.B.1}$$

$$\cdot\frac{\partial\tilde{\theta}}{\partial\begin{pmatrix}\xi_1\\ \xi_{21}\\ \xi_{22}\end{pmatrix}}\left(\xi_1^0,\xi_{21}^*,\xi_{21}^*\right)^\top\cdot\Omega\cdot\sqrt{T}\left[\hat{\theta}_T-\frac{1}{S}\sum_{s=1}^{S}\tilde{\theta}_T^s\left(\xi_1^0,\xi_{21}^*,\xi_{22}^*\right)\right].$$

(3.B.2)

The last term on the r.h.s of the previous equation represents the difference between the estimated instrumental parameters from the empirical and simulated data respectively. It is a key ingredient when deriving the asymptotic distribution of the structural parameters.

Therefore, the next step is to determine how this term is asymptotically distributed. In order to do so, the asymptotic distribution of the instrumental parameters has to be derived.

The starting point is thus the GMM objective function that is used to estimate the instrumental parameters θ. Using the empirical data, this objective function is given in Equation (3.2.3) and is repeated here for convenience

$$Q_T\left(\{y_t\}_{t=1}^T, \theta\right) = \frac{1}{2}\, g_T\left(\{y_t\}_{t=1}^T, \theta\right)^\top \cdot \widehat{W}_T \cdot g_T\left(\{y_t\}_{t=1}^T, \theta\right).$$

Similar to how the structural parameters were dealt with, the first step is to get the FOC of this GMM objective function

$$\frac{\partial g_T^\top}{\partial \theta}\left(\{y_t\}_{t=1}^T, \hat{\theta}_T\right) \cdot \widehat{W}_{1,T} \cdot g_T\left(\{y_t\}_{t=1}^T, \hat{\theta}_T\right),$$

and expand $g_T(\,\cdot\,)$ around the limit value θ^0. After rearranging, this becomes

$$\begin{aligned}\left(\hat{\theta}_T - \theta^0\right) = -\left\{\frac{\partial g_T^\top}{\partial \theta}\left(\{y_t\}_{t=1}^T, \hat{\theta}_T\right)\widehat{W}_T \frac{\partial g_T}{\partial \theta^\top}\left(\{y_t\}_{t=1}^T, \theta^0\right)\right\}^{-1} \frac{\partial g_T^\top}{\partial \theta}\left(\{y_t\}_{t=1}^T, \hat{\theta}_T\right)\widehat{W}_T \\ \cdot\, g_T\left(\{y_t\}_{t=1}^T, \theta^0\right).\end{aligned}$$

Equation (3.2.20) in Section 3.2.2 indicates that asymptotically, the previous equation can be written as

$$\begin{aligned}&\sqrt{T}\left(\hat{\theta}_T - \theta^0\right) \\ &\simeq -\left\{\mathbb{E}\left[\frac{\partial u_t^\top}{\partial \theta}\left(\theta^0\right)\right] W \mathbb{E}\left[\frac{\partial u_t}{\partial \theta^\top}\left(\theta^0\right)\right]\right\}^{-1} \mathbb{E}\left[\frac{\partial u_t^\top}{\partial \theta}\left(\theta^0\right)\right] W \cdot \sqrt{T} g_T\left(\{y_t\}_{t=1}^T, \theta^0\right) \\ &\simeq -C^0 \cdot \sqrt{T} g_T\left(\{y_t\}_{t=1}^T, \theta^0\right).\end{aligned}$$

Using the altered Assumption 9 in Appendix 3.A, the instrumental parameters under the empirical data can be asymptotically distributed as follows

$$\sqrt{T}\left(\hat{\theta}_T - \theta^0\right) \underset{d}{\to} \mathcal{N}\left(0, C^0 V {C^0}^\top\right),$$

with V formulated as in Equations (3.2.21) and (3.2.22).

The same rationale is applied for the instrumental parameters evaluated using the simulated data. The FOC of the objective function is then

$$\frac{\partial g_T^\top}{\partial \theta}\left(\{\tilde{y}_T^s(\xi)\}_{t=1}^T, \tilde{\theta}_T^s\right) \cdot \widehat{W}_T \cdot g_T\left(\{\tilde{y}_T^s(\xi)\}_{t=1}^T, \tilde{\theta}_T^s\right).$$

Again, an expansion of $g_T(\,\cdot\,)$ around the limit value $\tilde{\theta}^0$ is performed and after rearrangement, the equation becomes

$$\left(\tilde{\theta}_T^s - \tilde{\theta}^0\right) = -\left\{\frac{\partial g_T^\top}{\partial \theta}\left(\tilde{\theta}_T^s\right) \widehat{W}_T \frac{\partial g_T}{\partial \theta^\top}\left(\tilde{\theta}^0\right)\right\}^{-1} \frac{\partial g_T^\top}{\partial \theta}\left(\tilde{\theta}_T^s\right) \cdot \widehat{W}_T \cdot g_T\left(\{\tilde{y}_T^s(\xi)\}_{t=1}^T, \tilde{\theta}^0\right).$$

Using Equation (3.2.23) and the altered Assumption 8 which provides the binding functions for full encompassing in II and FII estimation, $\theta^0 = \tilde{\theta}(\cdot)$, the previous equation asymptotically becomes

$$\begin{aligned}
\sqrt{T}\left(\tilde{\theta}_T^s - \theta^0\right) \simeq & -\left\{\mathbb{E}^*\left[\frac{\partial u_t^\top}{\partial \theta}\left(\{\tilde{y}_T^s(\xi)\}_{t=1}^T, \theta^0\right)\right] W \mathbb{E}^*\left[\frac{\partial u_t}{\partial \theta^\top}\left(\{\tilde{y}_T^s(\xi)\}_{t=1}^T, \theta^0\right)\right]\right\}^{-1} \\
& \cdot \mathbb{E}^*\left[\frac{\partial u_t^\top}{\partial \theta}\left(\{\tilde{y}_T^s(\xi)\}_{t=1}^T, \theta^0\right)\right] W \cdot \sqrt{T} g_T\left(\{\tilde{y}_T^s(\xi)\}_{t=1}^T, \theta^0\right) \\
\simeq & -C^{*0} \cdot \sqrt{T} g_T\left(\{\tilde{y}_T^s(\xi)\}_{t=1}^T, \theta^0\right),
\end{aligned}$$

and the CLT in the altered Assumption 10 provides that the instrumental parameters evaluated using the simulated data are asymptotically distributed as follows

$$\sqrt{T}\left(\tilde{\theta}_T^s - \theta^0\right) \underset{d}{\to} \mathcal{N}\left(0, C^{*0} V^* {C^{*0}}^\top\right),$$

with V^* formulated as in Equations (3.2.24) and (3.2.25). Note, however, that in II estimation, the DGP of the simulated series is assumed to be identical to that of the empirical series. In such a case, $C^0 = C^{*0}$ and $V = V^*$. Accordingly, the asymptotic distributions of $\sqrt{T}\left(\hat{\theta}_T - \theta^0\right)$ and $\sqrt{T}\left(\tilde{\theta}_T^s - \theta^0\right)$ are identical.

Using the above results, $\sqrt{T}\left[\hat{\theta}_T - \frac{1}{S}\sum_{s=1}^{S}\tilde{\theta}_T^s\left(\xi_1^0, \xi_{21}^*, \xi_{22}^*\right)\right]$ can be expressed as

$$\sqrt{T}\left(\hat{\theta}_T - \frac{1}{S}\sum_{s=1}^{S}\tilde{\theta}_T^s\left(\xi_1^0, \xi_{21}^*, \xi_{22}^*\right)\right) \simeq -C^0 \cdot \sqrt{T} g_T\left(\{y_t\}_{t=1}^T, \theta^0\right) + C^{*0}\sqrt{T} g_T\left(\{\tilde{y}_T^s(\xi)\}_{t=1}^T, \theta^0\right)$$

and it is asymptotically normally distributed with asymptotic covariance matrix $\Phi_{FII}^0(S, W)$ as in Equation (3.2.19) in FII estimation in the absence of exogenous variables in the model. This is repeated here for convenience

$$\Phi_{FII}^0(S, W) = C^0 V {C^0}^\top + \frac{1}{S} C^{*0} V^* {C^{*0}}^\top.$$

In II estimation, the two terms on the r.h.s of the above equation are identical and thus can be combined together. This is shown in Equation (3.2.28) and is also repeated here for convenience

$$\Phi_{II}^0(S, W) = \left(1 + \frac{1}{S}\right) C^0 V {C^0}^\top,$$

The last step is to determine the distribution of the structural parameters. This has been previously given in Section 3.2.2 in Equations (3.2.17) and (3.2.26) for FII and II estimation, respectively. The details of the asymptotic covariance matrices are given in Equations (3.2.18) and (3.2.27), respectively. They are a result of forming a quadratic form of Equation (3.B.1) around the relevant $\Phi^0(S, W)$ depending on whether FII or II estimation is being performed.

Chapter 4

Volatility Discovery in Cryptocurrency Markets *

4.1 Introduction

Investing in cryptocurrencies is a risky undertaking due to their high volatility which has frequently been documented in the empirical literature (see, for example, Baek and Elbeck, 2015; Klein, Thu and Walther, 2018). At the same time, it may offer attractive benefits in terms of the prospect of high returns (Resta, Pagnottoni and De Giuli, 2020) and due to their hedging capabilities (Borri, 2019; Guesmi, Saadi, Abid and Ftiti, 2019). Investment strategies such as tail hedging require the estimation of a volatility time series and it is not clear which exchange or which data source to consider (see also the critique of Alexander and Dakos, 2020[1]). Hence, it is preferable to turn to the leading market in terms of volatility discovery. We contribute to the literature with an investigation of the structural interdependence of volatility among a set of cryptocurrencies (Bitcoin, Ethereum, Litecoin, and Ripple) which are traded on several exchanges. We choose to conduct our analysis

*This chapter is based on Dimpfl and Elshiaty (2021)

[1]The authors find inconsistencies in the empirical results of cryptocurrencies using data obtained from different sources, and accordingly suggest several guidelines to approach the numerous data sources for cryptocurrencies

on three of those exchanges (Bitfinex, Bitstamp, and Kraken), as they have the highest trading volume in our selected cryptocurrencies.

Our theoretical approach is based on the price discovery framework which has recently been extended to the discovery of volatility by Dias et al. (2018). The key idea is that a latent, common volatility process governs the volatility on all exchanges, similar to the common efficient price in the price discovery model of Hasbrouck (1995). Short term deviations from the underlying latent volatility are possible, but do not persist. We reformulate the model of Dias et al. (2018) in discrete time, accounting for the long memory property of volatility which is a well-documented stylized fact in finance (Baillie, 1996; Bollerslev, Osterrieder, Sizova and Tauchen, 2013; da Silva and Robinson, 2008). With this long memory property adjustment in mind, the well-established price discovery theory is then applied to volatility discovery.

In the empirical application, we estimate each market's volatility using a discrete time stochastic volatility model (Sandmann and Koopman, 1998). To quantify the contribution of the individual markets to the common variance of the volatility, we rely on the information share measure of Hasbrouck (1995). As the volatility time series exhibit long memory, we model them with a fractionally cointegrated vector autoregressive (FCVAR) model which directly allows the computation of Hasbrouck (1995) information shares. However, the shares of Hasbrouck (1995) are not unique, and the often applied Cholesky decomposition would lead to extreme bounds in our application. Therefore, we rely on the method of Lien and Shrestha (2009) to identify a unique information share for each market. Their paper proposes an alternative to the Cholesky decomposition that relies on the correlation matrix of the innovations and involves the entire matrix rather than its lower triangular decomposition only. This in turn renders the ordering of the markets obsolete and results in unique information shares. While the methodology is readily used in stock market applications (Fricke and Menkhoff, 2011; Liu and An, 2011; Chen, Chung and Lien, 2016), this study is the first to use it in the context of cryptocurrency volatility.

This study is related to several strands in the literature due to the multitude of methods used. The application of the price discovery framework to cryptocurrency markets can now be considered a well-established part of the cryptocurrency research. The first article is Brandvold, Molnár, Vagstad and Valstad (2015) who find that the now closed Mt.Gox and Btce are the most informative markets for Bitcoin prices. Since then, further studies have considered different sets of markets and extended the analysis to other cryptocurrencies, driven by the need to update the results in a constantly changing environment (Brauneis and Mestel, 2018; Pagnottoni and Dimpfl, 2019; Dimpfl and Peter, 2020). Even more recently, the analysis has been extended to Bitcoin spot and futures markets by Alexander, Choi, Park and Sohn (2020), Alexander and Heck (2020), Baur and Dimpfl (2019), Corbet, Lucey, Peat and Vigne (2018), or Fassas, Papadamou and Koulis (2020).

Analyzing the structure of volatility dynamics, in contrast, is a more recent topic, and this is, to the best of our knowledge, the first study which considers volatility discovery in cryptocurrency markets. Existing studies so far have considered stock volatility on different exchanges (Dias et al., 2018), stock and options volatility (Baule, Frijns and Tieves, 2018; Wang, 2014), or the volatility of options and credit default swaps (Forte and Lovreta, 2019). In terms of cryptocurrencies, there are studies which consider the interrelatedness of volatility across different currencies (Chaim and Laurini, 2019; Katsiampa, 2019), but not of the same currency across different exchanges.

As regards the methodological approach, FCVAR models are readily used in empirical finance (e.g. Bollerslev et al., 2013; Caporin, Ranaldo and De Magistris, 2013; Rossi and Santucci de Magistris, 2013; Nielsen and Shibaev, 2018). However, applications with the goal of price or volatility discovery are scarce and there are, to the best of our knowledge, only two studies which use the FCVAR model in this context, namely Dolatabadi, Nielsen and Xu (2015) and Dias et al. (2018). Both studies use the model in a two market context: Dolatabadi et al. (2015) investigate price discovery among the spot and futures markets of five non-ferrous metals. Dias et al. (2018) investigate both price and volatility discovery in 30 stocks traded on three different exchanges, but limit the main analysis to two pairs of

exchanges at a time and only use the three markets together as a robustness check. In contrast, this study examines volatility discovery among the three cryptocurrency exchanges at once. Additionally, Dolatabadi et al. (2015) start from price time series which are $I(1)$ while their difference is fractionally integrated. In contrast but similar to our study, Dias et al. (2018) start from volatility time series which are fractionally integrated while their difference is stationary.

Our results may be summarized as follows. We find that all our volatility time series are fractionally integrated with an integration order $d > 0.5$ which confirms their long memory properties in line with established results in the literature (see for example the discussion in da Silva and Robinson, 2008). As regards volatility discovery, we find that Bitfinex and Bitstamp are the leading markets depending on the cryptocurrency. Kraken's information share is the lowest, but still around 30% for Ethereum, Litecoin, and Ripple. While Bitfinex is the most important market in terms of trading volume for all cryptocurrencies, it is only the leader in volatility discovery for Bitcoin and Ripple, whereas Bitstamp is found to be the leader for both Ethereum and Litecoin. Apart from Bitcoin, we cautiously consider our results for the other three cryptocurrencies, as the sampled data series studied are not long enough to ensure precision of our FCVAR parameter estimates.

In a further step, we investigate whether among the three studied cryptocurrencies, a certain coin[2] is considered the volatility leader. This examination provides a deeper insight into how volatility propagates through the three cryptocurrencies and their exchange markets in this study. Our analysis hints at Bitcoin having the highest volatility information content. Whether this is because it is the oldest and most established coin in the market, or because of its high volume as compared to the other considered cryptocurrencies is a question that will be answered with time as the other coins gain more vigour in the market.

The chapter proceeds as follows. Section 4.2 presents our theoretical framework and motivates the (fractionally) cointegrated nature between the volatility series of the same cryptocurrency in different markets. Subsequently, it introduces the FCVAR model, the

[2]We use the terms coins and cryptocurrencies interchangeably.

information share methodology of Hasbrouck (1995) and the implemented identification strategy. Section 4.3 describes the data and presents the volatility estimation, while Section 4.4 discusses the results of the volatility discovery analyses. Finally, Section 4.5 concludes.

4.2 Theoretical Framework and Modeling Strategy

Our theoretical framework is a discretized version of the model proposed by Dias et al. (2018). The authors extend the "one security - many markets" setting which is discussed in detail in Hasbrouck (1995) and with a follow up in Lehmann (2002). In such a setting, the (log-)prices of an asset traded in different markets may not drift apart in the long run as they are linked by the asset's fundamental value m_t, which is assumed to evolve as a random walk

$$m_t = m_{t-1} + u_t, \tag{4.2.1}$$

where u_t are pricing relevant innovations with $\mathbb{E}[u_t] = 0$ and $\mathbb{V}\text{ar}[u_t] = \sigma^2_{t,u}$. The difference to the standard model of Hasbrouck (1995) is that the variance of u_t is allowed to be time dependent. In particular, it is assumed that $\sigma^2_{t,u}$ has a long memory (as, e.g., in Bollerslev et al., 2013) and is, thus, best described by a fractionally integrated process of order d ($I(d)$). This specification allows the fundamental value to exhibit volatility clustering, heteroskedasiticty, and persistence which are often documented properties of prices. We give a brief description of long memory processes and their properties in Appendix 4.A.

The trading prices, $p_{i,t}$, which are realized on a given market i differ from the fundamental value m_t due to microstructure frictions (e.g., bid-ask bounce, price discreteness, or high latency). Hence, the observed (log-)price can be formulated as

$$p_{i,t} = m_t + \nu_t, \tag{4.2.2}$$

where ν_t captures the microstructure noise component with $\mathbb{E}[\nu_t] = 0$. In contrast to $\sigma^2_{t,u}$, $\sigma^2_{i,\nu}$ is assumed to be time independent, as microstructure effects are short-lived and should neither persist nor cluster, which makes them i.i.d. (which is a standard assumption in realized volatility literature, see, e.g., Andersen, Bollerslev and Meddahi, 2011). However, market microstructure effects probably depend on the market design which requires that $\sigma^2_{i,\nu}$ depends on market i. Hence, $\sigma^2_{i,\nu}$ itself represents the simplest form of a stationary process, a constant. In other words, it is $I(0)$. In addition, we assume that $\sigma^2_{i,\nu}$ is independent of the fundamental innovations' variance $\sigma^2_{t,u}$.

Taking first differences of Equation (4.2.2), the variance of the (log-)returns of the observed price can be calculated as

$$\mathbb{V}\mathrm{ar}[\Delta p_{i,t}] = \sigma^2_{t,u} + 2\sigma^2_{i,\nu}, \tag{4.2.3}$$

which is a fractionally integrated process of order d, as it inherits its properties from $\sigma^2_{t,u}$.

Similar to how the law of one price would govern the cointegration relationship between the prices of the asset on two different markets i and j, the volatility of the two markets can also not drift apart as the prices are linked by m_t. Therefore, the difference of the markets' variances which are both $I(d)$ will be stationary $I(0)$ again:

$$\mathbb{V}\mathrm{ar}[\Delta p_{i,t}] - \mathbb{V}\mathrm{ar}[\Delta p_{j,t}] = 2\sigma^2_{i,\nu} - 2\sigma^2_{j,\nu}. \tag{4.2.4}$$

As Equation (4.2.4) shows, calculating the difference between the variance of different markets cancels the dependence on $\sigma^2_{t,u}$. What is left is the sum of two $I(0)$ processes which is itself $I(0)$. Hence, the variances are fractionally cointegrated of order 0. This gives rise to the fractionally cointegrated vector autoregression (FCVAR) model proposed by Johansen (2008) and Johansen and Nielsen (2012), and which is briefly summarized in the next subsection.

4.2.1 FCVAR Model

Johansen (2008) and Johansen and Nielsen (2012) provide the fractional processes' counterpart of the Granger representation theorem (Engle and Granger, 1987). They derive the error correction representation of a vector autoregressive (VAR) model of order p that has fractionally integrated variables, Y_t, of dimensions $(n \times 1)$, with $t = \{1, \cdots, T\}$, as

$$\Delta^d Y_t = \alpha\beta' \Delta^{d-b} L_b Y_t + \sum_{i=1}^{p} \Gamma_i \Delta^d L_b^i Y_t + \varepsilon_t, \tag{4.2.5}$$

where Δ^d is the fractional difference operator, such that $\Delta^d Y_t$ is $I(0)$. L_b is the fractional lag operator, i.e., $L_b = 1 - \Delta^b$, d and b represent the fractional integration order and the degree of fractional co-integration, respectively, and $0 < b \leq d$. In other words, if $Y_t \sim I(d)$, then $\Delta^b Y_t \sim I(d-b)$. If $d = b = 1$, the cointegrated VAR (CVAR) model of Johansen (1995) -more commonly referred to as the Vector Error Correction Model (VECM)- arises as a special case of Equation (4.2.5). Hence, the remaining symbols in Equation (4.2.5) can be interpreted accordingly: β is an $(n \times l)$ matrix which contains the l cointegration vectors in its columns, the $(n \times l)$ matrix α contains the adjustment coefficients to the long-run equilibrium (or cointegration relations), and Γ_i are $(n \times n)$ matrices which account for the short-run dynamics of the system. The model innovations, ε_t, are assumed to be independently and identically distributed with mean zero and variance-covariance matrix Ω. For further mathematical details, the reader is referred to Johansen (2008).

Estimation of the set of parameters $\lambda = (d, b, \alpha, \beta, \Gamma)$ in Equation (4.2.5) is conducted via the conditional maximum likelihood (CML) method of Johansen and Nielsen (2012). Conditioning on N observations, the estimation requires maximizing

$$\log L_T(\lambda) = -\frac{n}{2}\left(\log(2\pi) + 1\right) - \frac{T}{2} \log \det \left\{ T^{-1} \sum_{t=N+1}^{T+N} \varepsilon_t(\lambda)\varepsilon_t(\lambda)' \right\} \tag{4.2.6}$$

with

$$\varepsilon_t(\lambda) = \Delta^d Y_t - \alpha\beta' \Delta^{d-b} L_b Y_t - \sum_{i=1}^{p} \Gamma_i \Delta^d L_b^i Y_t. \tag{4.2.7}$$

Before performing the estimation, we check whether our data are suitable for the analysis. In particular, we test whether the data are fractionally cointegrated and determine the cointegration rank using the trace test of Johansen and Nielsen (2012). As our application considers the volatility process of the same cryptocurrency on different exchanges, our working hypothesis is that there is only one common stochastic trend which governs volatility on all exchanges alike. In this case, we expect a cointegration rank of $n-1$. To conduct the test and to estimate the FCVAR model, the MATLAB toolbox provided by Nielsen and Popiel (2014) is adapted to our purposes.

4.2.2 Hasbrouck's (1995) Information Share

To identify the leading market in terms of volatility, we quantify the contribution of each of the exchanges to the common volatility component. For that purpose, we rely on the methodology proposed by Hasbrouck (1995) and calculate information shares. While most applications consider only two markets, information shares can be computed involving three or even more markets (see, for example, Huang, 2002; Ivanov, 2013; Grammig and Peter, 2018). As shown by Dias et al. (2018), the information shares can be directly computed from the parameters of the estimated FCVAR based on the decomposition of the variance of the long-run impact of the innovations in each market. Therefore, the first step is to examine the long-run dynamics of the system via the vector moving average (VMA) representation of a fractionally integrated process

$$Y_t = \Psi(L)\Delta_+^{-d}\varepsilon_t + X_t. \tag{4.2.8}$$

Johansen and Nielsen (2012) decompose the fractional process, Y_t, into $I(0)$ and $I(d)$ constituents. X_t, in Equation (4.2.8), refers to the $I(0)$ component, while the $I(d)$ dynamics are governed by the sequence of innovations $\{\varepsilon_t\}_{t=1}^T$ that are differenced using the truncated fractional difference operator[3], Δ_+^{-d}. Consequently, the long-term effects of

[3]See the detailed explanation of how a fractional difference operator works, and what it means to have a truncated version of it in Appendix 4.A.

these innovations are determined in the values of the $\Psi(1) = I + \sum_{s=0}^{\infty} \psi_s$ matrix which can be calculated as

$$\Psi(1) = \beta_\perp \left[\alpha'_\perp \left(I_n - \sum_{i=1}^{p} \Gamma_i \right) \beta_\perp \right]^{-1} \alpha'_\perp, \tag{4.2.9}$$

based on the estimates obtained from the estimation of the FCVAR in Equation (4.2.5). In the current setting, where we have only one common volatility component, we assume that the volatility across markets is equal in the long run (see Equation (4.2.4)). In the short run, deviations are possible. This setting gives rise to a cointegrating matrix $\beta = (I_{n-1}, -\mathbf{1}_{n-1})$, where $\mathbf{1}$ is a column vector of ones. The resulting rows of $\Psi(1)$ are identical and denoted by ψ.

Given that $\Omega = \mathbb{E}(\varepsilon_t \varepsilon'_t)$, with a suitable estimate of ε_t obtained from the residuals during the estimation of Equation (4.2.5), the total variance of the long-run impact of the innovations can be calculated as $\psi \Omega \psi'$. In order to attribute the share of each market's variance to the total variance, we need to isolate the variance contribution of each individual market. This is, however, not possible without further identifying restrictions if the innovations of the different markets are contemporaneously correlated, i.e., if Ω is not a diagonal matrix. In this case, Hasbrouck (1995) suggests decomposing $\Omega = CC'$ using Cholesky decomposition. The information share of market i can then be computed as

$$IS(i) = \frac{(\psi_i C_{ii})^2}{\psi \Omega \psi'}, \tag{4.2.10}$$

where ψ_i is the i-th element of ψ and C_{ii} is the row i column i element of C.

Yet, Cholesky decomposition entails a dependence of the information shares on the ordering of the markets in the dataset, i.e., the market which is ordered first will have a dominant share in the common variance as compared to the market which is ordered last. To circumvent this problem, an upper and a lower bound of the information share of each market can be determined by performing the previous analysis on all possible combinations of the markets. Naturally, this becomes more exhaustive as the number of markets increases. Additionally, the higher the correlation between the different markets, the more

the upper and lower bounds widen and become negligibly different across the different markets. This renders the average information share of a single market uninformative. Therefore, the literature has proposed various approaches to identify unique information shares. For example, Grammig and Peter (2013) assume a mixture of distributions for the innovations ε_t to obtain a unique decomposition of Ω. Another example is Lien and Shrestha (2009) who propose a factor structure for Ω. We rely on the second approach as it is more widely used in the literature.

4.2.3 Unique Identification Strategy of Lien and Shrestha (2009)

Lien and Shrestha (2009) propose a method to uniquely identify the contribution of each market to the variance of the fundamental volatility process. Their approach can be translated immediately to our application, as we similarly assume that the innovations are stationary and that the system entails one common stochastic trend (which is $I(d)$ here and $I(1)$ in their work). It is also directly applicable in a setup with more than two markets (see, for example, Arzandeh and Frank, 2019). Lien and Shrestha (2009) use a decomposition scheme for Ω that is dependent on the innovations' correlation matrix. They suggest a factor structure of the form

$$\varepsilon_t = F z_t \tag{4.2.11}$$

for the innovations in Equation (4.2.5), such that their variance results as $\Omega = \mathbb{E}(\varepsilon_t \varepsilon_t') = FF'$. The z_t are assumed to be of mean zero and to have a variance $\mathbb{E}[z_t z_t'] = I_n$. The factor F is defined as

$$F = \left[G \Lambda^{-\frac{1}{2}} G' V^{-1} \right]^{-1}, \tag{4.2.12}$$

where Λ is a diagonal matrix with the eigenvalues of the innovations correlation matrix on its main diagonal, G is the corresponding matrix of eigenvectors of the innovations' correlation matrix, and $V = diag(\sqrt{\Omega_{11}}, \sqrt{\Omega_{22}}, \ldots, \sqrt{\Omega_{nn}})$ is a diagonal matrix which

contains the standard deviation of each market's innovation on its main diagonal. Similar to Equation (4.2.10), the modified information share of market i is then defined as

$$MIS(i) = \frac{(\psi_i F_{ii})^2}{\psi \Omega \psi'}. \tag{4.2.13}$$

However, due to the fact that Equation (4.2.12) contains the matrix $\Lambda^{\frac{-1}{2}}$, the factors are not altogether unique. This is because the matrix contains on its diagonal the reciprocal of the square root of the eigenvalues of the correlation matrix. As such, both the positive as well as the negative roots could be used in this matrix. Yet, since Equation (4.2.13) requires using the square of the factor in the numerator, using either roots will not impact the information share obtained for each of the markets.

Given the previously discussed theoretical framework and the explanation of the estimation strategy for detecting the volatility leader, we next turn to a description of the cryptocurrency data used in the analysis.

4.3 Data Description and Volatility Estimation

For the analysis, daily (log-)prices of dollar denominated Bitcoin, Ethereum, Litecoin, and Ripple from the three exchanges Bitfinex, Bitstamp, and Kraken are used. The chosen cryptocurrencies have the highest trading volume of all cryptocurrencies (according to data from coinmarketcap.com retrieved in July, 2020) for which sufficiently long data series is available. The chosen markets are then the ones which exhibit the highest trading volume in USD in said cryptocurrencies. The dataset for Bitcoin extends from 1st of January 2015 till 30th of June 2020. For the other cryptocurrencies, the datasets are shorter. The first observation for Ethereum is on 29th of August 2017, while Litecoin and Ripple datasets start from 22nd of June 2017. The data have been retrieved from investing.com.[4]

For each coin, Figure 4.1 presents the daily trading volume share of each of the three exchanges over time. As can be seen, Bitfinex mostly dominates in terms of trading

[4] `https://www.investing.com/crypto/`

Figure 4.1: Daily share of market volume

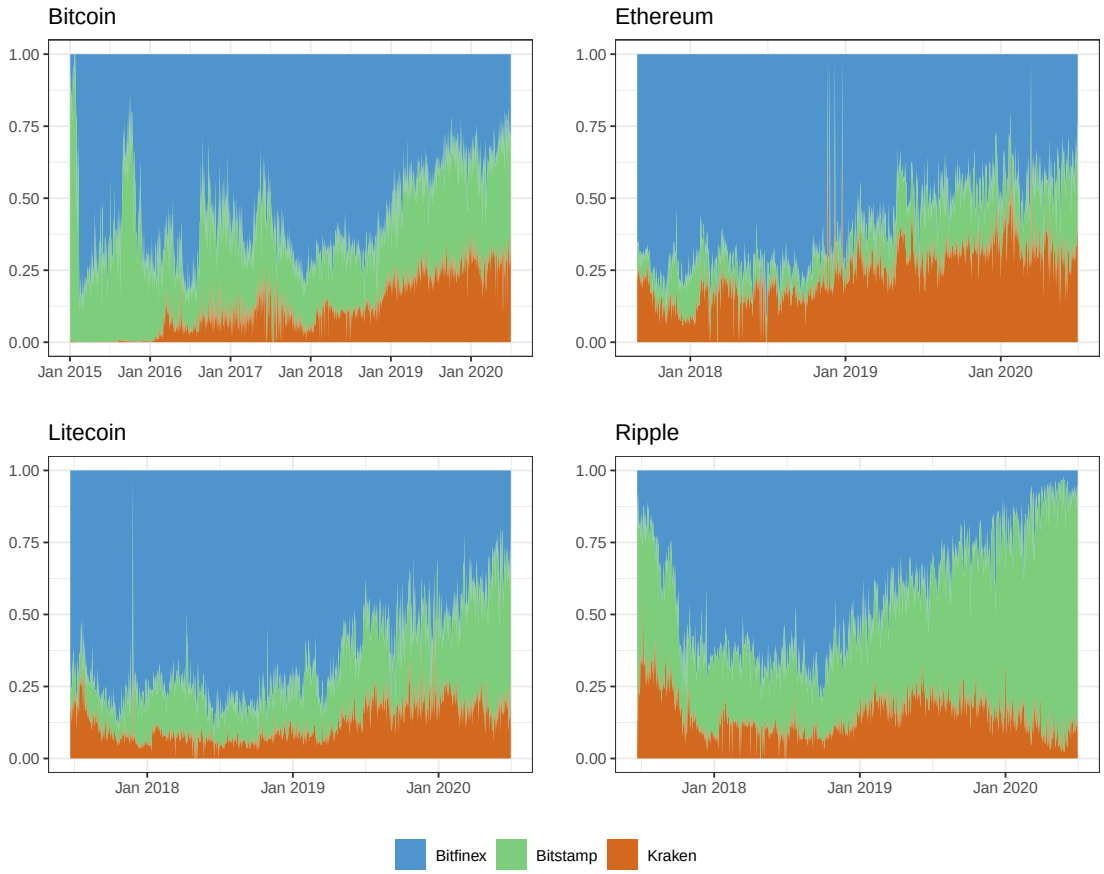

Note: The figure presents the evolution of the daily share of traded volume in Bitcoin and Etherum (upper panel), and Litecoin and Ripple (lower panel) across the three exchanges Bitfinex (blue), Bitstamp (green), and Kraken (orange).

volume for Bitcoin, Ethereum and Litecoin during the early period of the sample with few exceptions. Starting from 2019, however, the trading volume share of Bitstamp increases remarkably, and by the end of the data series, it dominates the other two markets in the trading of Bitcoin and Litecoin, while for Ethereum, the end of the data series shows an almost equal share of trading volume across the three exchanges. For Ripple, the beginning of the sample period shows a domination of Bitstamp, but it loses much trading volume between the end of 2017 and the end of 2018 in favor of Bitfinex. The end of the sample period, however, shows again a clear domination of Bitstamp.

In light of our theoretical framework discussion in Section 4.2, $\Delta p_{i,t}$ from Equation (4.2.3) is chosen to be modeled as a stochastic volatility (SV) process. In such a model, $\mathbb{V}\text{ar}\left[\Delta p_{i,t}\right]$ is an unobserved component that follows some latent stochastic process, usually an autoregressive process of order 1, AR(1). We follow Sandmann and Koopman (1998) and model our SV process in discrete time instead of the continuous time versions in Taylor (1994) and others. This SV model has also been previously used in the cryptocurrency literature, see for example Phillip, Chan and Peiris (2018) who use this model to examine the volatility process of 224 different cryptocurrencies among which are Bitcoin, Ethereum, and Ripple, and Chaim and Laurini (2018) who build on this model to examine volatility jumps in Bitcoin.

The SV model for each market/cryptocurrency is described by the following equations (the i index for the market is omitted for simplicity):

$$r_t = \exp\left(\frac{h_t}{2}\right)\xi_t \qquad \text{with} \qquad \xi_t \overset{iid}{\sim} \mathcal{N}(0,1), \tag{4.3.1}$$

$$h_t = \mu + \phi h_{t-1} + \eta_t \qquad \text{with} \qquad \eta_t \overset{iid}{\sim} \mathcal{N}(0,\sigma_\eta^2), \tag{4.3.2}$$

where $r_t = \Delta p_t$ refers to the daily log-returns and h_t is the latent log-volatility which follows an AR(1) process with a constant μ and a level of persistence ϕ. Both innovations ξ_t and η_t are assumed to be normally distributed with unit variance and σ_η^2, respectively. Thus, the goal is to estimate the set of parameters $\{\mu,\ \phi,\ \sigma_\eta^2\}$. This turns out to be a cumbersome task, as the linearization of Equation (4.3.1),

$$\ln\left(r_t^2\right) = h_t + \epsilon_t \qquad \text{with} \qquad \epsilon_t = \ln\left(\xi_t^2\right), \tag{4.3.3}$$

shows that the innovations ϵ_t in Equation (4.3.3) have a $\ln\left(\chi_1^2\right)$ distribution, for which there is no analytical expression. Some solutions to this problem are summarized in Sandmann and Koopman (1998) among which is a Bayesian approach using a Markov Chain Monte Carlo (MCMC) technique developed by Jacquier, Polson and Rossi (1994).

This technique is found to be superior to other methods, such as the Quasi-Maximum Likelihood (QML) and the Method of Moments (MM) estimation, yet it involves extensive simulations. Thus, we rely on its implementation in R by Kastner (2016) for our estimation purposes and keep the prior hyperparameters and the MCMC sampling configuration parameters at the suggested default values.[5]

Table 4.1 provides the estimates for the set of parameters $\{\mu, \phi, \sigma_\eta^2\}$ for each coin on each market. The small standard errors (reported in parentheses) for all the parameter estimates provide evidence that the MCMC sampler from the posterior distributions of the parameters has indeed converged without problems for all the exchanges and for all the cryptocurrencies. The estimated ϕ indicates that the latent log-volatility, h_t, is stationary for all entities in the sample as $\hat{\phi} < |1|$ in all cases. As expected, the differences among the estimates across exchanges for the same cryptocurrency are minor, due to the fact that we are modeling the prices of the same coin, and those, in turn, are cointegrated (as seen in the next subsection).

The differences across cryptocurrencies are more pronounced. As regards persistence, Bitcoin is found to have the highest persistence as $\hat{\phi}$ is in the vicinity of 0.90, while Ethereum is the least persistent with $\hat{\phi}$ around 0.7. Litecoin and Ripple occupy the middle-ground with $\hat{\phi}$ of approximately 0.8. Furthermore, Bitcoin has a higher mean stochastic volatility in levels as evidenced by its higher estimate of μ relative to the other cryptocurrencies, but has the lowest estimate for σ_η, the standard deviation of the innovation in the latent AR(1) volatility. Ethereum, on the other hand, has the highest estimate for σ_η.

Based on the estimates reported in Table 4.1, the latent volatility time series for our sample period is then reconstructed. The result is graphically illustrated in Figure 4.2 for Bitfinex. As can be seen, volatility reached a high at the end of December 2017 which is the time when Bitcoin reached its all-time high value of 19,141 USD. Overall, the figure reflects the pattern which is expected from the parameter estimates in Table 4.1, in particular that

[5]For further details, please refer to Kastner and Hosszejni (2019).

Table 4.1: Estimation results of the stochastic volatility model

	Bitfinex	**Bitstamp**	**Kraken**	**Bitfinex**	**Bitstamp**	**Kraken**
		A: Bitcoin			**B: Ethereum**	
$\hat{\mu}$	-7.14	-7.14	-7.15	-6.39	-6.39	-6.39
	(0.14)	(0.14)	(0.14)	(0.10)	(0.10)	(0.11)
$\hat{\phi}$	0.91	0.91	0.90	0.69	0.69	0.72
	(0.02)	(0.02)	(0.02)	(0.10)	(0.10)	(0.08)
$\hat{\sigma}_\eta$	0.54	0.54	0.57	0.78	0.78	0.75
	(0.05)	(0.05)	(0.05)	(0.13)	(0.13)	(0.12)
		C: Litecoin			**D: Ripple**	
$\hat{\mu}$	-6.18	-6.18	-6.21	-6.38	-6.38	-6.41
	(0.11)	(0.11)	(0.11)	(0.14)	(0.14)	(0.14)
$\hat{\phi}$	0.80	0.80	0.79	0.84	0.84	0.82
	(0.05)	(0.05)	(0.05)	(0.04)	(0.04)	(0.04)
$\hat{\sigma}_\eta$	0.60	0.60	0.62	0.68	0.68	0.73
	(0.08)	(0.08)	(0.08)	(0.08)	(0.08)	(0.08)

Note: The table presents the parameter estimates of the stochastic volatility model for each coin and market in the sample. Robust standard errors of the estimates are provided in parentheses. Panel A (B, C, D) holds the results for Bitcoin (Ethereum, Litecoin, and Ripple).

the three other cryptocurrencies have a higher standard deviation compared to Bitcoin. The time series plots for the remaining markets look similar and are therefore presented in Appendix 4.B.

Table 4.2 provides descriptive statistics for each coin and market. It shows that, on average, the volatility time series of Litecoin appears to be more volatile than the volatility of other currencies, while, consistent with Table 4.1 and Figure 4.2, Bitcoin is the least volatile in our sample period. Additionally, across the different market exchanges, Bitstamp has on average the highest volatility for all the cryptocurrencies except for Ripple, where Kraken, on average, is shown to have the highest volatility.

To motivate the application of the FCVAR model, Figure 4.3 presents the estimated autocorrelation coefficients along with their 95% confidence bounds (based on robust standard errors which are estimated using GMM) of the latent volatility of Bitcoin traded on the three exchanges. Similar to the illustrations in Appendix 4.A, it can be seen that

Figure 4.2: Latent volatility time series in Bitfinex market

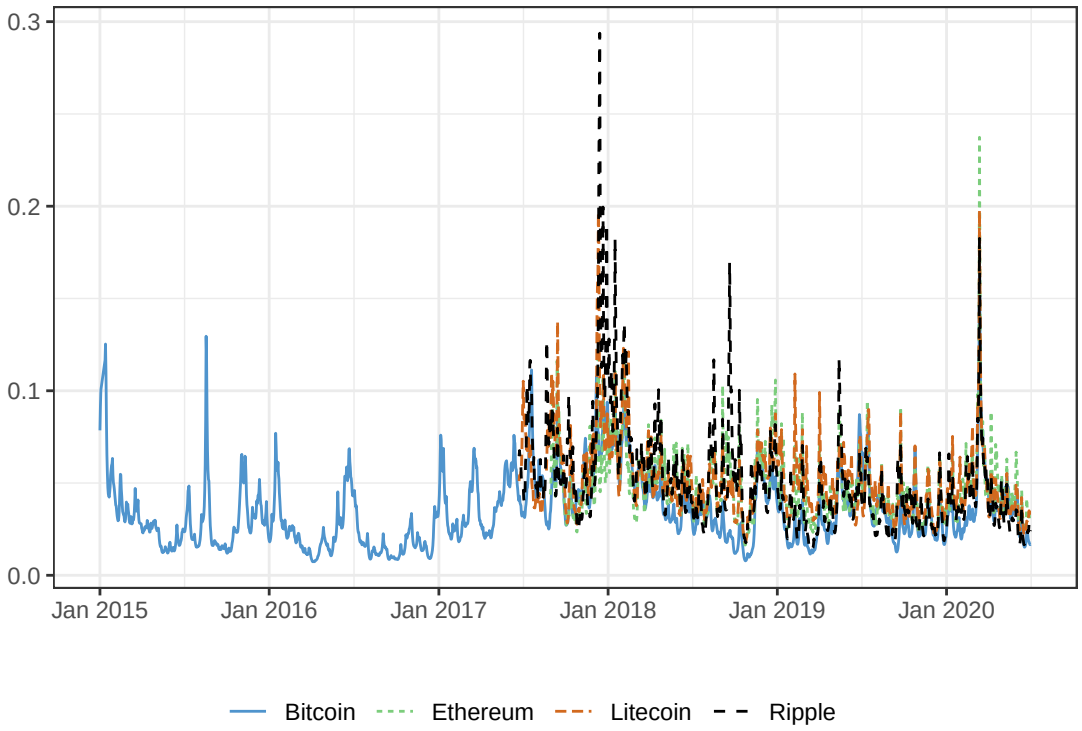

Note: The figure presents the time series of the latent volatility of the four cryptocurrencies Bitcoin, Ethereum, Litecoin, and Ripple based on data from Bitfinex market.

the autocorrelation is rather persistent, as it takes around 700 lags before the confidence bounds start oscillating around zero. This indicates that our latent volatility process, albeit an AR(1) process with $\mid \hat{\phi} \mid < 1$, exhibits the slow decline associated with long memory processes. The autocorrelation functions of the remaining cryptocurrencies show a similar pattern and, thus, support the assumption of a long memory in the volatility process and are provided in Appendix 4.C.

4.4 On the Origin of Volatility

4.4.1 Volatility Discovery among Cryptocurrency Markets

The FCVAR model in Equation (4.2.5) is estimated for the three markets; Bitfinex, Bitstamp, and Kraken ($n = 3$), with $Y_t = \left(\hat{h}_{1,t}, \hat{h}_{2,t}, \hat{h}_{3,t}\right)$, and $\hat{h}_{i,t}$ estimated according to

Table 4.2: Descriptive statistics of the latent volatility

	Mean	S.D.	Min	Max	Mean	S.D.	Min	Max
	A: Bitcoin				**B: Ethereum**			
Bitfinex	0.0344	0.0191	0.0073	0.1740	0.0476	0.0187	0.0164	0.2373
Bitstamp	0.0339	0.0201	0.0055	0.2172	0.0473	0.0193	0.0143	0.2388
Kraken	0.0345	0.0193	0.0059	0.1839	0.0474	0.0189	0.0147	0.2400
	C: Litecoin				**D: Ripple**			
Bitfinex	0.0516	0.0205	0.0179	0.1977	0.0502	0.0286	0.0145	0.2938
Bitstamp	0.0514	0.0211	0.0172	0.2108	0.0500	0.0287	0.0141	0.2882
Kraken	0.0512	0.0208	0.0166	0.2020	0.0501	0.0291	0.0147	0.2925

Note: The table presents descriptive statistics (mean, standard deviation (S.D.), minimum (Min), and maximum (Max)) of the latent volatility estimated on daily data for Bitfinex, Bitstamp, and Kraken. Panel A (B, C, D) holds the results for Bitcoin (Ethereum, Litecoin, and Ripple).

Equation (4.3.2). The number of lags p is chosen according to the Bayesian Information Criterion for each coin and a cointegration rank of $n - 1 = 2$ is used as evidenced by the trace test of Johansen and Nielsen (2012) shown in Table 4.D.1. The test supports our working hypothesis of a single stochastic trend driving the volatility processes in the different markets. Additionally, and following our theoretical scheme presented in Equation (4.2.4) in Section 4.2, we expect the deviations of the single markets from the long-run equilibrium to be short-term, and as such, $\beta' Y_t$ should be an $I(0)$ mean-reverting process. Thus, we impose a restriction of $d = b$ while estimating Equation(4.2.5). A white noise test on the residuals of the resulting FCVAR model for each of the cryptocurrencies indicates that the residuals are uncorrelated. We, thus, conclude that the model, given the imposed restrictions, fits the data reasonably well.

Table 4.3 holds the results of the FCVAR estimation. It can be seen that $\hat{d}$ is statistically significant for all the cryptocurrencies under consideration, thus, supporting the assumption of a fractional nature of the latent stochastic volatility processes in all the markets for all the cryptocurrencies. Furthermore, we find that the order of magnitude of $\hat{d}$ is quite similar across the different cryptocurrencies and varies around 0.7. Turning to the cointegration matrix, $\hat{\beta}$, by means of LR-tests, it is found that we cannot reject

Figure 4.3: Autocorrelation plots of the latent volatility of Bitcoin

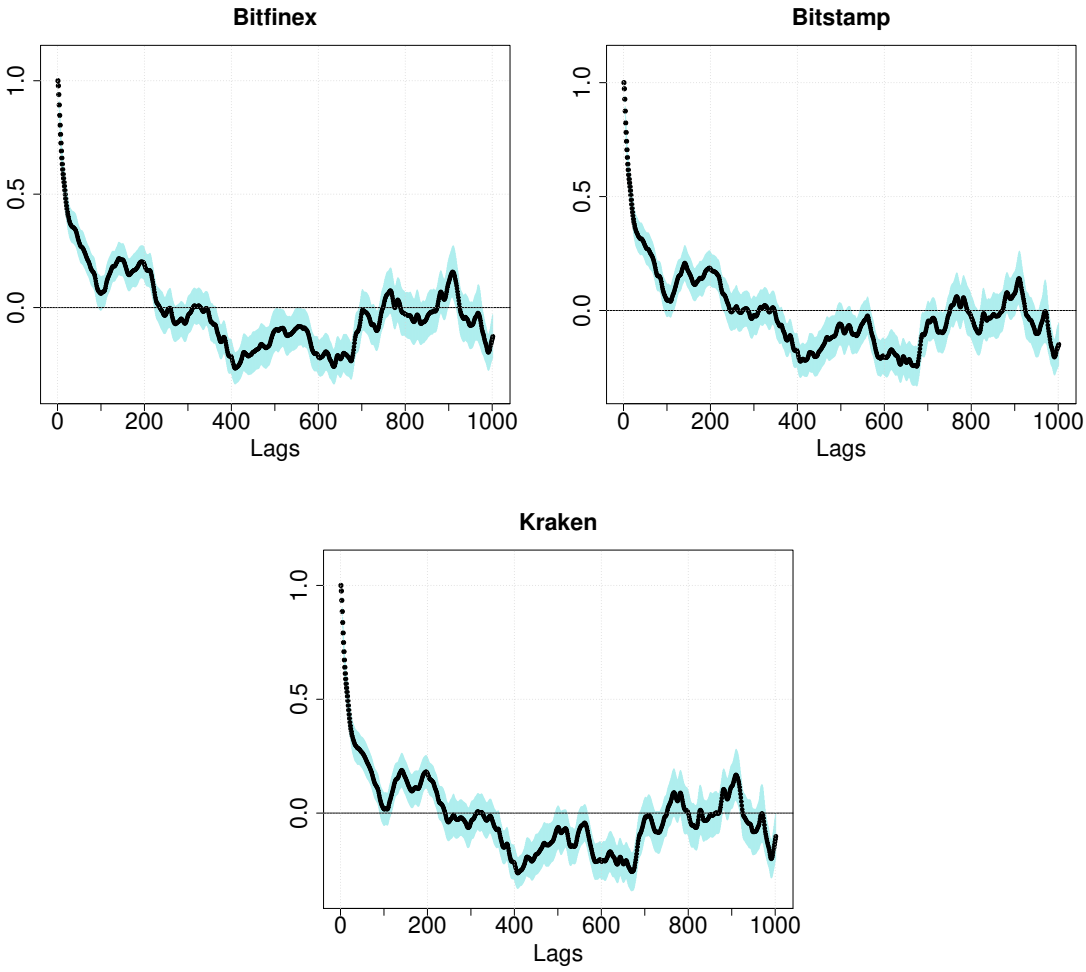

Note: The figure presents the autocorrelation plots and their 95% GMM based bounds for the three exchanges Bitfinex, Bitstamp (upper panel), and Kraken (lower panel) for the cryptocurrency Bitcoin.

the hypothesis of a matrix structure of $\hat{\beta} = (I_{n-1}, -\mathbf{1}_{n-1})'$ for all the cryptocurrencies on a 5% significance level. This indicates that the latent stochastic volatilities of the cryptocurrencies traded on the different exchanges are expected to behave similarly in equilibrium.

As mentioned previously, $\hat{\alpha}$, for each coin, reflects the adjustment coefficients of the different exchanges to the $n-1$ equilibrium/cointegration equations. It is, therefore, interesting to determine the significance level of each $\hat{\alpha}_{j,i}$, where $j = 1, \ldots, n-1$ denotes

Table 4.3: FCVAR model estimates

	Bitfinex	**Bitstamp**	**Kraken**	**Bitfinex**	**Bitstamp**	**Kraken**
	A: Bitcoin (p =2)			**B: Ethereum** (p =2)		
$\hat{\alpha}'$	0.002	0.061	0.067	-0.236	-0.106	0.067
	(0.018)	(0.022)	(0.019)	(0.152)	(0.149)	(0.144)
	-0.040	-0.102	0.065	0.137	-0.024	0.524
	(0.025)	(0.029)	(0.025)	(0.195)	(0.190)	(0.185)
	$\hat{d}$	0.775	(0.033)	$\hat{d}$	0.744	(0.029)
	C: Litecoin (p =5)			**D: Ripple** (p =2)		
$\hat{\alpha}'$	-0.170	0.003	-0.068	-0.000	0.092	0.113
	(0.118)	(0.119)	(0.123)	(0.115)	(0.122)	(0.125)
	0.114	-0.077	0.126	-0.110	-0.220	-0.061
	(0.121)	(0.124)	(0.126)	(0.142)	(0.150)	(0.154)
	$\hat{d}$	0.852	(0.032)	$\hat{d}$	0.716	(0.034)

Note: The table presents selected FCVAR estimates for the latent log-volatility $\hat{h}_t$. Robust standard errors are given in parentheses. Panel A (B, C, D) holds the results for Bitcoin (Ethereum, Litecoin, and Ripple) for the given number of lags p chosen according to the Bayesian Information Criterion.

the equilibrium equation, and i = (Bitfinex,Bitsamp,Kraken) is the relevant exchange market. If $H_0 : \hat{\alpha}_{j,i} = 0$, then this market does not adjust to the equilibrium, and it is, thus, the one driving the volatility. From Table 4.3, it is seen that for Bitcoin, Bitfinex does not adjust to the two cointegration equations, as $\hat{\alpha'}_{1,1}$ and $\hat{\alpha'}_{2,1}$ are statistically insignificant at the 5% significance levels. Bitstamp and Kraken, however, have statistically significant results, and adjust according to the magnitude and sign of their respective $\hat{\alpha}_{j,i}$. Therefore, it is expected that Bitfinex would be the volatility leader in the Bitcoin market. Unfortunately, a similar clear story cannot be told for the other three cryptocurrencies, as most of the values in their respective $\hat{\alpha}$ are statistically insignificant. It is our belief that this is in part due to the considerably shorter time series of Ethereum, Litecoin, and Ripple as compared to Bitcoin (cp. Section 4.3). Rossi and Santucci de Magistris (2013) show in a Monte Carlo simulation study that the CML estimation precision of the FCVAR model, described in Section 4.2.1, is highly dependent on the sample size

of the dataset. It becomes more reliable for $T = 2000$, as the finite sample distribution of the estimates resemble more closely their asymptotic limiting Gaussian distribution. Thus, it can be concluded that Bitfinex is the leading market in terms of bitcoin volatility, while the two other markets, Bitstamp and Kraken, merely adjust to the volatility process which is determined by Bitfinex. If statistical significance is temporarily disregarded, the $\hat{\alpha}$ estimates for Ethereum and Litecoin would suggest that Bitstamp is the market which adapts the least while Bitfinex and Kraken might exhibit similar adaptation mechanisms. Yet, for Ripple, similar to Bitcoin, Bitfinex appears to be the leading market. However, these interpretations should only be viewed with caution due to the imprecise nature of the estimation.

The $\hat{\alpha}$ results for Bitcoin are clearly reflected in the Hasbrouck information share results presented in panel A in Table 4.4. It is found that for Bitcoin, the Bitfinex exchange has the highest upper and lower information share bounds relative to the other two exchanges. For Ethereum and Litecoin, Bitstamp appears to have the largest upper and lower bounds, whereas for Ripple, Bitfinex is again the dominating exchange market. However, we remain skeptical about the results of the latter three cryptocurrencies due to their insignificant $\hat{\alpha}$, as previously explained. It is noticeable from Table 4.4 that the Hasbrouck information share bounds are very wide, due to the high correlation between the different markets. Consequently, we also report the Lien and Shrestha (2009) information shares in panel B. Again, here, Bitfinex dominates the market for Bitcoin with almost 60% of the information share followed by Kraken and then Bitstamp. For Ethereum, Litecoin and Ripple, the information shares are more evenly distributed across the three markets, which is in line with the insignificant $\hat{\alpha}$ results. Yet, in line with the Hasbrouck information shares, some dominance is achieved by Bitstamp, for Ethereum and Litecoin, and by Bitfinex for Ripple.

The last panel in Table 4.4 contains the traded volume shares of each exchange market in each of the cryptocurrencies under examination. It is evident that Bitfinex largely dominates in this aspect for all the cryptocurrencies, although it is not that outstandingly dominant in Ripple, while Bitstamp is the second highest market in all of the cryptocur-

Table 4.4: Information and volume shares

	Bitfinex		**Bitstamp**		**Kraken**	
A: Hasbrouck's 1995 information shares in %						
	upper	lower	upper	lower	upper	lower
Bitcoin	97.0	13.2	81.5	0.7	69.3	1.8
Ethereum	95.0	0.6	98.8	2.8	90.7	0.6
Litecoin	96.5	0.03	99.0	1.3	98.6	0.8
Ripple	98.8	1.6	95.7	0.04	97.6	0.4
B: Lien and Shrestha's 2009 information shares in %						
Bitcoin	59.1		17.8		23.1	
Ethereum	25.0		45.6		29.4	
Litecoin	25.7		38.3		36.0	
Ripple	42.0		21.9		36.1	
C: Volume shares in %						
Bitcoin	62.3		27.3		10.4	
Ethereum	62.6		14.6		23.2	
Litecoin	70.6		18.8		10.6	
Ripple	44.8		42.2		13.0	

Note: The table presents the information and volume shares of each cryptocurrency traded on the three exchanges: Bitfinex, Bitstamp and Kraken. Panels A and B display the Hasbrouck information share bounds and the modified information shares using Lien and Shrestha's method, respectively, and Panel C calculates the traded volume share which is an average of the daily shares presented in Figure 4.1.

rencies with the exception of Ethereum. These results indicate that for Bitcoin, the market with the highest volume share is also the market which contributes most to the common volatility process. This is a result frequently documented in the price discovery literature where high trading activity and a high information share often correspond. For Ripple, the result is also in line with this conjecture. For the two remaining cryptocurrencies, the result is not as clear-cut. For Ethereum, Bitstamp has the highest information share, but the lowest share in volume, while in the case of Litecoin, Bitstamp also dominates the volatility process, but has a decisively lower volume share than Bitfinex.

Given the low statistical significance of the FCVAR results, a clear statement can only be made about the volatility discovery of Bitcoin where Bitfinex turns out to be the leading market. For the remaining (younger) cryptocurrencies, estimation is very imprecise due to the low number of observations available at present. Nevertheless, they point to a dominating position of Bitfinex in the case of Ripple and of Bitstamp for Ethereum and Litecoin.

As a robustness check, we compare the out-of-sample forecasts of the estimated FCVAR model with that of a standard CVAR to determine whether the added complications of fractional differencing actually play a role in the representation of our data. The results are displayed in the two figures presented in Appendix 4.E. For conciseness, only the results of Bitcoin are displayed. The figures show that a 9-month out-of-sample forecast using FCVAR is able to match the trend (and sometimes the level) of the actual data, while a standard CVAR performs quite poorly. Thus, we abide by our choice of a fractional differencing cointegration scheme to investigate the volatility discovery in cryptocurrency markets.

4.4.2 Volatility Discovery among Cryptocurrencies

In this subsection, we investigate whether among the four examined cryptocurrencies, a certain coin is considered a volatility leader. Table 4.5 shows the cointegrating rank test performed on the four coins using the leading exchange market for each coin retrieved from the first stage results presented in the previous section. Our results suggests that there are three different cointegrating relations between the four coins, and thus, only one stochastic trend. This indicates that the markets and cryptocurrencies are linked by a common fundamental volatility process which could be considered the fundamental risk of cryptocurrencies.

The next step is to find which coin acts as the volatility leader in the cryptocurrency market. Thus, a second-stage volatility discovery analysis is run with the four cryptocurrencies. The second-stage FCVAR results are presented in Table 4.6. Interestingly, we

Table 4.5: Second stage cointegration rank test

Rank	d	b	Log-Likelihood	LR statistic	P-value
0	0.934	0.934	7235.041	199.748	0.000
1	0.960	0.960	7280.432	108.967	0.000
2	0.976	0.976	7314.298	41.234	0.000
3	0.994	0.994	7334.668	0.495	0.544
4	0.995	0.995	7334.916	–	–

Note: The table presents Johansen's trace test (Johansen and Nielsen, 2012) for the cointegrating rank conducted on the four coins in our study: Bitcoin, Ethereum, Litecoin and Ripple. The results are achieved with $p = 1$ according to the Bayes Information Criterion.

find that $\hat{d}$ is considerably higher than the results in the first stage of the analysis and lies more in the vicinity of one. This indicates that, whereas the volatility series of different exchange markets trading in a single coin are fractionally cointegrated, the volatility series of the different coins are governed by a cointegrated rather than a fractionally cointegrated relation. The $\hat{\alpha}'$ results indicate that Bitcoin may be the volatility leader while all the other coins follow suit, as the first cointegrating equation shows that only Bitcoin's adjustment coefficient estimate is not significantly different from zero. The second cointegrating equation, however, indicates that both Litecoin and Ripple do not adjust to the disequilibrium (with adjustment coefficients not significantly different from zero) and that Bitcoin and Ethereum follow their lead, as their adjustment coefficients are significantly different from zero. In the third equation, the adjustment coefficients of all the coins are significantly different from zero. Yet, if the order of magnitude is considered, Bitcoin is again viewed as the volatility leader, as its respective $\hat{\alpha}$ is the smallest compared to the other coins.

The second-stage Hasbrouck (1995) and Lien and Shrestha (2009) information share results presented in Table 4.7 confirm the preliminary $\hat{\alpha}$ results and indicate that Bitcoin is indeed the volatility leader among the other cryptocurrencies in the analysis. The Hasbrouck information shares of Bitcoin lie between an upper bound of 91% and a lower bound of 25%, while all the other coins have considerably smaller upper and lower bounds.

Table 4.6: Second stage estimates of the FCVAR model

	Bitcoin	**Ethereum**	**Litecoin**	**Ripple**
$\hat{\alpha}'$	-0.004	0.047	0.036	0.033
	(0.008)	(0.014)	(0.010)	(0.012)
	-0.034	-0.146	-0.005	-0.012
	(0.013)	(0.023)	(0.016)	(0.019)
	0.026	0.087	-0.045	0.041
	(0.014)	(0.024)	(0.017)	(0.020)
$\hat{d}$	0.994	(0.025)		

Note: The table presents the relevant FCVAR estimates for the latent log-volatility $\hat{h}_t$ of the second-stage results. Robust standard errors are presented in parentheses. The results are achieved with $p = 1$ according to the Bayes Information Criterion.

Table 4.7: Second stage information shares

	HIS		**MIS**
	upper	lower	
Bitcoin	91.0	25.5	60.8
Ethereum	39.4	0.2	1.6
Litecoin	63.3	0.8	21.5
Ripple	48.7	1.6	16.1

Note: The table presents Hasbrouck's (HIS) and Lien and Shrestha's modified (MIS) information shares of volatility among the different cryptocurrencies.

Similary, the Lien and Shrestha information share puts Bitcoin at a dominant 60% while the next market, Litecoin, has only a third of that share.

Hence, it seems that the established nature of Bitcoin makes it a volatility leader for the other cryptocurrencies. Only time will tell whether it will withhold its superiority as the other cryptocurrencies become more established.

4.5 Conclusion

Cryptocurrency markets are characterized by high risk which is reflected in the high volatility of the currencies' trading prices. Understanding how the volatility of different cryp-

tocurrencies or among different markets is related can open up hedging strategies and even provide opportunities for high returns. In this study, we investigate the interrelatedness of the volatility (estimated based on a discrete stochastic volatility model) of cryptocurrencies (Bitcoin, Ethereum, Litecoin and Ripple) traded in the most prominent cryptocurrency markets (Bitfinex, Bitstamp and Kraken).

Our theoretical framework and empirical approach extend the usual strategies for price discovery into the realm of volatility discovery. A detour has to be taken along the way, as volatility series tend to possess long memory properties, and thus, fractional cointegration, rather than standard cointegration, governs the relationship between the different volatility series. Towards this end, we rely on Johansen and Nielsen's 2012 fractionally cointegrated vector autoregressive model and exploit its results to calculate Hasbrouck's 1995 information shares and the refinement to modified information shares by Lien and Shrestha (2009).

Our results indicate that the dominating market for volatility of Bitcoin is Bitfinex. It is found to have both the highest trading volume share and the highest volatility information share. For the other coins, we cautiously consider our results, as the FCVAR estimation is imprecise due to the considerably lower number of observations available to date. We find that while Bitfinex still dominates the share of traded volume, Bitstamp has the highest volatility information share for both Ethereum and Litecoin, and for Ripple, Bitfinex has both the highest traded volume and information shares, but only with a small margin from the other two exchange markets in the analysis.

In a second step, we consider whether volatility in the cryptocurrency market may actually originate from a particular coin and then diffuse to the other coins in the market. Our findings indicate that Bitcoin might be a volatility leader in this regard, as it exhibits the highest volatility information share. Nevertheless, it remains to be seen whether in such a dynamic market Bitcoin will be able to maintain its distinction, as the other cryptocurrencies gather more momentum and a larger dataset is available for examination.

To address the problem of a limited dataset which we face in our study, a panel volatility discovery approach could be fruitful. For price discovery, panel estimation is used already (e.g., Narayan, Sharma and Thuraisamy, 2014; Karabiyik, Westerlund and Narayan, 2022). In the present context, however, a panel approach would have to take the fractional nature of volatility into account. To the best of our knowledge, there is no theory on fractionally integrated panel vector autoregressive models (yet). This is, thus, left for future research.

Appendix

4.A Long memory processes and the principles of fractional integration

This appendix section explains some time series properties of long memory processes and their underlying mathematical concepts to the extent that is relevant to the current study. The section depends heavily on the review provided in Baillie (1996), which relies on the work of Granger and Joyeux (1980) and Granger (1980, 1981). For further details, the aforementioned papers should be consulted.

In standard time series analysis, an autoregressive moving average process is denoted as ARMA (p, q), where p and q refer to the number of autoregressive and moving average lags, respectively. If this ARMA (p, q) process is covariance stationary, then it can be expressed using Wold's decomposition as:

$$Y_t = \mu + \sum_{j=0}^{\infty} \psi_j \varepsilon_{t-j}, \tag{4.A.1}$$

where ε is a white noise process[6] and square summability is assumed, i.e., $\sum_{j=0}^{\infty} \psi_j^2 < \infty$. As a result, the Wold decomposition coefficients, ψ_j, exhibit an exponential rate of decay (Hamilton, 1995). The covariance stationary ARMA (p, q) processes are, thus, seen as short memory processes. Long memory processes, in contrast, have a slower rate

[6]Not to be confused with ε used otherwise in the FCVAR model described in Section 4.2.1. This appendix has standalone symbols.

of decay. Specifically, they exhibit a hyperbolic rate of decay, which makes them ideal for representing shocks and autocorrelations that have some degree of persistence. They are, thus, thought of as processes that are integrated of order d, or $I(d)$ processes, where $0 < d < 1$, and pose a flexible compromise between covariance stationary processes, $I(0)$, and unit root processes, $I(1)$.

For many useful applications, such as forecasting exercises, ARMA (p, q) processes that have unit roots outside the unit circle need to be differenced in order to reduce their order of integration to zero, i.e., to make them covariance stationary. In that sense, the autoregressive integrated moving average process, denoted as ARIMA(p, d, q) is modeled. If d is allowed to take noninteger numbers, the autoregressive fractionally integrated moving average process, ARFIMA (p, d, q) then arises. It is modeled as:

$$\phi(L)\,(1-L)^{d}\,Y_t = \mu + \theta(L)\varepsilon_t, \tag{4.A.2}$$

where $\phi(L) = 1 - \phi_1 L - \phi_2 L^2 - \cdots - \phi_p L^p$, and $\theta(L) = 1 + \theta_1 L + \theta_2 L^2 + \cdots + \theta_q L^q$. Here, $(1-L)^d$ is the fractional difference operator, and it works via binomial expansion as follows:

$$(1-L)^d = \Delta^d = \sum_{i=0}^{\infty} (-1)^i \binom{d}{i} L^i \tag{4.A.3}$$

$$= 1 - dL + \frac{d(d-1)}{2!}L^2 - \frac{d(d-1)(d-2)}{3!}L^3 + \cdots \tag{4.A.4}$$

Yet, this poses a mathematical problem, as the fractional differencing process can extend to infinity. Therefore, in many cases, the differencing is truncated at a certain value,

usually at $t-1$, as in practice initial values rarely exist. Therefore, following Jensen and Nielsen (2014), to calculate the truncated fractional difference of a process, Y_t,

$$\Delta_+^d Y_t = \sum_{i=0}^{t-1} \pi_i(-d) Y_{t-i}, \qquad t = 1, \cdots, T \tag{4.A.5}$$

$$\text{with} \qquad \pi_i(-d) = \frac{-d(-d+1)\cdots(-d+i-1)}{i!}. \tag{4.A.6}$$

The '+' subscript in Equation (4.A.5) indicates that the differencing is restricted to only positive values of t, as no initial values exist in this case. Nevertheless, as T increases, the complexity of the fractional difference solution increases, and in turn its computation time. Jensen and Nielsen (2014) develop a fractional difference algorithm in MATLAB that utilizes discrete Fourier transform, and is thus fast. We rely on their algorithm in this study.

A simple simulation study

In order to illustrate the properties of a long memory process, a simple simulation study is carried out. Figure 4.A.1 shows the ensemble mean and variance of four different ARFIMA (1,d,0) processes simulated with different degrees of integration, $d = \{0, 0.3, 0.6, 1\}$. Panel A, with $d = 0$ is thus the standard AR(1) process with ensemble mean and variance that oscillates around their respective theoretical values without any persisting deviations. Panel D, on the other hand, represents an AR(1) process with unit root, as $d = 1$. As expected, it is a non stationary process, and predictably, the ensemble variance is time-dependent. The two other in-between panels represent different degrees of deviations from the completely stationary AR(1) process. Panel C with $d = 0.3$ more closely resembles the stationary AR(1) process, as the ensemble variance, although oscillating to higher values, does not exhibit a clear trend. Conversely, panel C with $d = 0.6$ shows an ensemble variance with an upward trend, but it accelerates at a slower pace relative to the unit root process.

Figure 4.A.1: Ensemble simulations of various ARFIMA(1,d,0) processes

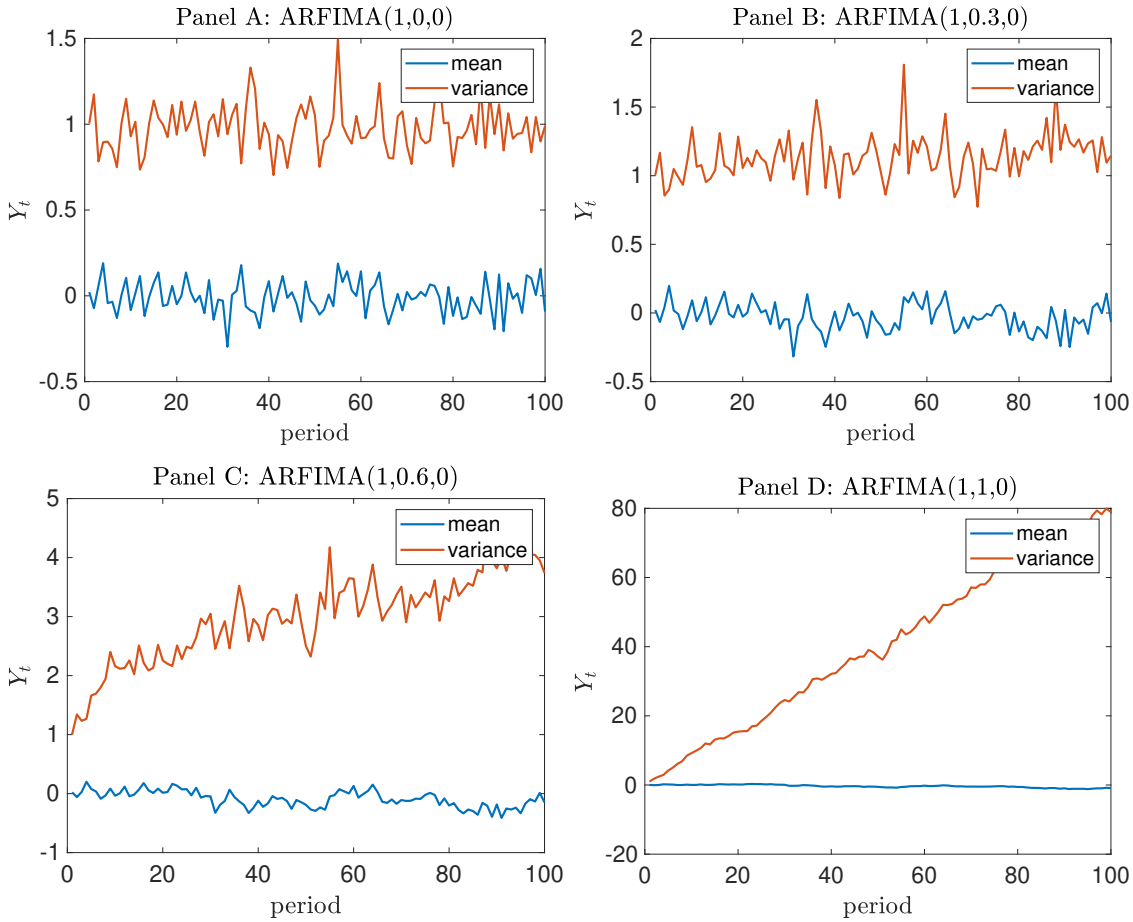

Note: The figure presents the ensemble mean and variance of 100 simulations of different ARFIMA(1,d,0) process with $\phi = 0.1$ and $T = 100$. Panel A presents an ARFIMA(1,0,0) process, i.e a standard AR(1) process. Panel B presents an ARFIMA(1,0.3,0) process. Panel C presents an ARFIMA(1,0.6,0) process. Panel D presents an ARFIMA(1,1,0) process, i.e. a unit root AR(1) process.

To illustrate the persistence of the long memory, Figure 4.A.2 shows the ensemble autocorrelations of the ARFIMA (1,d,0) processes in Figure 4.A.1. The figure illustrates the slower rate of decay of the autocorrelations of the different processes as d approaches 1. Panels B and C, which represent the long memory processes, have autocorrelations of zero only after 15 and 20 lags, respectively. In comparison, panel A, the standard AR(1) process, reaches zero in less than 5 lags, while panel D, representing the unit root process, does not reach zero at all and is thus permanently persistent.

Figure 4.A.2: Autocorrelations of various ARFIMA(1,d,0) processes

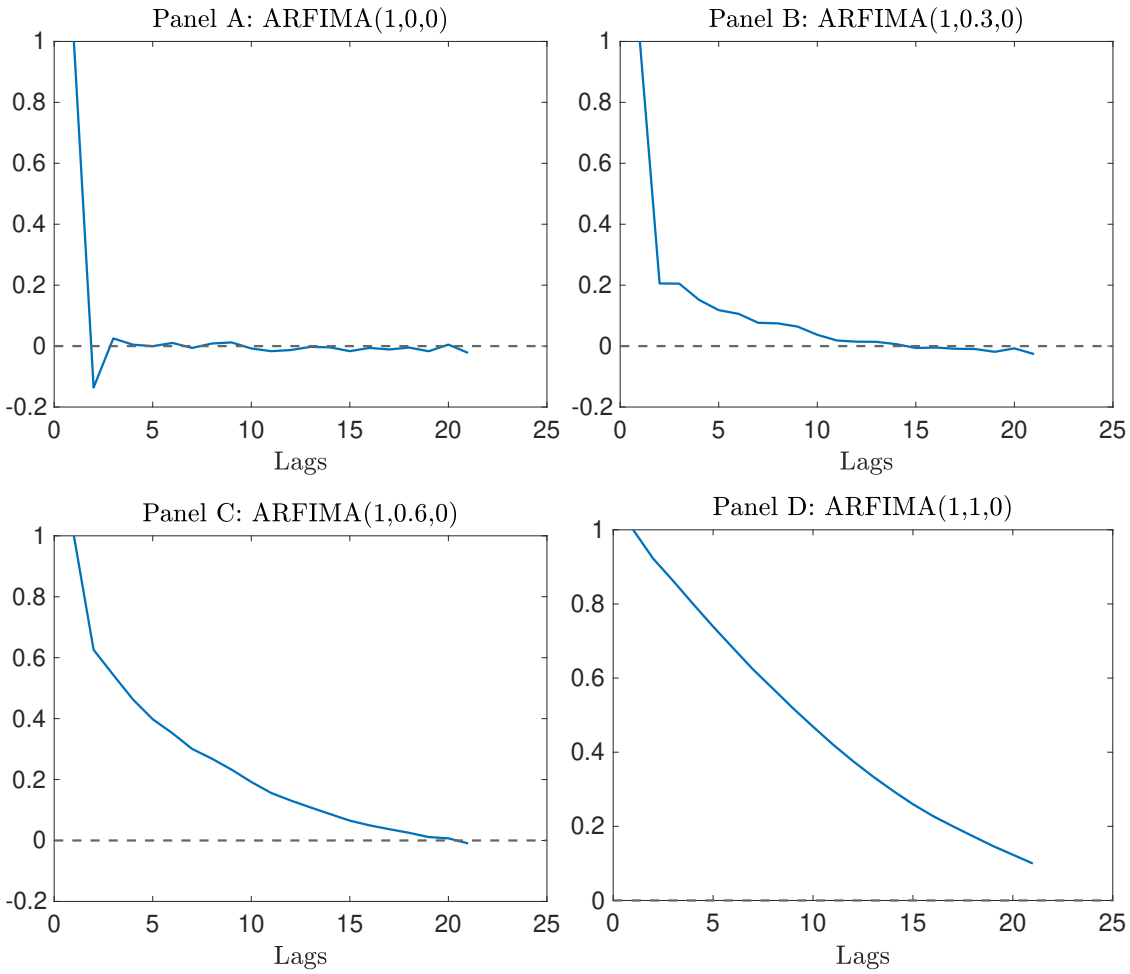

Note: The figure presents the mean autcorrelations of 100 simulations of different ARFIMA(1,d,0) process with $\phi = 0.1$ and $T = 100$. Panel A presents an ARFIMA(1,0,0) process, i.e a standard AR(1) process. Panel B presents an ARFIMA(1,0.3,0) process. Panel C presents an ARFIMA(1,0.6,0) process. Panel D presents an ARFIMA(1,1,0) process, i.e. a unit root AR(1) process.

4.B Time series plots of the latent volatility (continued)

Figure 4.B.1: Latent volatility time series in Bitstamp and Kraken markets

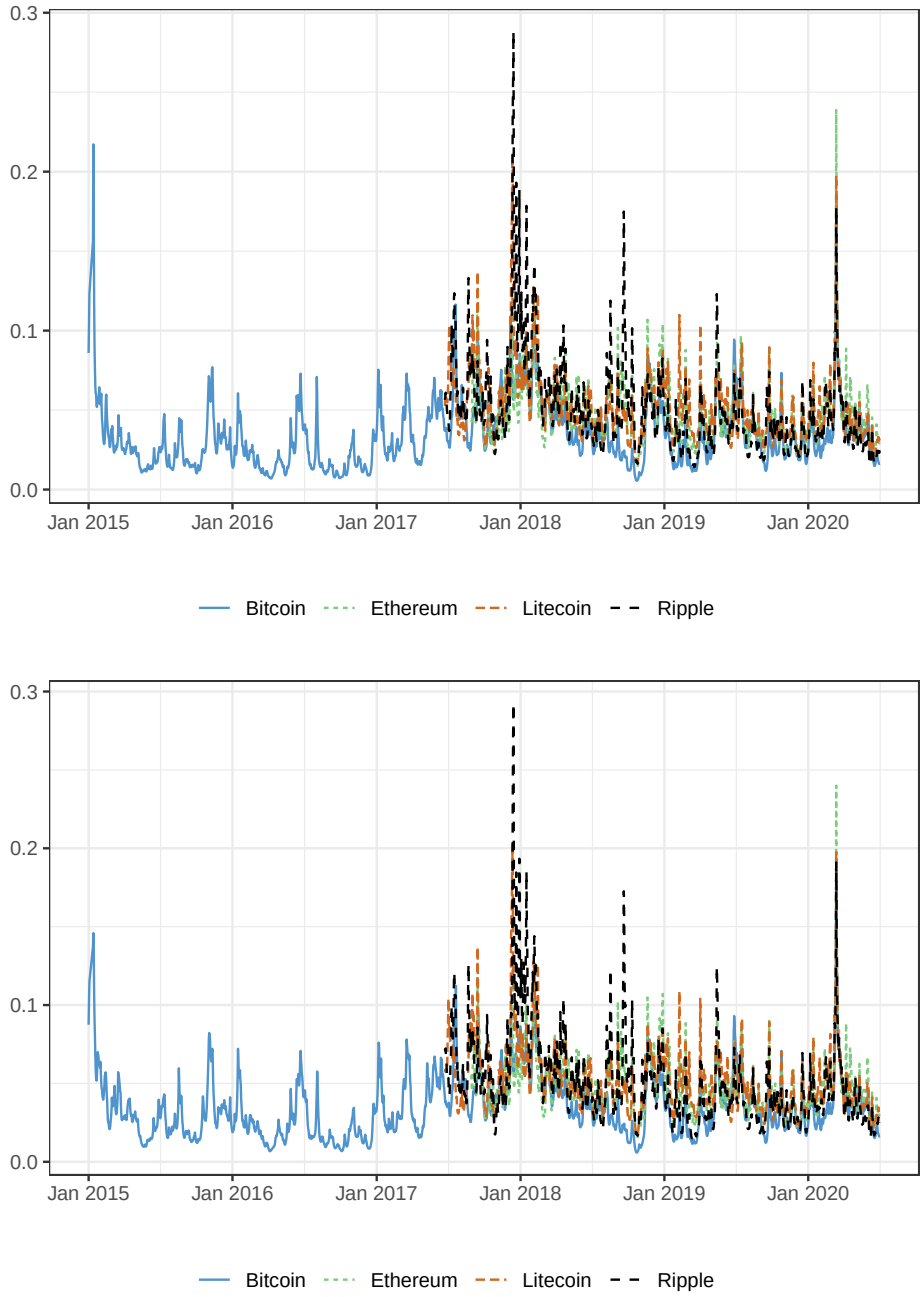

Note: The figure presents the time series of the latent volatility of the four cryptocurrencies Bitcoin, Ethereum, Litecoin, and Ripple based on data from Bitstamp (upper panel) and Kraken (lower panel) markets.

4.C Autocorrelation plots of the latent volatility (continued)

Figure 4.C.1: Autocorrelation plots of the latent volatility of Ethereum

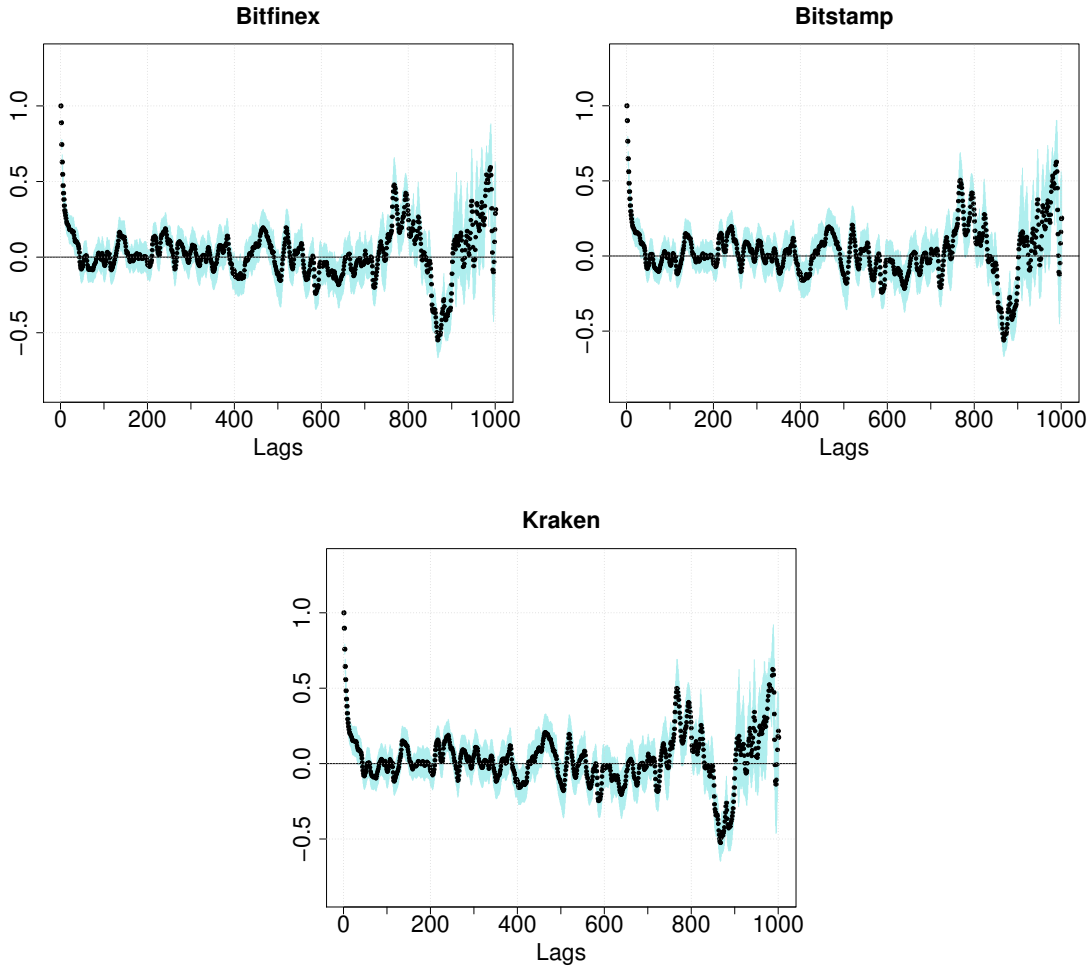

Note: The figure presents the autocorrelation plots and their 95% GMM based bounds for the three exchanges Bitfinex, Bitstamp (upper panel), and Kraken (lower panel) for the latent volatility of the cryptocurrency Ethereum.

Figure 4.C.2: Autocorrelation plots of the latent volatility of Litecoin

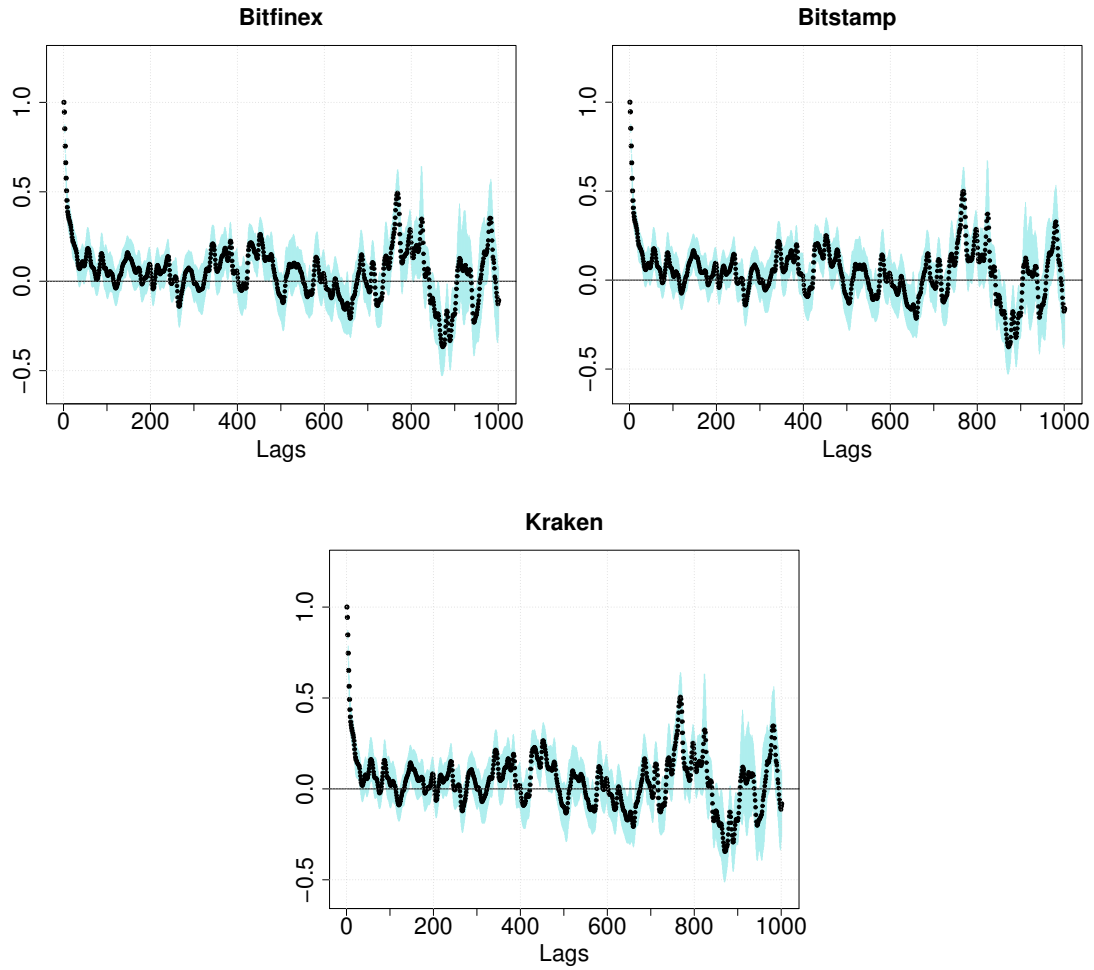

Note: The figure presents the autocorrelation plots and their 95% GMM based bounds for the three exchanges Bitfinex, Bitstamp (upper panel), and Kraken (lower panel) for the latent volatility of the cryptocurrency Litecoin.

Figure 4.C.3: Autocorrelation plots of the latent volatility of Ripple

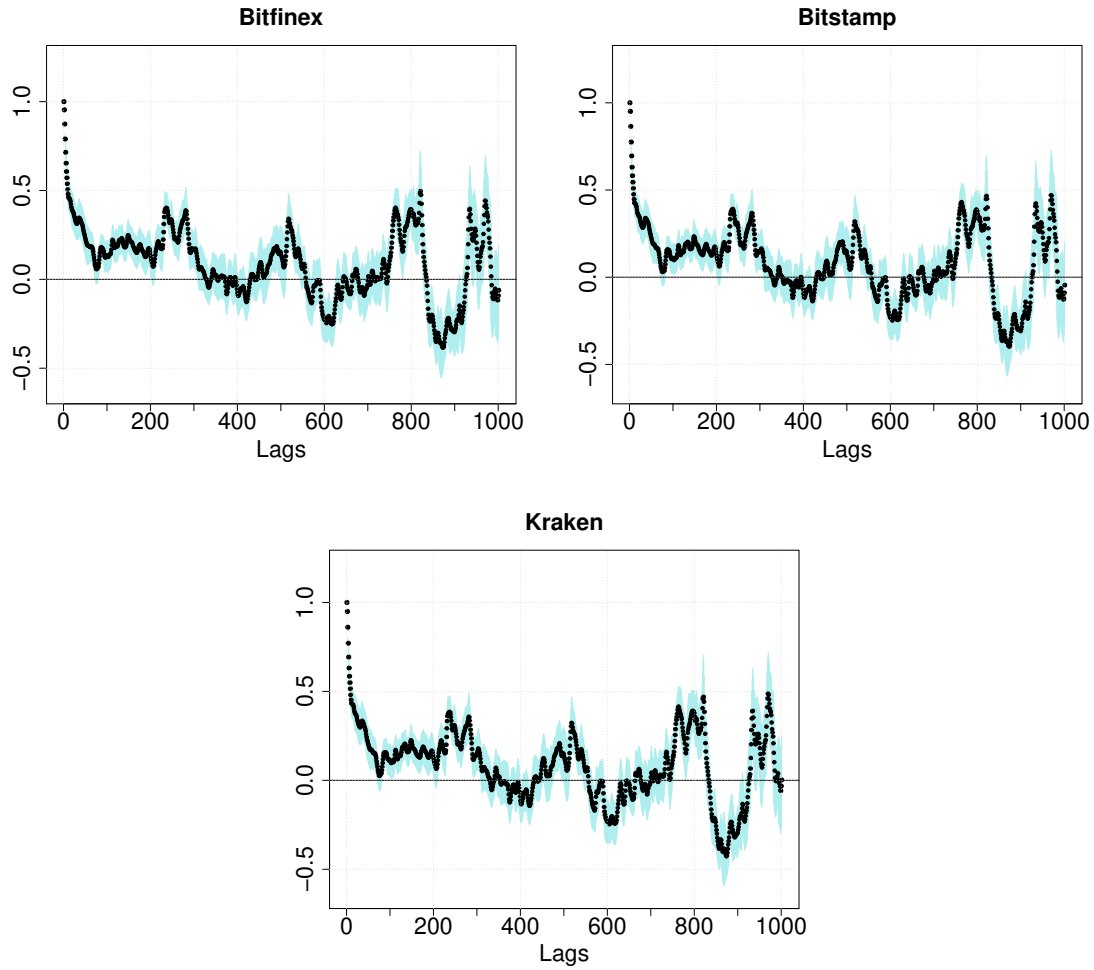

Note: The figure presents the autocorrelation plots and their 95% GMM based bounds for the three exchanges Bitfinex, Bitstamp (upper panel), and Kraken (lower panel) for the latent volatility of the cryptocurrency Ripple.

4.D Results of the cointegration rank tests

Table 4.D.1: Cointegration rank tests of the different cryptocurrencies

Rank	d	b	Log-Likelihood	LR statistic	P-value
A: Bitcoin					
0	0.642	0.642	13390.900	155.029	0.000
1	0.673	0.673	13438.129	60.570	0.000
2	0.775	0.775	13467.987	0.854	0.350
3	0.760	0.760	13468.414	–	–
B: Ethereum					
0	0.410	0.410	6825.426	143.560	0.000
1	0.700	0.700	6871.657	51.098	0.000
2	0.744	0.744	6894.247	5.917	0.014
3	0.688	0.688	6897.206	–	–
C: Litecoin					
0	0.743	0.743	8866.598	104.714	0.000
1	0.788	0.788	8894.642	48.624	0.000
2	0.852	0.852	8918.648	0.613	0.451
3	0.839	0.839	8918.955	–	–
D: Ripple					
0	0.602	0.602	8555.480	84.879	0.000
1	0.651	0.651	8580.804	34.230	0.000
2	0.716	0.716	8594.863	6.113	0.012
3	0.651	0.651	8597.919	–	–

Note: The table presents Johansen's trace test (Johansen and Nielsen, 2012) for the cointegration rank conducted on the three cryptocurrency markets in our study for each of the coins; Bitcoin (panel A), Ethereum (panel B), Litecoin (panel C) and Ripple (panel D).

4.E Comparison of out-of-sample forecasts of Bitcoin using FCVAR and standard CVAR

Figure 4.E.1: Out-of-sample forecasts

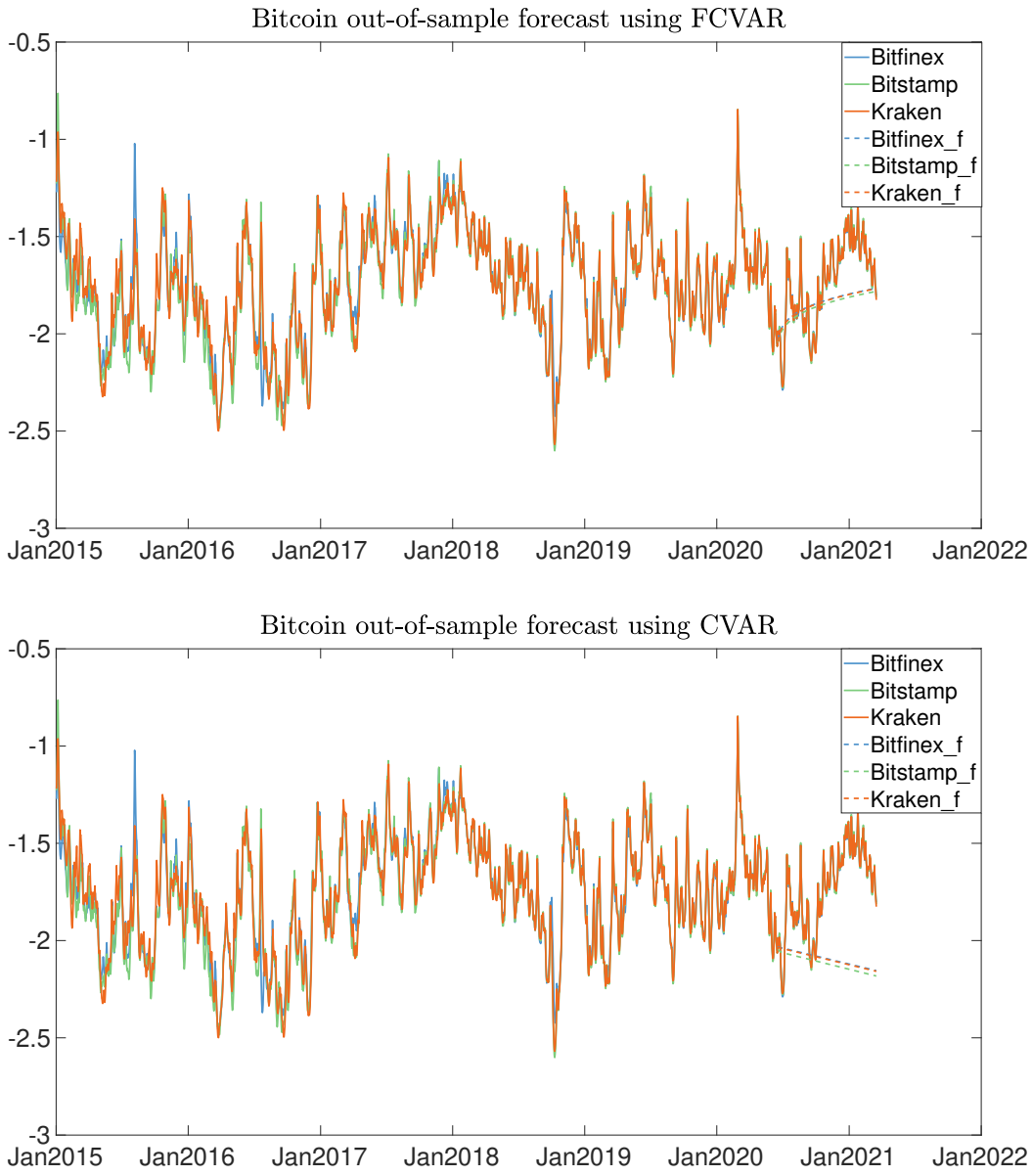

Note: The figure shows the out-of-sample daily forecasts of Bitcoin from 1st of July 2020 till 31st of March 2021. The solid blue (green, orange) line in both panels represents the latent log-volatility, $\hat{h}_t$, of the Bitfinex (Bitstamp, Kraken) market. The dashed blue (green, orange) line represents the out-of-sample forecast of the latent log-volatility of the Bitfinex (Bitstamp, Kraken) market using FCVAR estimates in the upper panel versus CVAR estimates in the lower panel.

Chapter 5

Summary and Conclusion

This dissertation is an assortment of three distinct studies that attempt to methodically contribute to the field of financial econometrics. They collectively tackle different challenges resulting from the uncertainty taking place in financial markets. The first two studies, presented in Chapters 2 and 3, are concerned with asset pricing and its challenges in the context of a DSGE model with habit preferences. The final study, presented in Chapter 4, looks beyond prices to the volatility taking place in cryptocurrency markets. It attempts to discover the volatility leader among the different cryptocurrency markets as well as among the different cryptocurrencies.

The methodical contributions of Chapters 2 and 3 lie in adapting estimation techniques that can withstand misspecification in highly structured models. In Chapter2, this is the PII estimation which encloses calibration within its folds. It can thus deliver consistent estimates of a subset of the structural model's parameters in the presence of misspecification in its calibrated part. This estimation technique is used to deliver a critical assessment of a DSGE asset pricing model with habit preferences, the model in Chen (2017). The findings indicate the successful identification of the parameters of interest; the asset pricing parameters. This leads to the resolution of the equity premium puzzle, provided that a high estimate of the relative risk aversion parameter is accepted. The risk-free rate puzzle

remains problematic; though we manage to estimate a slightly lower value for the volatility of the risk-free rate, we fail to match its level relative to its empirical counterpart. As such, we caution against the overstatement of the calibration results of DSGE asset pricing models.

Chapter 3 draws from the conclusions in Chapter 2, and asks what happens if misspecification in those highly structured DSGE asset pricing models is not taken into account? The methodical contribution lies in the comparison between three indirect inference strategies; the classical II estimation which does not account for misspecification, and the FII estimation and the PII estimation from Chapter 2. The latter two account for misspecification with differing degrees. An additional contribution is in tailoring the "dark matter" measure of Chen et al. (2019) to fit indirect inference estimation strategies. This measure goes beyond statistical inference and determines how fragile the estimation process is to the potentially misspecified moment conditions in the underlying GMM instrumental model. The findings indicate that, as expected, not accounting for the misspecification in the macroeconomic moments via II estimation results in unidentifiable parameter estimates. Yet, using FII estimation does not alter these unfortunate results. The dark matter measure, however, reveals that there is a better option than simply disregarding all of the macroeconomic dynamics by calibrating their parameters, as in the PII estimation in Chapter 2. Rather, adding the first two moments of GDP to the original PII estimation results in identifiable parameters. This modified PII method is found to deliver slightly improved estimates for the asset pricing moments and remarkably improved implied macroeconomic moments.

Finally, Chapter 4 departs from the macro-level view of the economy and dissects at close the market for cryptocurrencies. Since the same cryptocurrencies are traded on many different exchange platforms, the aim is to find out which exchange market is the volatility leader. Given the leading exchange market, the overall cryptocurrency volatility driver can also be discovered. The contribution here is not methodical per se, but lies in extending the price discovery framework to a volatility discovery scheme that takes into

account the long memory nature of volatility series. This is a novel attempt in the context of cryptocurrencies. As such, the FCVAR estimation of Johansen (2008) and Johansen and Nielsen (2012) is utilized, which then allows for the computation of Hasbrouck (1995) and Lien and Shrestha (2009) information shares. The findings indicate that the different cryptocurrencies tend to have different market volatility leaders. For Bitcoin, it can be confidently stated that this is Bitfinex. For the other cryptocurrencies under investigation, the estimation results are imprecise due to the considerably shorter time series available at the time of analysis. The dominance of Bitcoin is also demonstrated, as it is found to be the volatility leader among the three other cryptocurrencies under examination. Yet with the market for cryptocurrencies gaining more traction with time, it is possible that the "younger" cryptocurrencies may outshine Bitcoin. The investigation of this possibility is left for future research.

Overall the studies presented in this dissertation, while diverse in nature, all provide additional insights into some of the current research themes in financial econometrics. The possibilities for future research in these areas are far from limited; cryptocurrency is still a novice financial market with much to be discovered, cointegration analysis of time series with long memory properties is still far from developed, the resolution of asset pricing puzzles is still unattainable, and finally the DSGE asset pricing models which hope to be their salvation remain troublesome to estimate. My hope is that this dissertation serves as a stepping stone for future research in these areas.

Bibliography

Ainslie, G. (1992): *Picoeconomics: The strategic interaction of successive motivational states within the person*: Cambridge University Press.

Alexander, C., J. Choi, H. Park, and S. Sohn (2020): "BitMEX Bitcoin derivatives: Price discovery, informational efficiency, and hedging effectiveness," *Journal of Futures Markets*, 40(1), 23–43.

Alexander, C., and M. Dakos (2020): "A critical investigation of cryptocurrency data and analysis," *Quantitative Finance*, 20(2), 173–188.

Alexander, C., and D. F. Heck (2020): "Price discovery in Bitcoin: The impact of unregulated markets," Available at SSRN: https://ssrn.com/abstract=3583843.

Almeida, C., and R. Garcia (2012): "Assessing misspecified asset pricing models with empirical likelihood estimators," *Journal of Econometrics*, 170(2), 519–537.

Altig, D., L. J. Christiano, M. Eichenbaum, and J. Linde (2011): "Firm-specific capital, nominal rigidities and the business cycle," *Review of Economic Dynamics*, 14(2), 225–247.

Altug, S. (1989): "Time-to-build and aggregate fluctuations: some new evidence," *International Economic Review*, 30(4), 889–920.

An, S., and F. Schorfheide (2007): "Bayesian analysis of DSGE models," *Econometric reviews*, 26(2-4), 113–172.

Andersen, T. G., T. Bollerslev, and N. Meddahi (2011): "Realized volatility forecasting and market microstructure noise," *Journal of Econometrics*, 160(1), 220–234.

Andrews, I., M. Gentzkow, and J. M. Shapiro (2017): "Measuring the sensitivity of parameter estimates to estimation moments," *The Quarterly Journal of Economics*, 132(4), 1553–1592.

Antoine, B., K. Proulx, and E. Renault (2020): "Pseudo-true SDFs in conditional asset pricing models," *Journal of Financial Econometrics*, 18(4), 656–714.

Arzandeh, M., and J. Frank (2019): "Price discovery in agricultural futures markets: Should we look beyond the best Bid-Ask spread?" *American Journal of Agricultural Economics*, 101(5), 1482–1498.

Baek, C., and M. Elbeck (2015): "Bitcoins as an investment or speculative vehicle? A first look," *Applied Economics Letters*, 22(1), 30–34.

Baillie, R. T. (1996): "Long memory processes and fractional integration in econometrics," *Journal of Econometrics*, 73(1), 5–59.

Baule, R., B. Frijns, and M. E. Tieves (2018): "Volatility discovery and volatility quoting on markets for options and warrants," *Journal of Futures Markets*, 38(7), 758–774.

Baur, D. G., and T. Dimpfl (2019): "Price discovery in Bitcoin spot or futures?" *Journal of Futures Markets*, 39(7), 803–817.

Bollerslev, T. (2001): "Financial econometrics: Past developments and future challenges," *Journal of Econometrics*, 100(1), 41–51.

Bollerslev, T., D. Osterrieder, N. Sizova, and G. Tauchen (2013): "Risk and return: Long-run relations, fractional cointegration, and return predictability," *Journal of Financial Economics*, 108(2), 409–424.

Borri, N. (2019): "Conditional tail-risk in cryptocurrency markets," *Journal of Empirical Finance*, 50, 1–19.

Brandvold, M., P. Molnár, K. Vagstad, and O. C. A. Valstad (2015): "Price discovery on Bitcoin exchanges," *Journal of International Financial Markets, Institutions and Money*, 36, 18–35.

Brauneis, A., and R. Mestel (2018): "Price discovery of cryptocurrencies: Bitcoin and beyond," *Economics Letters*, 165, 58–61.

Burnside, C., M. Eichenbaum, and S. Rebelo (1993): "Labor hoarding and the business cycle," *The Journal of Political Economy*, 101(2), 245–273.

Campbell, J. Y., and J. H. Cochrane (1999): "By Force of Habit: A Consumption-Based Explanation of Aggregate Stock Market Behavior," *The Journal of Political Economy*, 107(2), 205–251.

Campbell, J. Y., A. W. Lo, and A. MacKinlay (1997): *The econometrics of financial markets*: Princeton University Press, `http://www.jstor.org/stable/j.ctt7skm5`.

Caporin, M., A. Ranaldo, and P. S. De Magistris (2013): "On the predictability of stock prices: A case for high and low prices," *Journal of Banking & Finance*, 37(12), 5132–5146.

Chaim, P., and M. P. Laurini (2018): "Volatility and return jumps in Bitcoin," *Economics Letters*, 173, 158–163.

——— (2019): "Nonlinear dependence in cryptocurrency markets," *North American Journal of Economics and Finance*, 48, 32–47.

Chen, A. Y. (2013): "External habit in a production economy,"Technical report, Ohio State University, Charles A. Dice Center for Research in Financial Economics.

——— (2017): "External habit in a production economy: A model of asset prices and consumption volatility risk," *The Review of Financial Studies*, 30(8), 2890–2932.

Chen, H., W. W. Dou, and L. Kogan (2019): "Measuring "Dark Matter" in asset pricing models," Working Paper 26418, National Bureau of Economic Research, `http://www.nber.org/papers/w26418`.

Chen, W.-P., H. Chung, and D. Lien (2016): "Price discovery in the S&P 500 index derivatives markets," *International Review of Economics & Finance*, 45, 438–452.

Chen, X., and S. C. Ludvigson (2009): "Land of addicts? an empirical investigation of habit-based asset pricing models," *Journal of Applied Econometrics*, 24(7), 1057–1093.

Christiano, L. J., and M. Eichenbaum (1992): "Current real-business-cycle theories and aggregate labor-market fluctuations," *The American Economic Review*, 82(3), 430–450.

Christiano, L. J., M. Eichenbaum, and C. L. Evans (2005): "Nominal rigidities and the dynamic effects of a shock to monetary policy," *The Journal of Political Economy*, 113(1), 1–45.

Cochrane, J. H. (2009): *Asset Pricing*: Princeton University Press.

——— (2016): "The Habit Habit," Economics Working Papers 16105, Hoover Institution, Stanford University, `https://ideas.repec.org/p/hoo/wpaper/16105.html`.

——— (2017): "Macro-finance," *Review of Finance*, 21(3), 945–985.

Corbet, S., B. Lucey, M. Peat, and S. Vigne (2018): "Bitcoin Futures–What use are they?" *Economics Letters*, 172, 23 – 27.

Dias, G. F., C. M. Scherrer, and F. Papailias (2018): "Volatility Discovery," CREATES Research Papers 2016-07, Department of Economics and Business Economics, Aarhus University, `https://ideas.repec.org/p/aah/create/2016-07.html`.

Dimpfl, T., and D. Elshiaty (2021): "Volatility discovery in cryptocurrency markets," *The Journal of Risk Finance*, 22(5), 313–331.

Dimpfl, T., and F. J. Peter (2020): "Nothing but noise? Price discovery between cryptocurrency exchanges," Available at SSRN: https://ssrn.com/abstract=3565209.

Dolatabadi, S., M. O. Nielsen, and K. Xu (2015): "A fractionally cointegrated VAR analysis of price discovery in commodity futures markets," *Journal of Futures Markets*, 35(4), 339–356.

Dridi, R., A. Guay, and E. Renault (2007): "Indirect inference and calibration of dynamic stochastic general equilibrium models," *Journal of Econometrics*, 136(2), 397–430.

Dridi, R., and E. Renault (2000): "Semi-parametric indirect inference," *LSE STICERD Research Paper No. EM392*.

Duffie, D., and K. J. Singleton (1993): "Simulated moments estimation of Markov models of asset prices," *Econometrica*, 61(4), 929–952.

Engle, R. F., and C. W. Granger (1987): "Co-integration and error correction: representation, estimation, and testing," *Econometrica*, 55(2), 251–276.

Fassas, A. P., S. Papadamou, and A. Koulis (2020): "Price discovery in Bitcoin futures," *Research in International Business and Finance*, 52, 101116.

Fernald, J. (2014): "A quarterly, utilization-adjusted series on total factor productivity," Federal Reserve Bank of San Francisco.

Fernández-Villaverde, J. (2010): "The econometrics of DSGE models," *SERIEs*, 1(1-2), 3–49.

Fernández-Villaverde, J., J. F. Rubio-Ramírez, and F. Schorfheide (2016): "Solution and estimation methods for DSGE models," *Handbook of Macroeconomics*, 2, 527–724.

Forte, S., and L. Lovreta (2019): "Volatility discovery: Can the CDS market beat the equity options market?" *Finance Research Letters*, 28, 107–111.

Fricke, C., and L. Menkhoff (2011): "Does the "Bund" dominate price discovery in Euro bond futures? Examining information shares," *Journal of Banking & Finance*, 35(5), 1057–1072.

Gallant, A. R., and G. Tauchen (1996): "Which moments to match?" *Econometric Theory*, 12(4), 657–681.

Gospodinov, N., R. Kan, and C. Robotti (2014): "Misspecification-robust inference in linear asset-pricing models with irrelevant risk factors," *The Review of Financial Studies*, 27(7), 2139–2170.

Gourieroux, C., A. Monfort, and E. Renault (1993): "Indirect inference," *Journal of Applied Econometrics*, 8(S1), 85–118.

Grammig, J., and F. J. Peter (2013): "Telltale tails: A new approach to estimating unique market information shares," *Journal of Financial and Quantitative Analysis*, 48(2), 459–488.

——— (2018): "Tumbling Titans? The changing patterns of price discovery in the U.S. equity market," Available at SSRN: `https://ssrn.com/abstract=3194484`.

Grammig, J., J. Schnaitmann, and D. Elshiaty (2020): "Empirical asset pricing in a DSGE framework: Reconciling calibration and econometrics using partial indirect inference," Available at SSRN: https://ssrn.com/abstract=3648085.

Granger, C. W. (1980): "Long memory relationships and the aggregation of dynamic models," *Journal of Econometrics*, 14(2), 227–238.

——— (1981): "Some properties of time series data and their use in econometric model specification," *Journal of Econometrics*, 16(1), 121–130.

Granger, C. W., and R. Joyeux (1980): "An introduction to long-memory time series models and fractional differencing," *Journal of Time Series Analysis*, 1(1), 15–29.

Guesmi, K., S. Saadi, I. Abid, and Z. Ftiti (2019): "Portfolio diversification with virtual currency: Evidence from Bitcoin," *International Review of Financial Analysis*, 63, 431 – 437.

Guvenen, F. (2009): "A parsimonious macroeconomic model for asset pricing," *Econometrica*, 77(6), 1711–1750.

Hamilton, J. D. (1995): *Time series analysis*: Princeton University Press.

Hansen, L. P. (1982): "Large sample properties of generalized method of moments estimators," *Econometrica*, 50(4), 1029–1054.

Hansen, L. P., and J. J. Heckman (1996): "The empirical foundations of calibration," *The Journal of Economic Perspectives*, 10(1), 87–104.

Hansen, L. P., and R. Jagannathan (1997): "Assessing specification errors in stochastic discount factor models," *The Journal of Finance*, 52(2), 557–590.

Hasbrouck, J. (1995): "One security, many markets: Determining the contributions to price discovery," *The Journal of Finance*, 50(4), 1175–1199.

Hodrick, R. J., and X. Zhang (2001): "Evaluating the specification errors of asset pricing models," *Journal of Financial Economics*, 62(2), 327–376.

Huang, R. D. (2002): "The quality of ECN and Nasdaq market maker quotes," *The Journal of Finance*, 57(3), 1285–1319.

Ireland, P. N. (2004): "Technology shocks in the new Keynesian model," *Review of Economics and Statistics*, 86(4), 923–936.

Ivanov, S. I. (2013): "The influence of ETFs on the price discovery of gold, silver and oil," *Journal of Economics and Finance*, 37(3), 453–462.

Jacquier, E., N. G. Polson, and P. E. Rossi (1994): "Bayesian analysis of stochastic volatility models," *Journal of Business & Economic Statistics*, 12(4), 371–389.

Jensen, A. N., and M. Ø. Nielsen (2014): "A fast fractional difference algorithm," *Journal of Time Series Analysis*, 35(5), 428–436.

Jermann, U. J. (1998): "Asset pricing in production economies," *Journal of Monetary Economics*, 41(2), 257–275.

——— (2010): "The equity premium implied by production," *Journal of Financial Economics*, 98(2), 279–296.

Johansen, S. (1995): "Identifying restrictions of linear equations with applications to simultaneous equations and cointegration," *Journal of Econometrics*, 69(1), 111–132.

——— (2008): "A representation theory for a class of vector autoregressive models for fractional processes," *Econometric Theory*, 24(3), 651–676.

Johansen, S., and M. Ø. Nielsen (2012): "Likelihood inference for a fractionally cointegrated vector autoregressive model," *Econometrica*, 80(6), 2667–2732.

Kaltenbrunner, G., and L. A. Lochstoer (2010): "Long-run risk through consumption smoothing," *The Review of Financial Studies*, 23(8), 3190–3224.

Kan, R., and C. Robotti (2008): "Specification tests of asset pricing models using excess returns," *Journal of Empirical Finance*, 15(5), 816–838.

Kan, R., and C. Zhang (1999): "Two-pass tests of asset pricing models with useless factors," *The Journal of Finance*, 54(1), 203–235.

Karabiyik, H., J. Westerlund, and P. Narayan (2022): "Panel data measures of price discovery," *Econometric Reviews*, 41(3), 269–290.

Kastner, G. (2016): "Dealing with stochastic volatility in time series using the R package stochvol," *Journal of Statistical Software*, 69(5), 1–30.

Kastner, G., and D. Hosszejni (2019): "stochvol: Efficient Bayesian inference for stochastic volatility (SV) models," `https://CRAN.R-project.org/package=stochvol`, R package version 2.0.4.

Katsiampa, P. (2019): "Volatility co-movement between Bitcoin and Ether," *Finance Research Letters*, 30, 221–227.

Kim, K., and A. R. Pagan (1999): "The econometric analysis of calibrated macroeconomic models," in *Handbook of Applied Econometrics* ed. by Pesaran, H., and Wickens, M. Volume 1: Macroeconomics, Oxford: Blackwell Publishing Ltd. Chap. 7, 309–338.

Klein, T., H. P. Thu, and T. Walther (2018): "Bitcoin is not the new gold – A comparison of volatility, correlation, and portfolio performance," *International Review of Financial Analysis*, 59, 105–116.

Kogan, L. (2004): "Asset prices and real investment," *Journal of Financial Economics*, 73(3), 411–431.

Kogan, L., and D. Papanikolaou (2012): "Economic activity of firms and asset prices," *Annual Review Financial Economics*, 4(1), 361–384.

Leeper, E. M., and C. A. Sims (1994): "Toward a modern macroeconomic model usable for policy analysis," *NBER Macroeconomics Annual*, 9, 81–118.

Lehmann, B. N. (2002): "Some desiderata for the measurement of price discovery across markets," *Journal of Financial Markets*, 5(3), 259–276.

Lien, D., and K. Shrestha (2009): "A new information share measure," *Journal of Futures Markets*, 29(4), 377–395.

Liu, Q., and Y. An (2011): "Information transmission in informationally linked markets: Evidence from US and Chinese commodity futures markets," *Journal of International Money and Finance*, 30(5), 778–795.

Ludvigson, S. C. (2013): "Advances in consumption-based asset pricing: Empirical tests," *Handbook of the Economics of Finance*, 2, 799–906.

McFadden, D. (1989): "A method of simulated moments for estimation of discrete response models without numerical integration," *Econometrica*, 57(5), 995–1026.

McGrattan, E. R., R. Rogerson, and R. Wright (1997): "An equilibrium model of the business cycle with household production and fiscal policy," *International Economic Review*, 38(2), 267–290.

Mehra, R., and E. C. Prescott (1985): "The equity premium: A puzzle," *Journal of Monetary Economics*, 15(2), 145–161.

Narayan, P. K., S. S. Sharma, and K. S. Thuraisamy (2014): "An analysis of price discovery from panel data models of CDS and equity returns," *Journal of Banking & Finance*, 41, 167–177.

Newey, W. K., and K. D. West (1987): "A simple, positive semi-definite, heteroskedasticity and autocorrelation consistent covariance matrix," *Econometrica*, 55(3), 703–708.

Nielsen, M. Ø., and M. K. Popiel (2014): "A Matlab program and user's guide for the fractionally cointegrated VAR model,"Technical report, Queen's Economics Department Working Paper.

Nielsen, M. Ø., and S. S. Shibaev (2018): "Forecasting daily political opinion polls using the fractionally cointegrated vector auto-regressive model," *Journal of the Royal Statistical Society: Series A (Statistics in Society)*, 181(1), 3–33.

Pagnottoni, P., and T. Dimpfl (2019): "Price discovery on Bitcoin markets," *Digital Finance*, 1(1-4), 139–161.

Phillip, A., J. S. Chan, and S. Peiris (2018): "A new look at cryptocurrencies," *Economics Letters*, 163, 6–9.

Resta, M., P. Pagnottoni, and M. E. De Giuli (2020): "Technical analysis on the Bitcoin market: Trading opportunities or investors' pitfall?" *Risks*, 8(2).

Rossi, E., and P. Santucci de Magistris (2013): "A no-arbitrage fractional cointegration model for futures and spot daily ranges," *Journal of Futures Markets*, 33(1), 77–102.

Rotemberg, J. J., and M. Woodford (1997): "An optimization-based econometric framework for the evaluation of monetary policy," *NBER Macroeconomics Annual*, 12, 297–346.

Rouwenhorst, G. (1995): *Asset returns and business cycles in frontiers of business cycle research*: Princeton University Press.

Ruge-Murcia, F. J. (2007): "Methods to estimate dynamic stochastic general equilibrium models," *Journal of Economic Dynamics and Control*, 31(8), 2599–2636.

——— (2012): "Estimating nonlinear DSGE models by the simulated method of moments: With an application to business cycles," *Journal of Economic Dynamics and Control*, 36(6), 914–938.

——— (2014): "Indirect inference estimation of nonlinear dynamic general equilibrium models: with an application to asset pricing under skewness risk,"Technical report, Centre interuniversitaire de recherche en économie quantitative, CIREQ.

Samuelson, P. A. (1938): "A note on the pure theory of consumers behavior," *Economica*, 5(17), 61–71.

Sandmann, G., and S. J. Koopman (1998): "Estimation of stochastic volatility models via Monte Carlo maximum likelihood," *Journal of Econometrics*, 87(2), 271–301.

da Silva, A. G., and P. M. Robinson (2008): "Fractional cointegration in stochastic volatility models," *Econometric Theory*, 24(5), 1207–1253.

Singleton, K. J. (2009): *Empirical dynamic asset pricing: model specification and econometric assessment*: Princeton University Press.

Smith, A. A. (1993): "Estimating nonlinear time-series models using simulated vector autoregressions," *Journal of Applied Econometrics*, 8(S1), 63–84.

Taylor, S. J. (1994): "Modeling stochastic volatility: A review and comparative study," *Mathematical Finance*, 4(2), 183–204.

Wang, Q. (2014): "Volatility discovery across stock limit order book and options markets," *Journal of Futures Markets*, 34(10), 934–956.

Weil, P. (1989): "The equity premium puzzle and the risk-free rate puzzle," *Journal of Monetary Economics*, 24(3), 401–421.